UNIVERSITY OF CALIFORNIA, SAN DIEGO

Regulation of Cell Adhesion and Cell Death: the Roles of the Abl Tyrosine Kinase and the Retinoblastoma Protein

A dissertation submitted in partial satisfaction of the requirements for the Doctor of Philosophy

in

Biology

by

Xiaodong Huang

Committee in charge:

Professor Jean Y. J. Wang, Chair
Professor Tony Hunter, Co-Chair
Professor Michael David
Professor Stephen Hedrick
Professor Amy Kiger
Professor Sanford Shattil

2007

The Dissertation of Xiaodong Huang is approved, and it is acceptable in quality and form for publication on microfilm:

Co-Chair

Chair

University of California, San Diego

2007

DEDICATION

To

My parents and all the ones who I love

For constant encouragement and support

TABLE OF CONTENTS

LIST OF FIGURES

CHAPTER 1:

CHAPTER 2:

CHAPTER 3:

CHAPTER 4:

CHAPTER 5:

LIST OF TABLES

CHAPTER 1:

CHAPTER 3:

ACKNOWLEDGEMENT

I would like to express my deepest gratitude for my mentor, Dr. Jean Wang, for taking me as a graduate student. It would have been impossible for me to accomplish this dissertation without her consistent support. She not only trained me with her scientific expertise, but also influenced me with her passion to science and commitment to perfection. I especially admire her deep thoughts, sharp mind, unconventional views and tremendous respect for everyone in the scientific community. As an international student, I am also greatly indebted to her for her generosity and concerns about my life here over the years. It is my privilege to be her student.

I thank my committee members, Dr. Tony Hunter, Dr. Michael David, Dr. Steve Hedrick, Dr. Amy Kiger, Dr. Sanford Shattil, and Dr. Douglas Green for their consistent interest and guidance of my research projects. I thank Dr. Dwayne Stupack for giving me advice on my caspase-8 and integrin projects. I thank Dr. Xin Lu for bioinformatics help for my shRNA library screening project. I also thank Dr. Steve Frisch and Dr. Elena Pasquale for sharing reagents.

I thank all the past and present members of the Wang laboratory, for creating a positive working atmosphere. I thank Scott Stuart, Shun Lee, Vera Huang, and Benjamin O'Connor for helping me prepare my manuscripts. I thank Diana Wu, Lisa Kodadek, and Jennifer Chang for their dedication on all the projects in which they participated. I thank Nelson Chau and Anja Masselli for initiating the RB-MI project. I had many enjoyable conversations with Martin Preyer, Samantha Zetlin, Susana Chaves, Jiangyu Zhu, Helena Borges, Jacqueline Bergseid, Yong Jiang, Vincent Shu, Guangli Suo, and Yosuke

Minami. Thanks also to Irina Hunton, Rimma Levenzon, and Guizhen Sun for their technical support.

I consider myself lucky to have many friends who have made my life secure and enjoyable in this wonderful country. I thank Edward Chiang, Jennifer Collins, Zhengdao Lan, and Tony Chu for being fantastic friends. I thank Mrs. An-Ling Chiang, the Margolin family and the Collins family for taking care of me through all these years.

Chapter 2, in part, is being prepared for publication of the material as it may appear in "Abl tyrosine kinase induces cell detachment through Rap1-induced integrin inactivation and requires Rho activation, Xiaodong Huang, Diana Wu, Dwayne G. Stupack, and Jean Y. J. Wang (in preparation)". The dissertation author is the primary investigator and author of this paper.

Chapter 3, in part, is being submitted of the material as it may appear in "Systems analysis of quantitative shRNA-library screens identifies novel regulators of cell adhesion, Xiaodong Huang, Jean Y. J. Wang, and Xin Lu (in submission)". The author of the dissertation is the primary investigator and author of this paper.

Chapter 5, in full, is a reprint of the material as it appears in "Xiaodong Huang, Anja Masselli, Steven M. Frisch, Irina C. Hunton, Yong Jiang, and Jean Y. J. Wang, J. Biol. Chem., 2007 Oct 5;282(40):29401-13". The author of the dissertation is the primary investigator and author of this paper.

CURRICULUM VITAE

EDUCATION:

2007 Ph.D. University of California, San Diego
Thesis: Regulation of cell adhesion and cell death: the roles of Abl tyrosine kinase and the retinoblastoma protein.
Advisor: Dr. Jean Y. J. Wang

1997 M.S. Shanghai Institute of Biochemistry, Chinese Academy of Sciences
Thesis: Cloning and expression of penicillin G acylase gene from *Bacillus megaterium* and its expression in *Bacillus subtilis*.
Advisor: Dr. Zhongyi Yuan

1994 B.S. Beijing Normal University
Major: Organic Chemistry

PROFESSIONAL EXPERIENCE:

1997-2001 Consultant, Chongqing Science and Technology Consulting Committee, Chongqing, China

MAJOR RESEARCH INTEREST:

Signaling network that coordinates cell proliferation, differentiation and apoptosis; tumorigenesis; animal models of diseases.

HONORS AND AWARDS:

1990-1994 Beijing Normal University Fellowship

PATENT:

1999 Yuan, Z., Yang, S., Li, S., **Huang, X**., The Expression elements of penicillin G acylase in *Bacillus subtilis*. Patent Number: CN99113885.6

MAJOR COMMITTEE ASSIGNMENTS:

UNIVERSITY OF CALIFORNIA SAN DIEGO:

2006-2007 International Education Committee

TEACHING EXPERIENCE:

1994 **Instructor**, General Chemistry, Qinghua High School, Beijing, China

2004-2005 **Lab Course Teaching Assistant**, Recombinant DNA Technique, University of California San Diego, CA
2006 **Lecture Course Teaching Assistant**, Molecular Biology, University of California San Diego, CA

CONFERENCE PROCEEDINGS/PRESENTATIONS:

- **Huang, X,** Wang, J.Y.J. (2005) "Characterization of Cell Death Induced by Abl Tyrosine Kinase" Cellular Senescence and Cell Death, Keystone Symposia

- **Huang, X**., Masselli, A., Frisch, SM., Hunton, IC., Jiang, Y., and Wang JY.. (2006) "Impaired Caspase-8 Activation by Type I TNF Receptor in Cells Expressing Caspase-Resistant RB" Gordon Research Conference

- **Huang, X**., Masselli, A., Frisch, SM., Hunton, IC., Jiang, Y., and Wang JY.. (2007) "Blockade of TNF-Induced Bid Cleavage by Caspase-Resistant Rb" Cell Death Meeting, Cold Spring Harbor, New York

PUBLICATIONS:

PEER REVIEWED ARTICLES

1. Yang, S., **Huang, X**, Huang, Y., Li, S., Yuan, Z.. High expression of penicillin G acylase gene from *Bacillus megaterium* in *Bacillus subtilis*. *Acta. Biochim. Biophys. Sin*., 1999, 31(5): 601-603

2. Yang, S, Huang, H., Zhang, R., **Huang, X.**, Li, S., Yuan, Z.. Expression and purification of extracellular penicillin G acylase in *Bacillus subtilis*. *Protein Expression and Purification*, 2001, 21, 60-64

3. Huang, H., Yang, S., Li, R., **Huang, X.**, Yuan, Z.. Optimization of recombinant penicillin G acylase expression in *Bacillus subtilis*, *Chin. J. Biochem. Molecular Biol.*, 2001, 17(2): 173-177

4. **Huang, X**., Masselli, A., Frisch, S.M., Hunton, I.C., Jiang, Y., and Wang, J.Y.J. Vacuolar ATPase Inhibition Rescues Defect in TNF-Induced Bid Cleavage Caused by Caspase-Resistant Rb, *J. Biol. Chem., 2007 In press.*

5. **Huang, X.**, Wang, J.Y.J., Lu, X., Systems Analysis of Quantitative shRNA-Library Screens Identifies Novel Regulators of Cell Adhesion, *Molecular Systems Biology*, Submitted

6. **Huang, X**., Wu, D., Stupack, D., Wang, J.Y.J. Activated Abl Kinase Reduces Cell Adhesion by Inhibiting Rap1-GTP through Crk-C3G Pathway, in preparation

ABSTRACT OF THE DISSERTATION

Regulation of Cell Adhesion and Cell Death: the Roles of c-Abl Tyrosine Kinase and Retinoblastoma Protein

by

Xiaodong Huang

Doctor of Philosophy in Biology

University of California, San Diego, 2007

Professor Jean Y. J. Wang, Chair
Professor Tony Hunter, Co-Chair

The c-Abl kinase shuttles between the nucleus and cytoplasm. In the nucleus, Abl is activated by DNA damage or TNF to induce apoptosis. To examine the mechanism by which Abl regulates apoptosis, we employed dimerization as a means to control Abl activity by fusing an FKBP domain to the N-terminus of Abl. We found mutational inactivation of the NLS abrogated cell death, whereas FKBP-Abl was more efficient than FKBP-AblNuk, a nuclear-exclusive Abl, in inducing apoptosis, suggesting that while the nuclear pool is required for apoptosis, the cytoplasmic pool cooperates once apoptosis program is initiated.

To find out how cytoplasmic Abl regulates cell adhesion, we made an *AbPP* gene that encodes an Abl protein that is constitutively activated. We stably transfected this gene into HEK293 cells under the control of a TET-on promoter. AblPP induction caused the host cells to detach from the supporting matrix in the presence of serum. We found that this was due to phosphorylation of CrkII by AblPP, leading to dissociation of the complex CrkII-C3G and loss of the GEF activity of C3G, resulting in the inactivation of Rap1 GTPase. The inactivation of Rap1 caused a decrease of integrin affinity for fibronectin. We also found that the Rho-ROCK1 pathway activated by LPA or serum is required for the cell detachment. These two pathways function independently of each other, and also play a role in ephrin A1-induced PC3 cell detachment.

To further analyze the mechanisms of cell detachment induced by Abl, we employed shRNA library screening. We developed a new analytical strategy that combined quantitative microarray data with previous biological knowledge, i.e. Gene Ontology and pathway information, to increase the power of this technique. Using this strategy we identified 16 candidate shRNA-target genes associated with cell detachment induced by AblPP. Included in this set of genes was IL6ST, a membrane protein that we have experimentally confirmed.

We also found that the caspase-resistant Rb-MI protein caused type-1 cells defect in Bid cleavage despite caspase-8 activation. Inhibition of V-ATPase, which is essential in acidification of endosomes, specifically restored Bid cleavage in *Rb-MI* cells, thus sensitizing *Rb-MI* but not wild-type fibroblasts to TNF-induced apoptosis, and stimulated inflammation-associated colonic apoptosis in $Rb^{MI/MI}$ but not wild-type mice.

CHAPTER 1

Background

PROGRAMMED CELL DEATH

Cellular and tissue homeostasis reflects a dynamic balance of cell proliferation, differentiation and death. Programmed cell death (apoptosis) is a process of suicide by a cell in a multicellular organism, and involves an orchestrated series of biochemical events that leads to changes in characteristic cell morphology and eventually cell death [1].

Apoptosis is important during developmental processes in order to discard unneeded cells. For example, neurons and the immune system initially arise from highly proliferative cell populations. This overproduction is then followed by the death of those cells that fail to establish functional synaptic connections or productive antigen specificities [2, 3]. Mice that have had been genetically deleted of various key components of the apoptotic machinery show a characteristic set of developmental defects, including excess neurons in the brain.

Apoptosis also regulates adult tissue physiology. It is estimated that in the adult human body, around 1×10^{10} cells die by apoptosis each day [4]. Furthermore, apoptosis is essential during various developmental processes. During the development of red blood cells (erythropoiesis) more than 95% of the erythroblasts are eliminated as part of the routine operations of the bone marrow. Additionally, apoptosis is central to remodeling in the adult, such as the follicular atresia of the postovulatory follicle and past-weaning mammary gland involution [5].

The process of apoptosis is controlled by a diverse range of extracellular (extrinsic) or intracellular (intrinsic) signals [6]. Extracellular signals include hormones, growth factors, nitric oxide or cytokines, and therefore must either cross the plasma

membrane to induce a response. These signals may positively or negatively induce apoptosis. Intracellular apoptotic signaling is a response initiated by a cell in response to stress, and may ultimately result in cell suicide. The binding of nuclear receptors by glucocorticoids, heat, radiation, nutrient deprivation, viral infection and hypoxia are all factors that can lead to the release of intracellular apoptotic signals by a damaged cell.

Intrinsic cell death pathway

The intrinsic apoptosis pathways involve a variety of non-receptor-mediated stimuli that act directly on targets within the cell and involve mitochondria. The stimuli can behave either in a positive mode, such as damage to the genome, hypoxia, viral infections, and free radicals, or a negative mode, such as lack of growth or survival factors, hormones, and cytokines.

All of these stimuli cause changes in the inner mitochondrial membrane that result in mitochondrial outer membrane permeabilization (MOMP), loss of the mitochondrial transmembrane potential and release of two groups of normally sequestered pro-apoptotic proteins from the intermembrane space into the cytosol [7]. The first group consists of cytochrome c, Smac/DIABLO, and the serine protease HtrA2/Omi [8]. The released cytochrome c binds Apaf-1, a cytosolic protein; the binding of cytochrome c to the WD40 domain repeats generates a more open Apaf-1 conformation. The subsequent binding of dATP or ATP to the CARD domain then allows Apaf-1 to oligomerize, and to specifically recruit pro-caspase 9, to form a complex known as the apoptosome [9]. Activation of caspase-9 by the apoptosome can then activate other downstream caspases and trigger a cascade of events leading to apoptosis (Figure 1-1).

The second group of pro-apoptotic proteins, AIF, endonuclease G (Endo G) and caspase-activated DNase (CAD), are released from the mitochondria during apoptosis, but these are late events that occur after the cell has committed to apoptosis. AIF translocates to the nucleus and causes DNA fragmentation into 50-300 kb pieces and condensation of peripheral nuclear chromatin [10]. Endo G also translocates to the nucleus where it cleaves nuclear chromatin to produce oligonucleosomal DNA fragments [11]. CAD is subsequently released from the mitochondria and translocates to the nucleus where it leads to oligonucleosomal DNA fragmentation and a more pronounced and advanced chromatin condensation [12].

The control and regulation of intrinsic apoptotic pathways are largely performed by Bcl-2 family members, which can be either pro-apoptotic or anti-apoptotic, depending on their domain constitution [6]. To date, a total of 25 proteins have been identified in the Bcl-2 family [13]. The pro-apoptotic members are grouped into multi-domain pro-apoptotic proteins, which possess three out of four conserved, function-defining regions termed Bcl-2 homology (BH) domains; and BH3-only proteins, which possess only the amphipathic helix of the BH3 domain. Multi-domain pro-apoptotic proteins, including BAX and BAK, mediate cytochrome c release from the mitochondria as homo-oligomers; BH3-only proteins, such as BID and BAD, initiate the intrinsic apoptosis pathway by promoting BAX/BAK activation. The activity of BH3 proteins is subject to transcriptional control and post-translational modification. For example, PUMA and NOXA are induced by p53. BAD is activated by phosphorylation in response to a lack of survival signals and BID is converted to its active form (tBID) via caspase cleavage upon death receptor triggering [13, 14].

The activity of BAX and BAK is negatively regulated by the anti-apoptotic members of the Bcl-2 family, including Bcl-2, Bcl-X_L and MCL-1, A1, and Bcl-W, which have homology in all four BH domains. The founding member of the Bcl-2 family, the Bcl-2 proto-oncoprotein identified in B-cell lymphomas, was found to block apoptosis following multiple physiological and pathological stimuli [15, 16]. Accordingly, Bcl-2 deficient mice display excessive apoptosis of lymphocytes in thymus and spleen [17]. Anti-apoptotic Bcl-2 proteins are thought to bind and sequester BH3-only proteins to prevent BAX/BAK activation, and to directly bind to BAX and BAK to keep them in their inactive conformation [18, 19] (Figure 1-1). Because of the mutual inhibition of Bcl-2 and BH-3 only proteins, the ratio of these molecules within a cell is a crucial determinant of the cells susceptibility to intrinsic death signals. The cells doubly-deficient for BAX and BAK are resistant to all stimuli that trigger death via the mitochondrial apoptosis pathway [20, 21]. This supports the notion that BAX and BAK are a requisite gateway to the intrinsic apoptosis pathway [6, 21].

Since there are multiple pro- and anti-apoptotic Bcl-2 family members, a question arised is whether these proteins are redundant, or each of them has different functions. Recently, short peptides of the α helical BH3 domains provided evidence for a two-class model in which BAD-like BH3 regions occupy anti-apoptotic pockets serving as ‘sensitizing’ domains capable of displacing BID-like ‘activating’ domains which induce the oligomerization, activation of BAX and BAK, suggesting the different members have different functions.

Extrinsic cell death pathway

The extrinsic cell death pathway, also known as death receptor-induced apoptosis, is initiated by a death receptor on the plasma membrane such as the tumor necrosis factor (TNF) receptor superfamily [22] (Figure 1-2). Members of the TNF receptor family share similar cysteine-rich extracellular domains and have a cytoplasmic domain of about 80 amino acids called the 'death domain (DD)' [23]. This death domain plays a critical role in transmitting the death signal from the cell surface to the intracellular signaling pathways. To date, the best characterized death receptor family members include FAS (also known as APO-1 or CD95), TNF receptor 1 (TNFR1), DR3, DR4, DR5, and TRAIL (TNF-related apoptosis inducing ligand) receptor 1 and 2 [23].

The elucidation of events that define the extrinsic apoptosis is best characterized with the TNF-α/TNFR1 model. The binding of TNF-α to TNF receptor results in trimerization of receptor molecules or conformational changes in pre-formed receptor trimers [24]. In both situations, the adaptor protein TRADD and serine kinase RIP1 are recruited to TNFR1. However, this event does not initiate the death-inducing signaling complex (DISC) assembly at the plasma membrane. Instead, the TNFR1-DISC complex is detected in the endosomal fraction under conditions of synchronized endocytosis in several cell types. A cytosolic DISC free of TNFR1 has been observed in a human fibrosarcoma cell line that ectopically expresses a constitutive inhibitor of NF-κB. In this fibrosarcoma cell line, two distinct signaling complexes were identified. Complex-1 contains TNFR1, TRADD, RIP1, TRAF-2 and mediates NF-κB activation. This membrane complex appears to be further processed to recruit FADD through TRADD resulting in the formation of complex-2, *i.e.*, the DISC complex, which dissociates from TNFR1 and accumulates in the cytosol. FADD then associates with procaspase-8 via

dimerization of the death domain, resulting in the auto-catalytic activation of caspase-8/10 [25]. Once activated, caspase-8 further activates effector pro-caspases 3 and 7, thus initiating apoptosis. In this model, the balance between complex-1 and complex-2 rests with cFLIP, a homology and inhibitor of caspase-8. When the NF-κB pathway is activated, cFLIP is expressed to block caspase-8 activity, and complex-2 cannot be formed. Only when complex-1-mediated NF-κB pathway is insufficient, can the apoptosis-inducing complex-2 be formed (Figure 1-2) [25].

Depending on the biochemical milieu, however, direct effector caspase activation by caspase-8 varies in efficiency and is in certain cell types not sufficient for apoptosis execution. In these cells, sometimes referred to as type-2 cells, cleavage of the Bcl-2 family protein BID by death receptor-activated caspase-8 is required for apoptosis [26]. Upon cleavage, the truncated BID (tBID) translocates to the mitochondria to induce cytochrome c release via BAX/BAK oligomerization. In this way, the death receptor-initiated apoptotic response can be executed via the intrinsic apoptosis pathway. Thus, the extrinsic apoptosis pathway can initiate the caspase cascade both directly, via death receptor-induced formation of caspase-8 activating scaffolding complexes, as well as indirectly via caspase-8 mediated cleavage of BID, which activates the mitochondria pathway of caspase activation (Figure 1-2) [26].

Execution of cell death

The intrinsic and extrinsic pathways both end up at the point of the execution phase. Effector caspases activate cytoplasmic endonucleases, which degrade nuclear material, and proteases that degrade the nuclear and cytoskeletal proteins. Caspase-3,

caspase-6, and caspase-7 function as effector caspases, cleaving various substrates including cytokeratins, poly ADP ribose polymerase (PARP), gelsolin, etc., that ultimately cause the morphological and biochemical changes seen in apoptotic cells [27]. Caspase-3 is considered to be the most important executioner caspase and is activated by many of the initiator caspases, including caspase-2, caspase-8, caspase-9, and caspase-10 [27].

DNA condensation is a hallmark of apoptotic cells, and this is induced by the caspase-activated DNase (CAD). In proliferating cells, CAD forms a complex with its inhibitor, ICAD (inhibitor of CAD). Once the apoptosis program is initiated, the activated caspase-3 cleaves ICAD to release CAD, allowing CAD to translocate into nucleus [28]. CAD then degrades chromosomal DNA within the nucleus, causing the characteristic 'DNA ladder' seen in apoptotic cells.

The engulfment process is the last step of apoptosis. Normally, most phosphotidylserine is kept in the inner plasma membrane by aminophospholipid translocase. Early in apoptosis, aminophospholipid translocase is blocked, while a hypothetical scramblase is activated, so that phosphatidylserine asymmetry is lost, and phosphatidylserine is exposed on the cell surface [29]. The appearance of phosphatidylserine on the outer leaflet of apoptotic cells then facilitates noninflammatory phagocytic recognition, allowing for their early uptake and disposal. This process of early and efficient uptake with no release of cellular constituents, results in essentially no inflammatory response [29].

Regulation of apoptosis pathways

The process of apoptosis is subject to intricate regulation in multiple ways. Generally, apoptosis is counteracted by the parallel activation of survival pathways. Thus, the decision between survival and apoptosis results from the integration of multiple signals received by the cell. One important way of regulating the initiation of apoptosis is transcriptional and post-translational control of pro- and anti-apoptotic proteins. A critical control point in the intrinsic cell death pathway in mammals is the activity of pro-apoptotic and anti-apoptotic members of the aforementioned Bcl-2 protein family (Figure 1-1) [6].

A family of inhibitors of apoptosis proteins (IAPs) was initially identified in baculoviruses where they prevent apoptosis of the infected host cells, thus allowing time for viral replication [30]. The cellular counterparts of these proteins control caspase activity downstream of cytochrome c release [31]. Similar to Bcl-2 family proteins, IAPs are subject to transcriptional regulation and post-translational modifications. Wang *et al.* have shown that IAPs are induced by survival signals through activation of the NF-κB group of transcription factors [32]. Although all IAPs are characterized by zinc-binding baculoviral IAP repeat (BIR) domains, only a subset of IAPs has anti-apoptotic activity including c-IAP-1, c-IAP-2 and XIAP, which inhibit the activity of caspase-3, -7 and -9 [33, 34].

In mammals, the inhibition of caspases by IAPs is antagonized by binding of Smac/DIABLO and Omi/HtrA2, two mitochondrial proteins released during apoptosis (Figure 1-1) [8, 35, 36]. Both molecules possess a conserved N-terminal IAP binding motif (IBMs) (Ala-Val-Pro-Ile) [37, 38]. While Smac/DIABLO binds IAPs, thereby

preventing them from targeting caspases [38], Omi/HtrA2 is a serine protease that neutralizes IAPs, presumably by cleavage [39]. Thus, the balance between IAPs and IAP antagonizing proteins (Smac, Omi) is an important control factor for effector caspase activation.

There is a balance between cell death and survival in death receptor-induced apoptosis too. The activation of initiator caspases by death receptors is regulated by the expression of c-FLIP [40], which is a caspase-8 molecules homolog that lacks the catalytic cysteine, but can form hetero-dimers with caspase-8 that are catalytically active [41]. There are two isoforms of c-FLIP, c-FLIP-long and c-FLIP-short, both of which are able to form hetero-dimers with caspase-8 at the DISC and thereby block the processing and activation of this initiator caspase (Figure 1-2) [25]. Sohn *et al.* have found that proteasome inhibitors such as MG132 can block death receptor-induced cell death. The expression analysis suggested that c-FLIP is degraded through the proteasome pathway after TNF treatment, thus blocking c-FLIP degradation by proteasome inhibitor treatment substantially reduces caspase-8 activation at the DISC after treatment with TNF [42]. In addition, the very first step of the extrinsic apoptosis pathway - the activation of a death receptor - can be inhibited by the expression of decoy receptors - extracellular, truncated versions of death receptors that compete with receptors on the cell surface for ligand binding [43], and this further complicates the regulation of death receptor-induced apoptosis.

ANOIKIS

In contrast to transformed cells, normal cells only proliferate and differentiate in the correct context within a tissue. Cells sense their location through interactions with the proteins within the extracellular matrix (ECM) as well as neighboring cells. In the absence of proper attachment, many types of cells will activate a special type of death program termed anoikis [44]. Since single epithelial cells *in vivo* can potentially develop into cancer cells, getting rid of those cells by anoikis is a way to protect the whole body. However, metastatic tumor cells may escape from anoikis and invade other organs by perturbing their ECM [45].

Integrin signaling plays important role in cell survival

Integrins are the major cellular receptors for proteins within ECM. They are composed of two membrane-spanning polypeptide chains: an α chain and a β chain, both of them have an extracellular domain, a single transmembrane helix and a small cytoplasmic domain. At least 8 β and 18 α subunits have been identified, which assemble into 24 distinct integrins [46]. Integrins play an important role in adhesion of cells to ECM. They transmit signals from external environment to inside of cells, therefore function similarly to growth factor receptors. Both types of receptors activate many common downstream pathways, which are critical to keep cells alive. Besides the classic outside-in signaling pathways, signals from inside of the cells that change conformation of the cytoplasmic domains of integrins can be relayed to proteins in ECM, and either increase or decrease the affinity of integrins for ligands [47, 48]. Since most cellular

responses to growth factors are dependent on the cell's ability to adhere to substrate molecules via integrins, integrin-mediated adhesion regulates most signaling pathways that control apoptosis in growth factor-mediated survival, DNA damage responses and death receptor-mediated apoptosis [46].

Different integrins activate distinct outside-in signaling cascades (Figure 1-3). These signaling pathways generated by contact with the ECM proteins have profound effects on cells. For example, activation of some integrins leads to the recruitment of cytoplasmic protein kinases, including Src. One of the downstream effectors of Src kinase following integrin engagement is the focal adhesion kinase (FAK), which interacts with a variety of signaling and adaptor molecules, including PI3K, paxillin, and p130CAS, and has been linked to a number of signaling pathways controlling migration, proliferation and apoptosis [49]. In addition, the Src family kinases Fyn and Yes can also be recruited to the activated integrin molecules via an interaction with caveolin, which can then activate the classical ERK-MAPK pathway by recruiting Shc, Grb2, and Sos [50]. Furthermore, integrin-linked kinase (ILK) is also recruited to adhesion sites, and has been implicated in survival signaling [51].

Role of the cytoskeleton in anoikis

Adhesion to the correct ECM is necessary but not sufficient to provide a survival signal. Cell adhesion, spreading and cell shape also have a profound influence on the phenotype. These characteristics are all controlled by the cytoskeleton and its connections with integrins at cell/ECM and cell/cell junctions.

The link between anoikis and cytoskeleton is best illustrated by two proapoptotic Bcl-2 family member, BIM [52, 53] and BMF [54]. In normal cells, BIM protein is sequestered by microtubule-associated-dynein light chain-1 (DLC-1). When released from this sequestration upon treatment with taxol, a microtubule-disrupting agent, BIM interacts directly with Bcl-2 and stimulates release of cytochrome c from mitochondria [53]. Similarly, BMF is sequestered by the actin/myosin-associated dynein light chain-2 (DLC-2) in MCF7 cells. Cell suspension, cytochalasin treatment or UV-irradiation all induce the release of BMF from DLC-2, to allow BMF to complex with and neutralize Bcl-2 [54]. Interestingly, release of these two proteins occurs independently of caspase activation, thus they may regulate the initial stages of apoptosis, by serving as sensors for cytoskeleton integrity.

Gelsolin is an F-actin-severing protein. Cleavage of gelsolin also contributes to the death phenotype [55, 56]. The *in vitro* experiments suggested that full-length gelsolin prevents the BAX-stimulated release of cytochrome c, while the cleavage of gelsolin by caspase appears to be pro-apoptotic. Furthermore, when the neutrophils from gelsolin-deficient mice are exposed to TNF-α, they show a delay in blebbing phenotype [56]. Taken together, these findings suggest that cleavage of gelsolin by caspases contributes to the cytoskeleton alterations.

The intrinsic and extrinsic pathways of anoikis

Anoikis has been proposed to be regulated by both the intrinsic and extrinsic pathways. In the intrinsic pathway, caspase activation occurs as a consequence of mitochondrial permeabilization, which is regulated by the Bcl-2 family members [6]. The

extrinsic pathway is initiated by the ligation of death receptors on the cell surface and recruiting of different proteins to form the DISC complex to activate caspase-8 [57].

A lot of studies have indicated that anoikis proceeds through the intrinsic pathway. For example, the proapoptotic proteins BAX and BAK are activated following detachment of cells from ECM. In mammary epithelial cells, BAX translocates from the cytosol to the outer mitochondrial membrane (OMM) within 30 minutes after detachment from the ECM [58, 59]. This is accompanied by the exposure of N-terminal epitopes of BAX, indicating its switch from the inactive to proapoptotic conformation [60]. However, how detachment activates BAX and BAK is still not clear. Current data suggest that BH3-only proteins are likely to be involved. These proteins include NOXA and PUMA, which are transcriptionally regulated by p53; BIM and BAD can be controlled by the PI3-kinase and ERK pathways, and BID may be cleaved in the death receptor pathway. Another aforementioned BH3-only protein, BMF, has also been implicated in anoikis through its interaction with the myosin V motor complex, although further evidence is required to show it is activated in a causative way following detachment from the ECM [54].

Anoikis requires OMM permeabilization as it can be blocked by overexpression of Bcl-2 anti-apoptotic protein, in epithelial cells, but some studies have suggested that the initiating event is the activation of a death receptor, as overexpression of a dominant-negative form of FADD inhibits anoikis [61, 62]. Furthermore, it has been reported that anoikis in HUVEC cells requires interactions between the endogenous death receptor FAS and its cognate Fas ligand, further suggesting the extrinsic pathway is involved in anoikis [63]. However, extracellular inhibitors of death receptors failed to inhibit anoikis.

Furthermore, the detachment-induced activation of caspase-8 was inhibited by Bcl-2 overexpression, suggesting that caspase-8 activation occurs as a downstream event of the activated intrinsic pathway. Lastly, although extensive attempts have been tried from a number of laboratories to document the assembly of the DISC complex in detached epithelial cells, so far there is no evidence to suggest that this complex has been formed during anoikis [61]. Taken together, these data suggested that anoikis is probably performed by the cooperation of intrinsic and extrinsic pathways.

REGULATION OF ABL TYROSINE KINASE

The *c-Abl* proto-oncogene was isolated as the cellular counterpart to the Abelson murine leukemia virus oncogene, *v-abl* [64]. Its encoded protein, the Abl non-receptor tyrosine kinase is essential to the proper development of mice because homozygous deletion of mouse *c-abl* gene results in neonatal lethality [65, 66]. The surviving mice usually develop thymic and splenic atrophy and a T and B cell lymphopenia [65, 66]. Because the $abl^{-/-}$ mice show low penetrance and are pleiotropic, the exact physiologic role of Abl protein remains to be solved. There is also an *Abl*-related gene (*Arg*) in the mammalian genome [67]; although the knockout of *arg* gene did not cause any developmental defects, the combined ablation of *abl* and *arg* leads to an earlier embryonic lethality (E9-11) [68], suggesting there might be a functional redundancy between Abl and Arg proteins during early developmental stage.

The Abl tyrosine kinase family consists of two Abl isoforms, designated as type I and type IV in mice (type 1a and 1b in human) (Figure 1-4). The type IV isoform

contains a myristoylation site at the very N-terminus [69, 70]. The N-terminus of Abl contains 'CAP' region, SH3, SH2, and kinase domain, and is highly conservative with Src tyrosine kinase. The C-terminus of Abl contains a DNA-binding domain [71] and an F-actin binding domain (FABD) [72, 73]. Interestingly, the Abl protein also contains three nuclear localization signals [74] and a nuclear export signal [75], suggesting that Abl can shuttle between nucleus and cytoplasm (Figure 1-4, 1-5). Indeed, Abl kinase is ubiquitously expressed at multiple subcellular organelles, including nucleus, cytoplasm, mitochondria, the endoplasmic reticulum (ER) and the cell cortex, where Abl kinase interacts with a variety of cellular proteins, including signaling adaptors, kinases, transcription factors and cytoskeletal proteins [76].

The overall structure of Abl is tightly controlled through autoinhibition, which relies on a complex set of intramolecular interactions that involve the SH3 and SH2 domains, the CAP region, the myristoyl group, the SH3-SH2 linker, the SH2-kinase-domain linker, and the kinase domain [69, 70, 77-79]. Furthermore, the tyrosine kinase activity of Abl is inhibited by F-actin *in trans*, and the FABD of Abl is necessary for F-actin-mediated inhibition of its kinase activity, suggesting that trans-inhibition is mediated through direct binding to F-actin, which may enforce the folding of Abl into the inactive conformation [80].

The SH3 and SH2 domains of Abl protein interact with the two lobes of the kinase domain. The SH3-N-lobe assembly requires the SH2-kinase linker since the PXXP-binding surface of SH3 contacts the $_{242}$PTIY$_{245}$ sequence in this linker [81, 82]. Thus, the SH2-kinase linker functions as an internal scaffold to hold the SH3 domain and the N-lobe in place. The very N-terminal of CAP region in Abl-IV, but not in Abl-I

protein bears a myristoyl group. The C-lobe of the kinase domain has a hydrophobic pocket for insertion of the myristoyl group. Burial of the myristoyl group within the kinase domain induces a specific C-lobe conformation of kinase domain, which is important for the SH2-C-lobe assembly. In its absence, rearrangement of two helices that border the hydrophobic pocket destroys the docking surface for the SH2 domain. Thus, removal of the myristoyl group unlocks the clamp by destabilizing the SH2-C-lobe interaction [69]. Although Abl-I protein does not have the myristoyl group, deletion of its N-terminus can still activate its kinase activity, it is proposed that myristoyl group or some other fatty acids may be added *in trans* to assemble the auto-inhibited conformation [69].

Nuclear Abl is involved in apoptosis induced by DNA damage

Abl protein can be activated by a variety of stimuli (Table 1). In the nucleus, Abl tyrosine kinase activity can be stimulated by physiological and pharmacological agents that induce apoptosis (Figure 1-5). DNA damage inducers such as cisplatin and ionizing radiation preferentially activate the nuclear pool of Abl kinase. The activation of nuclear Abl kinase by ionizing radiation requires functional ATM kinase [83]. Furthermore, tumor necrosis factor can also activate Abl kinase activity [84]. The activation of nuclear Abl has been shown to induce cells to undergo apoptosis. For example, transient transfection of Abl in NIH3T3 cells weakly activates apoptosis in about 10% of transfected cells [85]. However, the molecular basis by which Abl contributes to apoptosis is not completely understood. The tumor suppressor p53 has been speculated to be the immediate downstream effector of Abl in Abl-induced apoptosis. However, a

functional interaction between Abl and p53 *in vivo* remains to be proved [86]. In contrast, p73, a p53 family member, has been proved to be the downstream effector of Abl by genetic evidence [87-89]. It has been proved that cisplatin can induce the accumulation of p73 protein in wild type mouse embryonic fibroblasts, but not in Abl-deficient cells, while the induction of p53 can occur without functional Abl, demonstrating an essential role of Abl in regulation of p73 protein by DNA damage [87]. It has also been proposed that p73 is a substrate of the Abl kinase and that the ability of Abl to phosphorylate p73 is markedly increased by gamma-irradiation [88]. Abl has also been shown to interact through its SH3 domain with the C-terminal homo-oligomerization domain of p73 and phosphorylates p73 on Y99 [89]. Furthermore, Vella *et al.* have found that in some p73α-expressing cancer cells, Abl is excluded from the nucleus, demonstrating that the apoptotic function of Abl-p73 pathway can be controlled by the subcellular segregation of these two proteins and suggesting an alternative mechanism to inactivate the p73 tumor suppression function [90].

In addition to DNA damage, tumor necrosis factor-α (TNF-α) also activates nuclear Abl [84]. A specific inhibitor of Abl, STI-571, can partially block TNF-α-induced apoptotic response. The retinoblastoma protein (RB) inhibits the kinase activity of Abl by binding to the Abl kinase domain [91], and Chau *et al.* have found that caspase-dependent cleavage of Rb is required for TNF-α to activate the nuclear Abl [92]. It has been proposed that in most death receptor-induced extrinsic apoptosis pathways, the nucleus is largely dispensable for cell death, but the discovery that Abl, Rb, and p73 are all involved in TNF signaling pathway suggested that the nuclear events are also required for death receptor-induced cell death. Interestingly, both Abl and p73 can shuttle

between nucleus and cytoplasm [75, 93], but whether the shuttling of these proteins has functions in death receptor-induced apoptosis remains to be resolved.

The apoptotic function of Abl kinase is best illustrated by its oncogenic version, the BCR-Abl tyrosine kinase [94]. BCR-Abl kinase is constitutively activated through the formation of homo-oligomers mediated by a coiled-coil domain at the N-terminus of BCR [72]. Normally, BCR-Abl protein is localized exclusively to the cytoplasm, although it has three functional nuclear localization signals. In the cytoplasm, BCR-Abl activates Akt kinase and is anti-apoptotic [95]. Vigneri and Wang have showed that inhibition of the BCR-Abl tyrosine kinase by using STI571 and blocking nuclear export by using LMB can entrap the oncogenic BCR-Abl into nucleus. Following reactivation of the kinase activity of BCR-Abl in the nucleus, the classic apoptosis markers, such as the activation of caspases, DNA laddering, and the appearance of phosphatidylserine on the cell surface could be observed [94], suggesting BCR-Abl is pro-apoptotic in nucleus.

Cytoplasmic Abl regulates cytoskeleton

Studies of BCR-Abl have made important contributions to the understanding of the function of the cytoplasmic pool of Abl kinase. Besides upregulating mitogenic and anti-apoptotic pathways [96], BCR-Abl phosphorylates several focal adhesion proteins and promotes dramatic changes in the actin cytoskeleton, leading to increases in cell migration, membrane ruffling and filopodial extension [97]. The cytoplasmic Abl also binds to F-actin through a conserved F-actin-binding domain (FABD) at the extreme C-terminus, suggesting it may also regulate cytoskeletal rearrangement [72]. Indeed, it has been found that during cell spreading over fibronectin-coated surfaces, Abl protein

promotes an increased number of F-actin microspikes and filopodia, allowing them to persist for longer periods of time on the surface of cells relative to cells lacking Abl [98]. Although the exact function of these structures are unknown, it is suggested that they likely to serve as sensors, being used by the cell to pick up spatial information about the nearby environment during the spreading process; thus Abl activity can prolong the exploratory phase of cell spreading [98]. Recently, the NMR structure of Abl protein has identified the critical residues of helix α-III that are responsible for F-actin binding and cytoskeletal association, and these interactions represent a major determinant for the cytoplasmic localization of Abl and BCR-Abl [99].

The kinase activity of Abl is increased by signals that stimulate F-actin rearrangement. These include ECM proteins, such as fibronectin, which promote cell spreading [100, 101], and growth factors such as PDGF, which induce membrane ruffling [102]. Fibronectin engagement of integrins stimulates the tyrosine kinase activity of Abl three- to five- fold in cultured fibroblasts. Normally, Abl is associated with F-actin at the cell perimeter of suspended cells, allowing Abl kinase to have an immediate effect on F-actin once activated by cell adhesion. Lewis *et al.* have shown that during the first 20-30 minutes of fibronectin stimulation, when Abl activity is the highest, the nuclear pool of Abl in 10T1/2 fibroblasts re-localizes transiently to focal adhesions; it was thought that this translocation could play a role in the activation of cytoplasmic Abl and that integrins may also regulate nuclear events through the translocation of nuclear Abl [100]. The localization of Abl to focal adhesion triggers the phosphorylation of several proteins, among them, is the protein paxillin. Although the physiological role of this

phosphorylation is still not clear, it has been suggested that it may behave as a docking site for the translocated Abl kinase [103].

Growth factors, such as PDGF and EGF can stimulate the kinase activity of a pool of Abl localized at the plasma membrane in fibroblasts. Treatment of mouse fibroblasts with PDGF increases the activity of Abl family kinases and is accompanied by F-actin-mediated membrane ruffling. However, Abl-deficient fibroblasts exhibit a reduced ruffling response, which can be rescued by the re-expression of Abl [102]. Although another tyrosine kinase, Src, which is also modestly activated by treatment of cells with PDGF, may act upstream of Abl stimulation by PDGF, the details of how PDGF stimulates Abl are still not clear [102]. Since tyrosine phosphorylation on Abl after PDGF treatment is not detected without pretreatment of cells with the tyrosine phosphatase inhibitor pervanadate, it is possible that a downstream substrate of Src is responsible for Abl activation by PDGF. Consistently, Src and Abl substrates (such as Abi) are susceptible to dephosphorylation by PTP-PEST phosphatase, and the activation of Abl by PDGF is prolonged in PTP-PEST-deficient fibroblasts [104]. Another study shows that phospholipase C-γ1 (PLC-γ1) and decreased levels of phosphatidylinositol (4,5)-bisphosphate (PIP2) are required for the activation of Abl kinase by PDGF, and expression of inositol pholyphosphate 5-phosphatase can also increase Abl activity [105].

Abl kinase promotes membrane ruffling but inhibits cell migration. Recently, Jin and Wang have found that through CrkII phosphorylation and in collaboration with dynamin-2, Abl protein can regulate the partitioning of Rac-GTP to favor dorsal ruffles during cell spreading, and thus this Abl-dependent dorsal membrane localization of activated Rac protein explains its positive role in ruffling and negative role in cell

spreading and migration [106]. The effects of Abl on cell motility contrast with those of BCR-Abl, since BCR-Abl stimulates both membrane protrusion and cell migration. This may due to the BCR moiety of BCR-Abl protein, which has a Dbl homology (DH) domain with GEF activity for Rho, Rac, and Cdc42 [107], thus BCR-Abl may have completely different regulating mechanisms than Abl protein.

THE RETINOBLASTOMA PROTEIN (RB) IS A REGULATOR OF BOTH PROLIFERATION AND APOPTOSIS

The retinoblastoma protein (RB), was the first tumor suppressor to be identified [108]. Germline mutation of the *RB* gene results in the development of retinoblastoma in early childhood [109]. The elimination of *RB* gene by gene targeting in mice was found to result in embryonic lethality (around embryonic day 13.5) and revealed additional functions of RB during development [110-112]. Furthermore, RB-null mutant embryos suffer from ectopic proliferation in the developing central nervous system (CNS), suggesting a role of RB in cell cycle regulation. Later on, it has been found that the active RB binds E2Fs and converts them into transcriptional repressors by recruiting chromatin-modifying factors such as histone deacetylases (HDAC) [113], SWI/SNF factors [114], methyltransferases [115], or polycomb group proteins [116]. Besides cell cycle regulation, RB protein also plays an important role in differentiation. For example, RB is necessary for the completion of the muscle differentiation and for myogenic helix-loop-helix-dependent transcription [117].

The RB family has three members: RB, p107, and p130. They share large regions of homology, especially in a bipartite region, which is called the 'pocket domain', and this domain is responsible for many of the protein-protein interactions during cell cycle. Besides E2F, RB also binds many other proteins with the LXCXE peptide motif, such as D-type cyclins [118], several DNA tumor virus proteins, such as SV40 large T antigen [119], and HDACs. Furthermore, RB family proteins can bind E2F and LXCXE protein at the same time, because the binding sites for them are distinct [120].

RB and cell cycle

Cyclin-dependent kinase and cyclins are the most important proteins involved in the cell cycle machinery. They form complexes during distinct phases of the cell cycle, and are specifically involved in the phosphorylation of different target proteins to orchestrate the advance of cell cycle. It has been demonstrated that the phosphorylation of RB by CDK/cyclin complexes is the underlying mechanism of cell cycle regulation (Figure 1-6, 1-7). More specifically, RB is unphosphorylated in G0 cells, hypophosphorylated after entrance into G1, and becomes hyperphosphorylated by cyclin D-CDK4/6 complexes in concert with advance of cells through the R point [118]. Once cells have passed through the R point, RB usually remains hyperphosphorylated throughout the remainder of the cell cycle [121]. The protein phosphatase type 1 (PP1) dephosphorylates RB once cells pass through and exit mitosis. The interaction between RB and E2F family transcription factors plays a central role in governing cell cycle progression and DNA replication by controlling the expression of E2F-regulated genes [113, 122]. RB protein has sixteen CDK phosphorylation sites, mutation of nine out of

them is required to create an RB variant (PSM-RB, phosphorylation site mutated RB) with constitutive growth suppressing function. PSM-RB lacks seven phosphorylation sites in the C-region and two phosphorylation sites in the insert region of RB [123]. PSM-RB is a potent inhibitors of proliferation in various cellular contexts [123-125].

RB also regulates the G1-S transition through E2F-independent mechanisms. It has been shown that RB can upregulate the expression of p27 and stabilize the p27 protein by binding the Skp2 protein and interfering with SCF-Skp2-p27 complex formation, thus avoiding p27 ubiquitination [126]. Furthermore, CDK inhibitors (CKIs) binding to the CDK/cyclin complex also affect the phosphorylation status of RB [127].

RB and cell death

Intriguingly, *RB*-null embryos also display massive apoptosis in the central nervous system (CNS) and exhibit defects in the terminal differentiation of myocytes and erythrocytes. These observations strongly indicated additional roles for RB in the process of terminal differentiation and apoptosis regulation [110-112]. The terminal differentiation of a progenitor cell into a quiescent post-mitotic cell is usually accompanied with the loss of its proliferative potential, a characteristic effectively preventing tumor development. Thus, the promotion of terminal differentiation, which has been confirmed in several contexts [128, 129], is another mechanism potentially contributing to the tumor suppressor activity of RB. At the same time, the phenotype of RB-deficient mice, which indicate that RB is normally required to inhibit apoptosis, seemed to contradict the well-established growth suppressing function of RB. Despite this apparent conundrum, several lines of evidence now support the ability of RB to

suppress apoptosis [113, 130]. For example, Masselli and Wang has shown that PSM-RB attenuated caspase activation by doxorubincin as a result of cell cycle arrest, while staurosporine caused RB-dependent G1 arrest or apoptosis; furthermore, PSM-RB stimulated the apoptotic response to TNF in Rat-16 cells, which mostly undergo necrosis in the absence of PSM-RB [131]. These results show that PSM-RB exerts disparate effects on apoptotic response to different stimuli, and that cell cycle arrest does not always associate with resistance to apoptosis.

In addition to changes in its phosphorylation status, regulated cleavage and degradation control the activity of the RB protein. RB is an effector caspase substrate and caspase cleavage induces its degradation during apoptosis [132]. Mutation of the C-terminal caspase cleavage site (Figure 1-7) generates a protein termed RB-MI (mutated in ICE-site) that is resistant to caspase cleavage and can suppress apoptosis in response to various stimuli [132-134]. The RB-MI mutation has moreover been introduced into the mouse *Rb* gene locus by gene targeting to create $RB^{MI/MI}$ 'knockin' mice [135]. The $RB^{MI/MI}$ mice do not have any detectable developmental or longevity defect. However, the RB-MI protein conferred tissue-specific protection from endotoxin-induced apoptosis in $RB^{MI/MI}$ mice. Moreover, fibroblasts derived from these animals were specifically protected from TNFR1-induced apoptosis, but not to apoptosis induced by DNA damage [135, 136]. These observations indicate that elimination of RB is a prerequisite in some apoptosis pathways. Since RB protein also has growth suppressing activity, the question here is whether the apoptosis suppression by RB is connected to its growth suppressing activity. E2F family transcription factors also initiate transcription of some pro-apoptotic proteins, such as Apaf-1 and caspase-3 [137]. These data suggest that RB controls

developmental apoptosis by suppressing the transcription of E2F regulated pro-apoptotic genes. On the other hand, RB is able to block the TNF-induced apoptosis pathway, which is independent of transcription [130, 136]. Furthermore, it has been shown that the cleavage of RB is an upstream event of Bid cleavage in TNF-induced cell death, and blocking cleavage of RB by RB-MI can protect type-2, but not type-1 cell death [136]. However, the underlying mechanisms of RB protection to type-2 cell death induced by TNF remain to be determined.

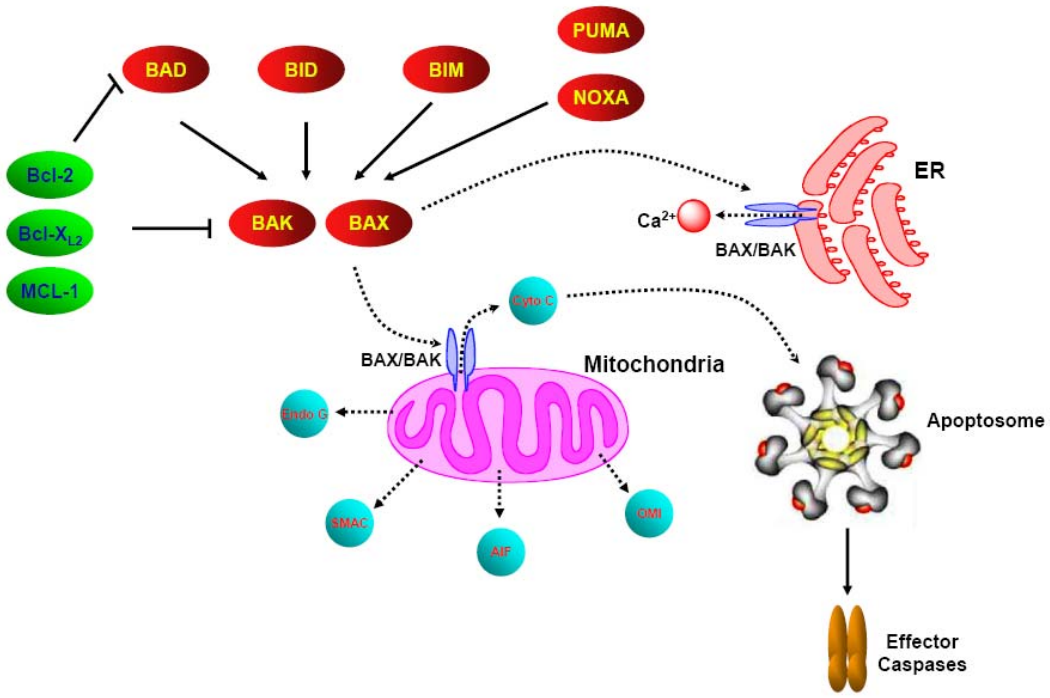

Figure 1-1: The intrinsic apoptosis pathway.
Various cellular stresses and developmental death cues induce the release of cytochrome c from mitochondria via the activation of pro-apoptotic members of the Bcl-2 family. Different pro-apoptotic BH3-only proteins (*e.g.* BAD, BIM, BID, PUMA, and NOXA) bind to anti-apoptotic Bcl-2-family members (Bcl-2, Bcl-X_L) and prevent them from interacting with BAX or BAK, two pro-apoptotic proteins that oligomerize and promote cytochrome c release from the mitochondria. Cytosolic cytochrome c triggers apoptosome formation and activation of pro-caspase-9, which in turn activates effector caspases. Caspase activation is inhibited by IAP proteins, which are counteracted by pro-apoptotic proteins that are released from the mitochondria (Smac, Omi). Additional proteins (Endo G, AIF) released from the mitochondria promote caspase-independent cell death pathways.

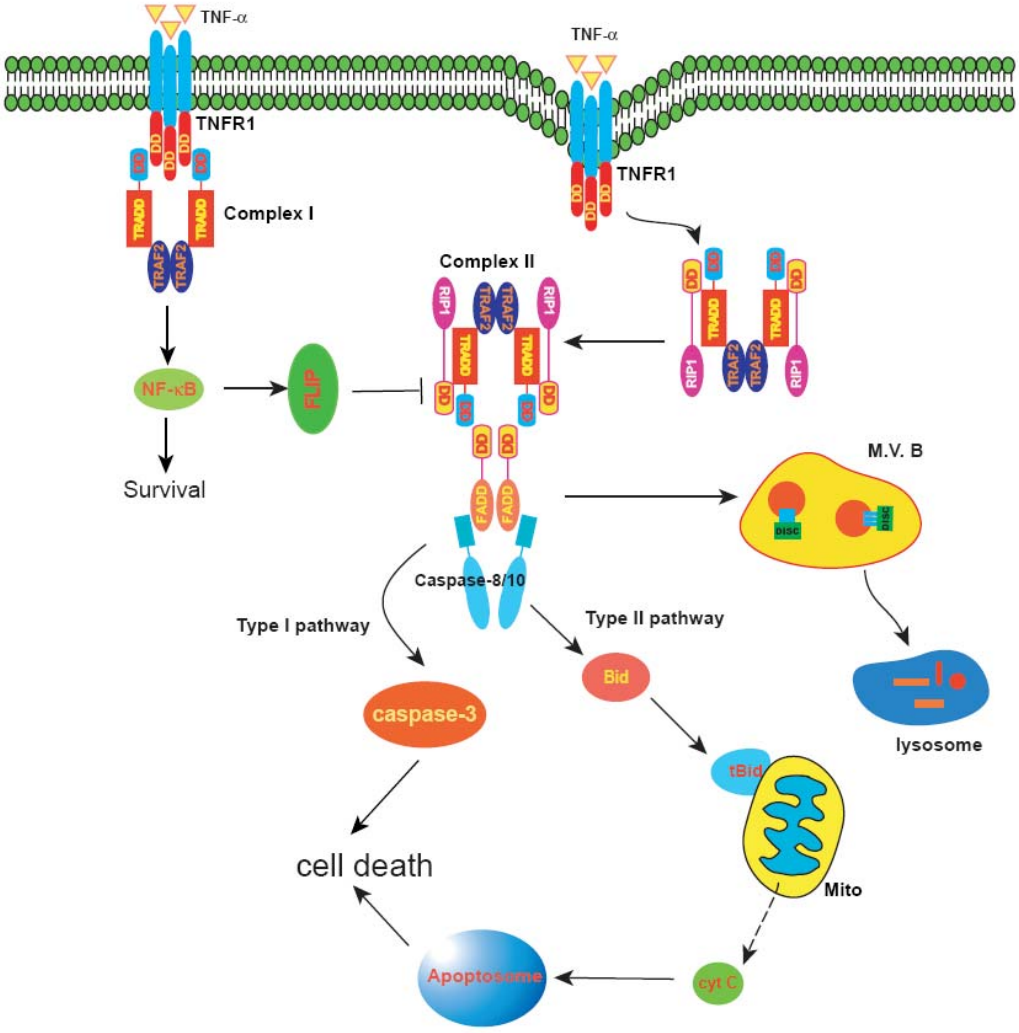

Figure 1-2: TNFR1 signaling pathways.
Engagement of TNF with TNFR1 results in the formation of a receptor-proximal complex containing the adaptor proteins TRADD, RIP1 and TRAF-2, which in turn recruit c-IAP proteins and IKK. This signaling complex (complex-1) initiates NF-κB activation and transcription of anti-apoptotic genes such as IAP and FLIP. A second complex (complex-2) based on TRADD, RIP1 and TRAF-2 is formed in the cytosol and recruits FADD and pro-caspase-8/10. Caspase-8 activation in this complex initiates the apoptotic caspase cascade. Caspase-8 activation is inhibited by NF-κB-induced expression of FLIP and other anti-apoptotic proteins. DISC complex may also go to MVB pathway and be degraded in lysosome.

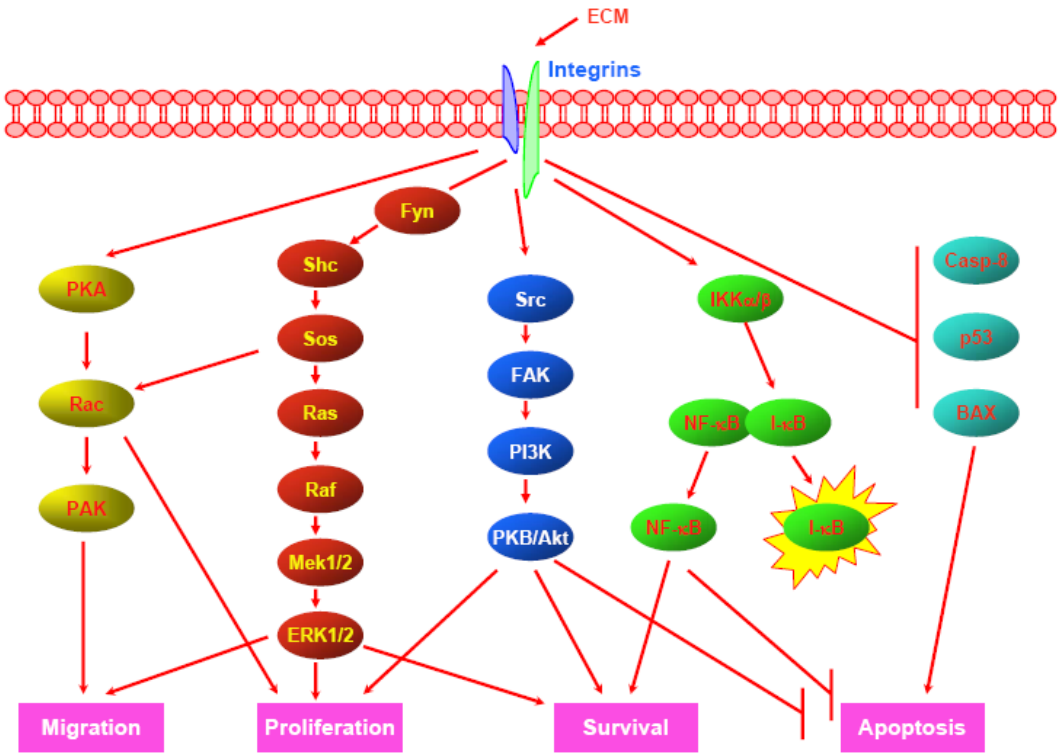

Figure 1-3: The major integrin signaling pathways.
Integrin ligation activates four major signaling pathways: the Rac GTPase, the MAPK, PI-3K-PKB/Akt and the NF-kB pathways. These pathways generate essential signals for cell migration, proliferation, survival, and apoptosis.

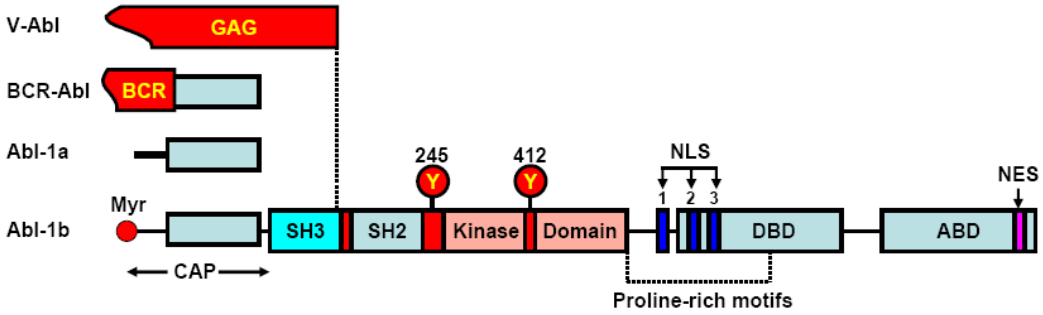

Figure 1-4: Structures of Abl protein and its variants.
Human Abl has two alternative N-termini, Abl-1a and Abl-1b. Abl-1b is myristoylated (Myr). The CAP region contains the variable N terminus and has a role in auto-inhibition. Phosphorylation at Tyr 245 in the SH2-kinase linker region, or Tyr 412 at the kinase domain, can activate Abl kinase. NLS, nuclear localization signal; NES, nuclear export signal; DBD, DNA-binding domain; ABD, actin-binding domain. Oncogenic v-Abl and BCR-Abl are N-terminal mutants of c-Abl. In v-Abl, the viral Gag sequence is fused to Abl at the SH3-SH2 linker. In BCR-Abl, cellular BCR sequence is fused to Abl in the CAP region.

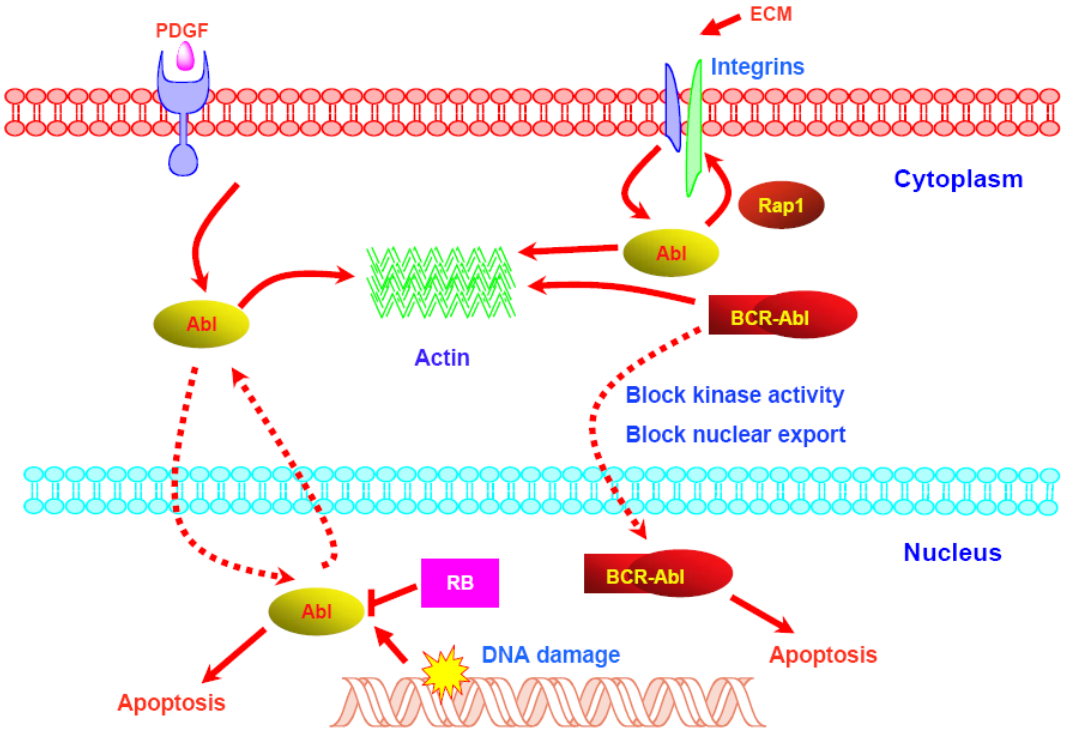

Figure 1-5: Nuclear and cytoplasmic Abl have distinct functions.
Cytoplasmic Abl is activated by growth factors such as PDGF and FGF, or binding of integrins with ECM proteins. Activation of cytoplasmic Abl is involved in cytoskeletal rearrangement. Nuclear pool of Abl is activated by DNA damage and the activation of nuclear Abl can induce cells to undergo apoptosis.

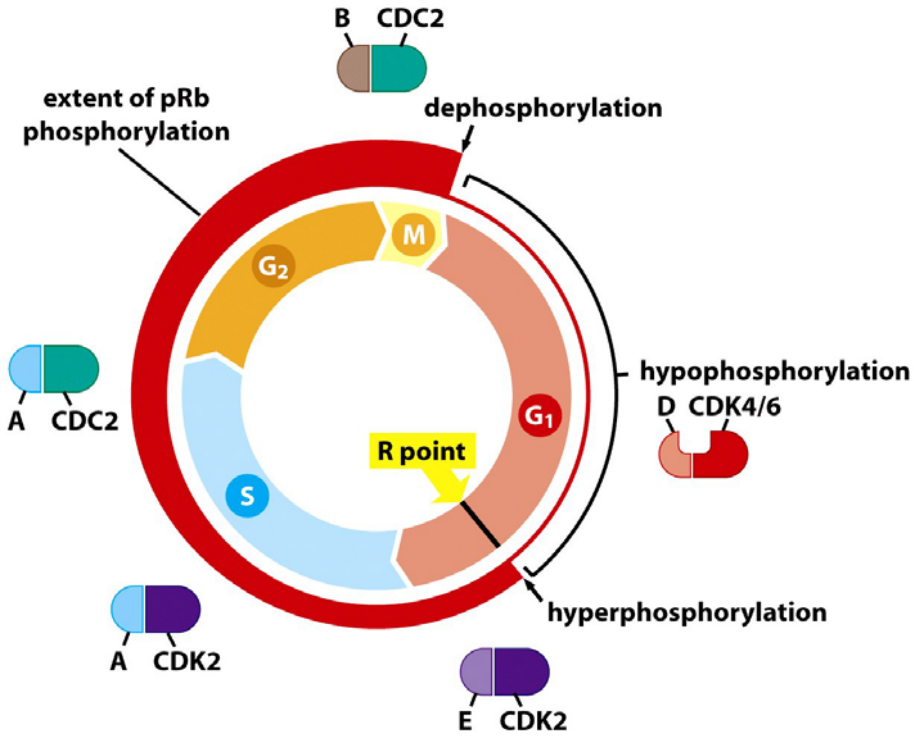

Figure 1-6: Inhibition of cell cycle progression by RB.
Hypophosphorylated RB binds the E2F transcription factor, a hetero-dimer of DP and E2F, and recruits chromatin-modifying enzymes to form a complex, which suppresses "S phase genes", whose transcription is required for DNA synthesis. Upon phosphorylation by CDKs in mid G1, RB dissociates from E2F, which then activates the transcription of S-phase genes. RB is re-activated through dephosphorylation at the end of mitosis (the figure is adapted from the Biology of Cancer, by Robert A. Weinberg).

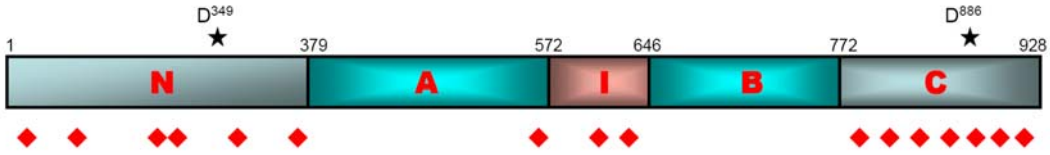

★ **Caspase-cleavage sites**

◆ **phosphorylation sites of CDK/cyclin complexes**

Figure 1-7: Domain structure of the Retinoblastoma protein.
The A and B pocket domains are shaded in blue; CDK phosphorylation sites are indicated by diamonds. Two conserved caspase consensus sites are indicated by stars, one - $DEAD^{886}G$- at the C terminus [133], the other - $DSID^{349}$- in the N-terminal domain [138].

Table 1-1: Signals that activate Abl tyrosine kinase.

Stimulus	Fold activation	Cell type	References
Ionizing radiation	~4	mouse thymocytes	[83]
DNA Damage	N.D.	NIH3T3, MCF-7 transfected with c-Abl	[87-89]
TNF	N.D.	U937	[84]
Ephrin B2	N.D.	MDA-MB-435c breast cancer cells	[139]
PDGF	1.3-3.5	NIH3T3 fibroblasts; 10T1/2 fibroblasts; Abl reconstituted *abl*$^{-/-}$ *arg*$^{-/-}$ MEFs	[102, 140]
EGF	1.7-3.3	10T1/2 fibroblasts overexpressing EGFR	[102]
HGF + collagen	1.5	Ca18/3 and WRO thyroid cancer cells	[141]
FN adhesion	1.9-6.8	NIH3T3 fibroblasts; 10T1/2 fibroblasts; Abl reconstituted *abl*$^{-/-}$*arg*$^{-/-}$ MEFs	[80, 98, 100]
CrkY221F expression	N.D.	HEK-293T overexpressing Abl and CrkY221F	[142]
Abi expression	N.D.	Drosophila S2 cells overexpressing Abl and Abi	[143]
H_2O_2	N.D.	COS-7, wild type and *Arg*-reconstituted *arg*$^{-/-}$ MEFs	[144, 145]

N.D., not determined

REFERENCES

1. Kerr, J.F., A.H. Wyllie, and A.R. Currie, *Apoptosis: a basic biological phenomenon with wide-ranging implications in tissue kinetics.* Br J Cancer, 1972. **26**(4): p. 239-57.

2. Nijhawan, D., N. Honarpour, and X. Wang, *Apoptosis in neural development and disease.* Annu Rev Neurosci, 2000. **23**: p. 73-87.

3. Opferman, J.T., et al., *Development and maintenance of B and T lymphocytes requires antiapoptotic MCL-1.* Nature, 2003. **426**(6967): p. 671-6.

4. Renehan, A.G., C. Booth, and C.S. Potten, *What is apoptosis, and why is it important?* Bmj, 2001. **322**(7301): p. 1536-8.

5. Lund, L.R., et al., *Two distinct phases of apoptosis in mammary gland involution: proteinase-independent and -dependent pathways.* Development, 1996. **122**(1): p. 181-93.

6. Danial, N.N. and S.J. Korsmeyer, *Cell death: critical control points.* Cell, 2004. **116**(2): p. 205-19.

7. Saelens, X., et al., *Toxic proteins released from mitochondria in cell death.* Oncogene, 2004. **23**(16): p. 2861-74.

8. Du, C., et al., *Smac, a mitochondrial protein that promotes cytochrome c-dependent caspase activation by eliminating IAP inhibition.* Cell, 2000. **102**(1): p. 33-42.

9. Adams, J.M. and S. Cory, *Apoptosomes: engines for caspase activation.* Curr Opin Cell Biol, 2002. **14**(6): p. 715-20.

10. Joza, N., et al., *Essential role of the mitochondrial apoptosis-inducing factor in programmed cell death.* Nature, 2001. **410**(6828): p. 549-54.

11. Li, L.Y., X. Luo, and X. Wang, *Endonuclease G is an apoptotic DNase when released from mitochondria.* Nature, 2001. **412**(6842): p. 95-9.

12. Enari, M., et al., *A caspase-activated DNase that degrades DNA during apoptosis, and its inhibitor ICAD.* Nature, 1998. **391**(6662): p. 43-50.

13. Cory, S. and J.M. Adams, *The Bcl2 family: regulators of the cellular life-or-death switch.* Nat Rev Cancer, 2002. **2**(9): p. 647-56.

14. Cory, S., D.C. Huang, and J.M. Adams, *The Bcl-2 family: roles in cell survival and oncogenesis.* Oncogene, 2003. **22**(53): p. 8590-607.

15. Vaux, D.L., S. Cory, and J.M. Adams, *Bcl-2 gene promotes haemopoietic cell survival and cooperates with c-myc to immortalize pre-B cells.* Nature, 1988. **335**(6189): p. 440-2.

16. McDonnell, T.J., et al., *bcl-2-immunoglobulin transgenic mice demonstrate extended B cell survival and follicular lymphoproliferation.* Cell, 1989. **57**(1): p. 79-88.

17. Veis, D.J., et al., *Bcl-2-deficient mice demonstrate fulminant lymphoid apoptosis, polycystic kidneys, and hypopigmented hair.* Cell, 1993. **75**(2): p. 229-40.

18. Cheng, E.H., et al., *BCL-2, BCL-X(L) sequester BH3 domain-only molecules preventing BAX- and BAK-mediated mitochondrial apoptosis.* Mol Cell, 2001. **8**(3): p. 705-11.

19. Martinou, J.C. and D.R. Green, *Breaking the mitochondrial barrier.* Nat Rev Mol Cell Biol, 2001. **2**(1): p. 63-7.

20. Lindsten, T., et al., *The combined functions of proapoptotic Bcl-2 family members bak and bax are essential for normal development of multiple tissues.* Mol Cell, 2000. **6**(6): p. 1389-99.

21. Wei, M.C., et al., *Proapoptotic BAX and BAK: a requisite gateway to mitochondrial dysfunction and death.* Science, 2001. **292**(5517): p. 727-30.

22. Locksley, R.M., N. Killeen, and M.J. Lenardo, *The TNF and TNF receptor superfamilies: integrating mammalian biology.* Cell, 2001. **104**(4): p. 487-501.

23. Ashkenazi, A. and V.M. Dixit, *Death receptors: signaling and modulation.* Science, 1998. **281**(5381): p. 1305-8.

24. Chen, G. and D.V. Goeddel, *TNF-R1 signaling: a beautiful pathway.* Science, 2002. **296**(5573): p. 1634-5.

25. Micheau, O. and J. Tschopp, *Induction of TNF receptor I-mediated apoptosis via two sequential signaling complexes.* Cell, 2003. **114**(2): p. 181-90.

26. Scaffidi, C., et al., *Two CD95 (APO-1/Fas) signaling pathways.* The EMBO Journal, 1998. **17**: p. 1675-1687.

27. Nicholson, D.W. and N.A. Thornberry, *Caspases: killer proteases.* Trends Biochem Sci, 1997. **22**(8): p. 299-306.

28. Sakahira, H., M. Enari, and S. Nagata, *Cleavage of CAD inhibitor in CAD activation and DNA degradation during apoptosis.* Nature, 1998. **391**(6662): p. 96-9.

29. Zwaal, R.F., P. Comfurius, and E.M. Bevers, *Surface exposure of phosphatidylserine in pathological cells.* Cell Mol Life Sci, 2005. **62**(9): p. 971-88.

30. Crook, N.E., R.J. Clem, and L.K. Miller, *An apoptosis-inhibiting baculovirus gene with a zinc finger-like motif.* J Virol, 1993. **67**(4): p. 2168-74.

31. Kasof, G.M. and B.C. Gomes, *Livin, a novel inhibitor of apoptosis protein family member.* J Biol Chem, 2001. **276**(5): p. 3238-46.

32. Wang, C.Y., et al., *NF-kappaB antiapoptosis: induction of TRAF1 and TRAF2 and c-IAP1 and c-IAP2 to suppress caspase-8 activation.* Science, 1998. **281**(5383): p. 1680-3.

33. Salvesen, G.S. and C.S. Duckett, *IAP proteins: blocking the road to death's door.* Nat Rev Mol Cell Biol, 2002. **3**(6): p. 401-10.

34. Riedl, S.J. and Y. Shi, *Molecular mechanisms of caspase regulation during apoptosis.* Nat Rev Mol Cell Biol, 2004. **5**(11): p. 897-907.

35. Suzuki, Y., et al., *A serine protease, HtrA2, is released from the mitochondria and interacts with XIAP, inducing cell death.* Mol Cell, 2001. **8**(3): p. 613-21.

36. Verhagen, A.M., et al., *Identification of DIABLO, a mammalian protein that promotes apoptosis by binding to and antagonizing IAP proteins.* Cell, 2000. **102**(1): p. 43-53.

37. Hegde, R., et al., *Identification of Omi/HtrA2 as a mitochondrial apoptotic serine protease that disrupts inhibitor of apoptosis protein-caspase interaction.* J Biol Chem, 2002. **277**(1): p. 432-8.

38. Wu, G., et al., *Structural basis of IAP recognition by Smac/DIABLO.* Nature, 2000. **408**(6815): p. 1008-12.

39. Suzuki, Y., et al., *Mitochondrial protease Omi/HtrA2 enhances caspase activation through multiple pathways.* Cell Death Differ, 2004. **11**(2): p. 208-16.

40. Krueger, A., et al., *Cellular FLICE-inhibitory protein splice variants inhibit different steps of caspase-8 activation at the CD95 death-inducing signaling complex.* J Biol Chem, 2001. **276**(23): p. 20633-40.

41. Micheau, O., et al., *The long form of FLIP is an activator of caspase-8 at the Fas death-inducing signaling complex.* J Biol Chem, 2002. **277**(47): p. 45162-71.

42. Sohn, D., et al., *The proteasome is required for rapid initiation of death receptor-induced apoptosis.* Mol Cell Biol, 2006. **26**(5): p. 1967-78.

43. Igney, F.H. and P.H. Krammer, *Death and anti-death: tumour resistance to apoptosis.* Nat Rev Cancer, 2002. **2**(4): p. 277-88.

44. Frisch, S.M. and H. Francis, *Disruption of epithelial cell-matrix interactions induces apoptosis.* J Cell Biol, 1994. **124**(4): p. 619-26.

45. Douma, S., et al., *Suppression of anoikis and induction of metastasis by the neurotrophic receptor TrkB.* Nature, 2004. **430**(7003): p. 1034-9.

46. Hynes, R.O., *Integrins: bidirectional, allosteric signaling machines.* Cell, 2002. **110**(6): p. 673-87.

47. Giancotti, F.G., *Complexity and specificity of integrin signalling.* Nat Cell Biol, 2000. **2**(1): p. E13-4.

48. Ginsberg, M.H., A. Partridge, and S.J. Shattil, *Integrin regulation.* Curr Opin Cell Biol, 2005. **17**(5): p. 509-16.

49. Schwartz, M.A. and M.H. Ginsberg, *Networks and crosstalk: integrin signalling spreads.* Nat Cell Biol, 2002. **4**(4): p. E65-8.

50. Frisch, S.M. and R.A. Screaton, *Anoikis mechanisms.* Curr Opin Cell Biol, 2001. **13**(5): p. 555-62.

51. Grashoff, C., et al., *Integrin-linked kinase: integrin's mysterious partner.* Curr Opin Cell Biol, 2004. **16**(5): p. 565-71.

52. Strasser, A., et al., *The role of bim, a proapoptotic BH3-only member of the Bcl-2 family in cell-death control.* Ann N Y Acad Sci, 2000. **917**: p. 541-8.

53. Puthalakath, H., et al., *The proapoptotic activity of the Bcl-2 family member Bim is regulated by interaction with the dynein motor complex.* Mol Cell, 1999. **3**(3): p. 287-96.

54. Puthalakath, H., et al., *Bmf: a proapoptotic BH3-only protein regulated by interaction with the myosin V actin motor complex, activated by anoikis.* Science, 2001. **293**(5536): p. 1829-32.

55. Koya, R.C., et al., *Gelsolin inhibits apoptosis by blocking mitochondrial membrane potential loss and cytochrome c release.* J Biol Chem, 2000. **275**(20): p. 15343-9.

56. Kothakota, S., et al., *Caspase-3-generated fragment of gelsolin: effector of morphological change in apoptosis.* Science, 1997. **278**(5336): p. 294-8.

57. Wajant, H., *Death receptors.* Essays Biochem, 2003. **39**: p. 53-71.

58. Valentijn, A.J., et al., *Spatial and temporal changes in Bax subcellular localization during anoikis.* J Cell Biol, 2003. **162**(4): p. 599-612.

59. Gilmore, A.P., et al., *Integrin-mediated survival signals regulate the apoptotic function of Bax through its conformation and subcellular localization.* J Cell Biol, 2000. **149**(2): p. 431-46.

60. Wolter, K.G., et al., *Movement of Bax from the cytosol to mitochondria during apoptosis.* J Cell Biol, 1997. **139**(5): p. 1281-92.

61. Frisch, S.M., *Evidence for a function of death-receptor-related, death-domain-containing proteins in anoikis.* Curr Biol, 1999. **9**(18): p. 1047-9.

62. Rytomaa, M., L.M. Martins, and J. Downward, *Involvement of FADD and caspase-8 signalling in detachment-induced apoptosis.* Curr Biol, 1999. **9**(18): p. 1043-6.

63. Aoudjit, F. and K. Vuori, *Matrix attachment regulates Fas-induced apoptosis in endothelial cells: a role for c-flip and implications for anoikis.* J Cell Biol, 2001. **152**(3): p. 633-43.

64. Wang, J.Y., et al., *The mouse c-abl locus: molecular cloning and characterization.* Cell, 1984. **36**(2): p. 349-56.

65. Tybulewicz, V.L., et al., *Neonatal lethality and lymphopenia in mice with a homozygous disruption of the c-abl proto-oncogene.* Cell, 1991. **65**(7): p. 1153-63.

66. Schwartzberg, P.L., et al., *Mice homozygous for the ablm1 mutation show poor viability and depletion of selected B and T cell populations.* Cell, 1991. **65**(7): p. 1165-75.

67. Kruh, G.D., et al., *A novel human gene closely related to the abl proto-oncogene.* Science, 1986. **234**(4783): p. 1545-8.

68. Koleske, A.J., et al., *Essential Roles for the Abl and Arg Tyrosine Kinases in Neurulation.* Neuron, 1998. **21**(6): p. 1259-1272.

69. Hantschel, O., et al., *A myristoyl/phosphotyrosine switch regulates c-Abl.* Cell, 2003. **112**(6): p. 845-57.

70. Nagar, B., et al., *Structural basis for the autoinhibition of c-Abl tyrosine kinase.* Cell, 2003. **112**(6): p. 859-71.

71. Kipreos, E.T. and J.Y. Wang, *Cell cycle-regulated binding of c-Abl tyrosine kinase to DNA.* Science, 1992. **256**(5055): p. 382-5.

72. McWhirter, J.R. and J.Y. Wang, *An actin-binding function contributes to transformation by the Bcr-Abl oncoprotein of Philadelphia chromosome-positive human leukemias.* Embo J, 1993. **12**(4): p. 1533-46.

73. Van Etten, R.A., et al., *The COOH terminus of the c-Abl tyrosine kinase contains distinct F- and G-actin binding domains with bundling activity.* J Cell Biol, 1994. **124**(3): p. 325-40.

74. Wen, S.T., P.K. Jackson, and R.A. Van Etten, *The cytostatic function of c-Abl is controlled by multiple nuclear localization signals and requires the p53 and Rb tumor suppressor gene products.* Embo J, 1996. **15**(7): p. 1583-95.

75. Taagepera, S., et al., *Nuclear-cytoplasmic shuttling of C-ABL tyrosine kinase.* Proc Natl Acad Sci U S A, 1998. **95**(13): p. 7457-62.

76. Woodring, P.J., T. Hunter, and J.Y. Wang, *Regulation of F-actin-dependent processes by the Abl family of tyrosine kinases.* J Cell Sci, 2003. **116**(Pt 13): p. 2613-26.

77. Schindler, T., et al., *Structural mechanism for STI-571 inhibition of abelson tyrosine kinase.* Science, 2000. **289**(5486): p. 1938-42.

78. Nagar, B., et al., *Crystal structures of the kinase domain of c-Abl in complex with the small molecule inhibitors PD173955 and imatinib (STI-571).* Cancer Res, 2002. **62**(15): p. 4236-43.

79. Nagar, B., et al., *Organization of the SH3-SH2 unit in active and inactive forms of the c-Abl tyrosine kinase.* Mol Cell, 2006. **21**(6): p. 787-98.

80. Woodring, P.J., T. Hunter, and J.Y. Wang, *Inhibition of c-Abl tyrosine kinase activity by filamentous actin.* J Biol Chem, 2001. **276**(29): p. 27104-10.

81. Brasher, B.B. and R.A. Van Etten, *c-Abl has high intrinsic tyrosine kinase activity that is stimulated by mutation of the Src homology 3 domain and by autophosphorylation at two distinct regulatory tyrosines.* J Biol Chem, 2000. **275**(45): p. 35631-7.

82. Tanis, K.Q., et al., *Two distinct phosphorylation pathways have additive effects on Abl family kinase activation.* Mol Cell Biol, 2003. **23**(11): p. 3884-96.

83. Baskaran, R., et al., *Ataxia telangiectasia mutant protein activates c-Abl tyrosine kinase in response to ionizing radiation.* Nature, 1997. **387**(6632): p. 516-9.

84. Dan, S., et al., *Activation of c-Abl tyrosine kinase requires caspase activation and is not involved in JNK/SAPK activation during apoptosis of human monocytic leukemia U937 cells.* Oncogene, 1999. **18**(6): p. 1277-83.

85. Cong, F. and S.P. Goff, *c-Abl-induced apoptosis, but not cell cycle arrest, requires mitogen-activated protein kinase kinase 6 activation.* Proc Natl Acad Sci U S A, 1999. **96**(24): p. 13819-24.

86. Ben-Yehoyada, M., I. Ben-Dor, and Y. Shaul, *c-Abl tyrosine kinase selectively regulates p73 nuclear matrix association.* J Biol Chem, 2003. **278**(36): p. 34475-82.

87. Gong, J.G., et al., *The tyrosine kinase c-Abl regulates p73 in apoptotic response to cisplatin-induced DNA damage.* Nature, 1999. **399**(6738): p. 806-9.

88. Agami, R., et al., *Interaction of c-Abl and p73alpha and their collaboration to induce apoptosis.* Nature, 1999. **399**(6738): p. 809-13.

89. Yuan, Z.M., et al., *p73 is regulated by tyrosine kinase c-Abl in the apoptotic response to DNA damage.* Nature, 1999. **399**(6738): p. 814-7.

90. Vella, V., et al., *Exclusion of c-Abl from the nucleus restrains the p73 tumor suppression function.* J Biol Chem, 2003. **278**(27): p. 25151-7.

91. Welch, P.J. and J.Y. Wang, *A C-terminal protein-binding domain in the retinoblastoma protein regulates nuclear c-Abl tyrosine kinase in the cell cycle.* Cell, 1993. **75**(4): p. 779-90.

92. Chau, B.N., et al., *Tumor necrosis factor alpha-induced apoptosis requires p73 and c-ABL activation downstream of RB degradation.* Mol Cell Biol, 2004. **24**(10): p. 4438-47.

93. Inoue, T., et al., *Nuclear import and export signals in control of the p53-related protein p73.* J Biol Chem, 2002. **277**(17): p. 15053-60.

94. Vigneri, P. and J.Y. Wang, *Induction of apoptosis in chronic myelogenous leukemia cells through nuclear entrapment of BCR-ABL tyrosine kinase.* Nat Med, 2001. **7**(2): p. 228-34.

95. Amarante-Mendes, G.P., et al., *Bcl-2-independent Bcr-Abl-mediated resistance to apoptosis: protection is correlated with up regulation of Bcl-xL.* Oncogene, 1998. **16**(11): p. 1383-90.

96. Chopra, R., Q.Q. Pu, and A.G. Elefanty, *Biology of BCR-ABL.* Blood Rev, 1999. **13**(4): p. 211-29.

97. Salgia, R., et al., *BCR/ABL induces multiple abnormalities of cytoskeletal function.* J Clin Invest, 1997. **100**(1): p. 46-57.

98. Woodring, P.J., et al., *Modulation of the F-actin cytoskeleton by c-Abl tyrosine kinase in cell spreading and neurite extension.* J Cell Biol, 2002. **156**(5): p. 879-92.

99. Hantschel, O., et al., *Structural basis for the cytoskeletal association of Bcr-Abl/c-Abl.* Mol Cell, 2005. **19**(4): p. 461-73.

100. Lewis, J.M., et al., *Integrin regulation of c-Abl tyrosine kinase activity and cytoplasmic-nuclear transport.* Proc Natl Acad Sci U S A, 1996. **93**(26): p. 15174-9.

101. Renshaw, M.W., J.M. Lewis, and M.A. Schwartz, *The c-Abl tyrosine kinase contributes to the transient activation of MAP kinase in cells plated on fibronectin.* Oncogene, 2000. **19**(28): p. 3216-9.

102. Plattner, R., et al., *c-Abl is activated by growth factors and Src family kinases and has a role in the cellular response to PDGF.* Genes Dev, 1999. **13**(18): p. 2400-11.

103. Lewis, J.M. and M.A. Schwartz, *Integrins regulate the association and phosphorylation of paxillin by c-Abl.* J Biol Chem, 1998. **273**(23): p. 14225-30.

104. Cong, F., et al., *Cytoskeletal protein PSTPIP1 directs the PEST-type protein tyrosine phosphatase to the c-Abl kinase to mediate Abl dephosphorylation.* Mol Cell, 2000. **6**(6): p. 1413-23.

105. Plattner, R., et al., *A new link between the c-Abl tyrosine kinase and phosphoinositide signalling through PLC-gamma1.* Nat Cell Biol, 2003. **5**(4): p. 309-19.

106. Jin, H. and J.Y. Wang, *Abl Tyrosine Kinase Promotes Dorsal Ruffles but Restrains Lamellipodia Extension during Cell Spreading on Fibronectin.* Mol Biol Cell, 2007. **18**(10): p. 4143-54.

107. Harnois, T., et al., *Differential interaction and activation of Rho family GTPases by p210bcr-abl and p190bcr-abl.* Oncogene, 2003. **22**(41): p. 6445-54.

108. Sherr, C.J., *Cancer cell cycles.* Science, 1996. **274**(5293): p. 1672-7.

109. Knudson, A.G., Jr., *Mutation and cancer: statistical study of retinoblastoma.* Proc Natl Acad Sci U S A, 1971. **68**(4): p. 820-3.

110. Clarke, A.R., et al., *Requirement for a functional Rb-1 gene in murine development.* Nature, 1992. **359**(6393): p. 328-30.

111. Jacks, T., et al., *Effects of an Rb mutation in the mouse.* Nature, 1992. **359**(6393): p. 295-300.

112. Lee, E.Y., et al., *Mice deficient for Rb are nonviable and show defects in neurogenesis and haematopoiesis.* Nature, 1992. **359**(6393): p. 288-94.

113. Harbour, J.W. and D.C. Dean, *Rb function in cell-cycle regulation and apoptosis.* Nat Cell Biol, 2000. **2**(4): p. E65-7.

114. Zhang, H.S., et al., *Exit from G1 and S phase of the cell cycle is regulated by repressor complexes containing HDAC-Rb-hSWI/SNF and Rb-hSWI/SNF.* Cell, 2000. **101**(1): p. 79-89.

115. Nielsen, S.J., et al., *Rb targets histone H3 methylation and HP1 to promoters.* Nature, 2001. **412**(6846): p. 561-5.

116. Dahiya, A., et al., *Linking the Rb and polycomb pathways.* Mol Cell, 2001. **8**(3): p. 557-69.

117. De Falco, G., F. Comes, and C. Simone, *pRb: master of differentiation. Coupling irreversible cell cycle withdrawal with induction of muscle-specific transcription.* Oncogene, 2006. **25**(38): p. 5244-9.

118. Weinberg, R.A., *The retinoblastoma protein and cell cycle control.* Cell, 1995. **81**(3): p. 323-30.

119. Lee, J.O., A.A. Russo, and N.P. Pavletich, *Structure of the retinoblastoma tumour-suppressor pocket domain bound to a peptide from HPV E7.* Nature, 1998. **391**(6670): p. 859-65.

120. Rubin, S.M., et al., *Structure of the Rb C-terminal domain bound to E2F1-DP1: a mechanism for phosphorylation-induced E2F release.* Cell, 2005. **123**(6): p. 1093-106.

121. Knudsen, E.S. and J.Y.J. Wang, *Differential Regulation of Retinoblastoma Protein Function by Specific Cdk Phosphorylation Sites.* J. Biol. Chem., 1996. **271**(14): p. 8313-8320.

122. Nevins, J.R., et al., *Role of the Rb/E2F pathway in cell growth control.* J Cell Physiol, 1997. **173**(2): p. 233-6.

123. Knudsen, E.S. and J.Y. Wang, *Dual mechanisms for the inhibition of E2F binding to RB by cyclin-dependent kinase-mediated RB phosphorylation.* Mol Cell Biol, 1997. **17**(10): p. 5771-83.

124. Knudsen, E.S., et al., *Inhibition of DNA synthesis by RB: effects on G1/S transition and S-phase progression.* Genes Dev, 1998. **12**(15): p. 2278-92.

125. Sever-Chroneos, Z., et al., *Retinoblastoma tumor suppressor protein signals through inhibition of cyclin-dependent kinase 2 activity to disrupt PCNA function in S phase.* Mol Cell Biol, 2001. **21**(12): p. 4032-45.

126. Ji, P., et al., *An Rb-Skp2-p27 pathway mediates acute cell cycle inhibition by Rb and is retained in a partial-penetrance Rb mutant.* Mol Cell, 2004. **16**(1): p. 47-58.

127. Sherr, C.J. and J.M. Roberts, *Inhibitors of mammalian G1 cyclin-dependent kinases.* Genes Dev, 1995. **9**(10): p. 1149-63.

128. Lipinski, M.M. and T. Jacks, *The retinoblastoma gene family in differentiation and development.* Oncogene, 1999. **18**(55): p. 7873-82.

129. Ferguson, K.L. and R.S. Slack, *The Rb pathway in neurogenesis.* Neuroreport, 2001. **12**(9): p. A55-62.

130. Chau, B.N. and J.Y. Wang, *Coordinated regulation of life and death by RB.* Nat Rev Cancer, 2003. **3**(2): p. 130-8.

131. Masselli, A. and J.Y. Wang, *Phosphorylation site mutated RB exerts contrasting effects on apoptotic response to different stimuli.* Oncogene, 2006. **25**(9): p. 1290-8.

132. Tan, X. and J.Y. Wang, *The caspase-RB connection in cell death.* Trends Cell Biol, 1998. **8**(3): p. 116-20.

133. Tan, X., et al., *Degradation of Retinoblastoma Protein in Tumor Necrosis Factor- and CD95-induced Cell Death.* J. Biol. Chem., 1997. **272**(15): p. 9613-9616.

134. Janicke, R.U., et al., *Specific cleavage of the retinoblastoma protein by an ICE-like protease in apoptosis.* EMBO J, 1996. **15**(24): p. 6969-6978.

135. Chau, B.N., et al., *Signal-dependent protection from apoptosis in mice expressing caspase-resistant Rb.* Nat Cell Biol, 2002. **4**(10): p. 757-65.

136. Huang, X., et al., *Blockade of Tumor Necrosis Factor-induced Bid Cleavage by Caspase-resistant Rb.* J Biol Chem, 2007. **282**(40): p. 29401-13.

137. Muller, H., et al., *E2Fs regulate the expression of genes involved in differentiation, development, proliferation, and apoptosis.* Genes Dev, 2001. **15**(3): p. 267-85.

138. Fattman, C.L., et al., *Sequential two-step cleavage of the retinoblastoma protein by caspase- 3/-7 during etoposide-induced apoptosis.* Oncogene, 2001. **20**(23): p. 2918-26.

139. Noren, N.K., et al., *The EphB4 receptor suppresses breast cancer cell tumorigenicity through an Abl-Crk pathway.* Nat Cell Biol, 2006. **8**(8): p. 815-25.

140. Dorey, K., et al., *Phosphorylation and structure-based functional studies reveal a positive and a negative role for the activation loop of the c-Abl tyrosine kinase.* Oncogene, 2001. **20**(56): p. 8075-84.

141. Frasca, F., et al., *Tyrosine kinase inhibitor STI571 enhances thyroid cancer cell motile response to Hepatocyte Growth Factor.* Oncogene, 2001. **20**(29): p. 3845-56.

142. Shishido, T., et al., *Crk family adaptor proteins trans-activate c-Abl kinase.* Genes Cells, 2001. **6**(5): p. 431-40.

143. Juang, J.L. and F.M. Hoffmann, *Drosophila abelson interacting protein (dAbi) is a positive regulator of abelson tyrosine kinase activity.* Oncogene, 1999. **18**(37): p. 5138-47.

144. Sun, X., et al., *Interaction between protein kinase C delta and the c-Abl tyrosine kinase in the cellular response to oxidative stress.* J Biol Chem, 2000. **275**(11): p. 7470-3.

145. Sun, X., et al., *Activation of the cytoplasmic c-Abl tyrosine kinase by reactive oxygen species.* J Biol Chem, 2000. **275**(23): p. 17237-40.

CHAPTER 2

Abl tyrosine kinase induces cell detachment through Rap1-induced integrin inactivation and requires Rho activation

ABSTRACT

A variety of cell adhesion mechanisms underlie the way that cells are organized in tissues. Among them, integrin molecules on the cellular membrane play a critical role to maintain cell integrity. Abl is a non-receptor tyrosine kinase and is activated by binding of integrins with proteins within the extracellular matrix (ECM). Here we made a mutant *Abl* gene (*AblPP*) that encodes a constitutively activated protein. We stably transfected this gene into HEK293 cells under the control of a TET-on promoter. The expression of AblPP caused the host cells to round up and detach from the supporting matrix in the presence of serum. We found that this was due to phosphorylation of the CrkII adaptor protein by AblPP, which disrupted the complex between CrkII and C3G and abolished the GEF activity of C3G, resulting in the inactivation of Rap1, a small GTPase. Furthermore, the inactivation of Rap1 caused a decrease of integrin affinity with fibronectin. We also found that the Rho-ROCK1 pathway activated by LPA or serum was required in order for the AblPP-induced cell detachment. These two pathways function independently of each other and also exist in ephrin A1-induced PC3 cell detachment.

INTRODUCTION

Integrins are heterodimeric transmembrane receptors composed of an α and a β subunit that bind proteins in extracellular matrix (ECM) such as fibronectin [1-3]. Integrins have two major functions: to allow cells to adhere to the ECM and to allow for

the transmission of information between cells and the external environment [1-3]. Integrins are able to respond to changes in the extracellular matrix and activate a number of pathways critical for cell motility, cell spreading, and cell survival [4, 5]. In order to exert these biological effects, integrins signal through a number of well characterized signaling proteins such as Rho, Rac, and Rap small GTPases, and PI3K, focal adhesion kinase (FAK), Src, and Abl kinases.

c-Abl is a non-receptor tyrosine kinase that is ubiquitously expressed in mammals [6]. It has three nuclear localization signals (NLS) and one nuclear export signal (NES) and therefore can shuttle between nucleus and cytoplasm [6, 7]. The nuclear fraction of Abl is activated upon DNA damage and activation of this pool of Abl can induce cells to undergo apoptosis [6, 8, 9]. The cytoplasmic fraction of Abl can be activated in several ways including growth factors such as PDGF or by integrins in an outside-in manner after attachment to the ECM [10-12]. In the case of Abl activation by cell adhesion, it has been shown that after integrin activation Abl kinase activity increases and Abl is recruited to early focal contacts. It is also suggested that cell adhesion activates cytoplasmic c-Abl and that this activation can transmit integrin signals to the nucleus where it may function to integrate adhesion and cell cycle signals [10].

Rap1 is a small GTPase and the closest homolog of the Ras oncoprotein [13, 14]. A variety of extracellular signals control its activity through the regulation of several guanine nucleotide exchange factors (GEFs), such as C3G (CrkII SH3-domain binding GEF) [15] and Epacs (exchange protein directly activated by cAMP) [16, 17], and GTPase activating proteins (GAPs), such as Rap1GAP [18]. It was originally thought that Rap1 inhibits Raf-Erk pathway by binding to Raf [19, 20], but activation of endogenous

Rap1 fails to antagonize the subsequent Ras-dependent activation of ERK pathway, suggesting that the inhibition of Raf-ERK pathway might be a cell context-dependent event [21]. Rap1 has also been implied to regulate integrins that are associated with the actin cytoskeleton, i. e. the β1, β2, and β3 families, to control both integrin affinity and avidity depending on the cell type and integrin molecules [22-24]. Although these studies have clearly shown that Rap1 functions in 'inside-out' signaling to integrins, the mechanisms of this regulation remain unknown at this point.

The Rho-like family members are involved in the formation of stress fibers and focal adhesions [25, 26]. Rho activation leads to the subsequent activation of the downstream Rho-kinase (ROCK) that phosphorylates and inhibits the myosin light chain (MLC) phosphatase, leading to an elevation in MLC phosphorylation and to enhanced myosin activation [27]. The resulting tension drives the formation of stress fibers and focal adhesions [28]. Another effector of Rho is mDia [29], which stimulates actin polymerization [30]. Expression of activated mDia promotes assembly of more normal stress fibers than the constitutively activated ROCK kinase [29]. In stress fibers and focal adhesion assembly, both myosin contractility generated by ROCK, and an activity from mDia, are required [26].

In this study, we found that induction of a constitutively active Abl mutant, (AblPP) induced HEK293 cells to round up and detach from the supporting matrix. We found this phenotype was due to integrin inactivation caused by AblPP's inactivation of a CrkII-C3G-Rap1-integrin pathway. Furthermore, our data suggest that the Rho-ROCK1 pathway is also required for this process of cell detachment.

RESULTS

Abl kinase activity causes HEK293 cells to detach

Normally the Abl kinase adopts an auto-inhibited conformation in which the SH3 domain and N-lobe play important roles in keeping the kinase inactive. It has been shown that the linker between the SH2 domain and the kinase domain is also important for maintenance of this autoinhibitory conformation as it functions as an internal scaffold to hold the SH3 domain and the N-lobe in place [31]. By mutating two proline residues in this linker region ($_{242}$**P**TIYGVS**P**$_{249}$) with glutamic acid (*AblPP*), the auto-inhibited structure of the kinase is disrupted, and the kinase becomes constitutively active.

To determine how expression of a constitutively active Abl kinase affects cells, we stably transfected this AblPP construct under the control of a Tet-On protomer into HEK293 cells (HEK293-AblPP). As controls, we also stably transfected wild type Abl and kinase defective *Abl* (K290H; *AblKD*) into HEK293 cells (HEK293-Abl, and HEK293-AblKD) [32]. In this system, the expression of Abl, AblPP, or AblKD was tightly controlled and was quickly induced by 2 μg/ml of doxycycline (Figure 2-1A, 2-1E). Interestingly, we found that the expression of AblPP caused the HEK293-AblPP cells to detach from the supporting matrix (Figure 2-1B). This detachment was a fast process. In 2 hours, around 80% of the cells had detached from the dish (Figure 2-1C), and these cells did not re-attach even after doxycycline was removed from the media, suggesting that this process is not reversible (data not shown). Because the Abl tyrosine kinase is known to regulate cytoskeletal rearrangement and induce apoptosis [12], we did a kinetic study to determine whether the induction of AblPP also led to cell death in our

system. We found that although HEK293-AblPP cells underwent cell death after AblPP induction, they lost attachment to the supporting matrix at a much earlier timepoint (Figure 2-1D), suggesting that the cell death induced by AblPP might be a secondary effect of cell detachment.

To determine if this phenotype of cell detachment was kinase dependent, we induced wild type Abl or AblKD in our HEK293-Abl and HEK293-AblKD cells. Although the level of Abl expression in these cells was actually higher than in HEK-AblPP cells at 5 hours (Figure 2-1E), the cells did not detach from the supporting matrix, suggesting that this phenotype was in fact kinase-dependent (Figure 2-1F). We further demonstrated the kinase-dependence of this phenotype by treating the HEK293-AblPP cells with STI571, a specific inhibitor of the Abl kinase, which completely abolished the cell detachment phenotype even after expression of AblPP for 24 hours (Figure 2-1B, 2-1C).

AblPP expression causes β1 integrin inactivation

Since the expression of AblPP caused host HEK293-AblPP cells to detach from the supporting matrix, we checked the ability of host cells to adhere to fibronectin-coated plates after the induction of AblPP or AblKD. While the expression of AblKD did not cause any significant change, the expression of AblPP led to a significant decrease in cell adhesion to fibronectin (Figure 2-2A, 2-2B). The major cellular receptor for fibronectin is β1 integrin. The expression of AblPP did not change the expression level of β1 integrin (Figure 2-2C), and so we monitored integrin activation status by using an antibody

specific for the active conformation of β1 integrin. Interestingly, although the expression of AblKD did not change the integrin binding activity, the expression of AblPP caused a 50% reduction in integrin binding activity (Figure 2-2D, 2-2E), and this effect was completely blocked by treatment of induced cells with STI571 (data not shown). Taken together, these data suggest that the AblPP-induced cell detachment is likely caused by a decrease in the affinity of integrins for the supporting matrix.

Abl kinase activity caused Rap1-GTP level goes down

Rap1 is a small GTPase, which is capable of regulating integrin activity in response to intracellular signals [22-24]. We speculated that the integrin inactivation we observe in our AblPP system was due to a change in the level of active Rap1 (Rap1-GTP) after AblPP expression. To test this hypothesis, we used a Rap1 pulldown assay to check Rap1-GTP levels in the presence and absence of AblPP expression. Indeed, the induction of AblPP caused roughly a 3-fold reduction in the level of Rap1-GTP (Figure 2-3A, 2-3B). In contrast, expression of AblKD did not cause Rap1-GTP levels to change (data not shown). Furthermore, STI571 treatment of induced HEK293-AblPP cells completely abrogated the AblPP-induced reduction in Rap1-GTP levels. To further prove that changes in Rap1 activity were responsible for the loss of cell adhesion in our system, we analyzed cell detachment after transfection of HEK-AblPP cells with Rap1GAP (which inactivates Rap1) or the constitutively active Rap1-V12 mutant. As expected, Rap1GAP transfection led to a minor increase in the number of detached cells before induction of AblPP. Transfection of cells with Rap1V12, on the other hand, largely blocked cell

detachment induced by AblPP induction (Figure 2-3C), further indicating that Rap1 inactivation is a downstream event of AblPP induction.

Abl phosphorylates CrkII to disrupt CrkII-C3G complex

The first identified guanine nucleotide exchange factor (GEF) for Rap1 was C3G, which regulates Rap1 activity induced by tyrosine kinases [15]. C3G contains several proline-rich sequences that associate with the first SH3 domain of the CrkII adaptor protein. If the formation of this CrkII-C3G complex is inhibited, Rap1 activation is also blocked [33]. Since CrkII is a well-known Abl kinase substrate, we asked whether the activation of Abl kinase causes Rap1-GTP levels to go down through disruption of the CrkII-C3G complex. As expected, we found that the CrkII protein was phosphorylated with the expression of AblPP, and that treatment with 5 μM STI571 completely abrogated the phosphorylation (Figure 2-3D). Furthermore, we found that while CrkII forms a complex with C3G under normal condition, this complex was disrupted after induction of AblPP. Pretreating the cells with STI571 prevented AblPP from forming a complex with CrkII, and rescued CrkII-C3G complex formation (Figure 2-3E). To further prove that CrkII is a downstream effector of AblPP, we examined the effect of transiently expressing a CrkII mutant that lacks the Abl phosphorylation site (CrkII-Y221F) on AblPP-induced cell detachment and Rap1 inactivation. Transfection of CrkII-Y221F into AblPP cells, almost completely rescued the cell detachment phenotype (Figure 2-3F). We next checked the effect of CrkII-Y221F transfection on Rap1-GTP levels and found that, in the presence of CrkII-Y221F, Rap1-GTP levels no longer decreased following AblPP

induction. Taken together, these data led us to believe that AblPP phosphorylates CrkII on Y221, which disrupts the CrkII-C3G complex and leads to a decrease in Rap1-GTP levels which then lowers integrin affinity and causes host cells to detach.

Rho activity is required for Abl kinase-induced cell detachment

During the course of our experiments, we noticed that the induction of AblPP did not cause the HEK293-AblPP cells to detach under serum-free conditions (Figure 2-4A, 5-4B), suggesting a pathway induced by serum is also required for AblPP-induced cell detachment. Because growth factors can activate the Rho-ROCK1 pathway that can generate the active myosin contractility important for cell adhesion and de-adhesion [27, 34], we tested whether the Rho-ROCK1 pathway was involved in AblPP-induced cell detachment. To do this, we induced AblPP expression in serum-free media in the absence or presence of lysophosphatidic acid (LPA), which is one of the most important serum mitogens, and a strong activator of hetero-trimeric G proteins (Gα12 and Gα13) and the Rho-ROCK1 pathway [35, 36]. To monitor the process of cell detachment, we checked the morphology of actin and found that, as expected, neither AblPP alone nor LPA alone caused cells to round up and detach (Figure 2-4C, 2-4D). However, when AblPP was induced in the presence of LPA, HEK293-AblPP cells rounded up and detached from the supporting matrix (Figure 2-4C, 2-4D), suggesting that a pathway activated by LPA is also required in order for HEK293-AblPP cells to detach when AblPP is induced. To further test whether this pathway is the Rho-ROCK1 pathway, we transfected HEK293-AblPP cells with either constitutively active (RhoV14) or dominant negative (RhoN19)

Rho constructs and monitored cell detachment. Interestingly, we found that HEK293-AblPP cells expressing RhoV14 could round up and detach after AblPP induction even in the absence of LPA or serum (Figure 2-4E), demonstrating that Rho activity could supplant the LPA or serum requirement. Furthermore, the dominant negative RhoN19 largely, if not completely abrogated the cell detachment phenotype even when AblPP was expressed in the presence of LPA or serum (Figure 2-4E). Taken together, these data suggest that Rho activation is required for the cell rounding, and therefore for the cell detachment that occurs following Abl induction in HEK293-AblPP cells.

ROCK1 kinase activation is required for Abl kinase-induced cell detachment

One of the downstream effectors of Rho is the ROCK1 kinase [27, 34], and so we asked whether ROCK1 kinase activity also plays a role in AblPP-induced cell detachment. Indeed, a specific ROCK1 kinase inhibitor, Y27632, completely blocked the cell detachment phenotype induced by AblPP expression (Figure 2-5F). Furthermore, we used a ROCK1 specific siRNA to knockdown ROCK1 expression in HEK293-AblPP cells and found that the knockdown of ROCK1 significantly lowered the percentage of detached cells (Figure 2-5G, 2-5H). These data provide further evidence that the Rho-ROCK1 pathway is required for the AblPP-induced detachment of HEK293-AblPP cells.

It has been shown that Abl-related gene, Arg, can inhibit Rho activity by phosphorylating p190RhoGAP [37]. Therefore we asked that whether the induction of AblPP directly affects the Rho-ROCK1 pathway or whether these two pathways are independent of each other. Despite extensive effort, we were not able to detect any

tyrosine phosphorylation of ROCK1 after AblPP induction, nor were we been able to detect any change in its expression level (data not shown). In addition, expression of AblPP did not have any significant effect on Rho-GTP levels or myosin light chain phosphorylation, irrespective of the presence of serum (Figure 2-5B and data not shown). Finally, although LPA addition increased Rho-GTP levels in 5 minutes, it did not have any effect on Rap1-GTP levels, irrespective of AblPP expression level (Figure 2-5A). Taken together, these data suggest that the Abl-CrkII-C3G-Rap1 pathway induced by AblPP and the Rho-ROCK1 pathway induced by serum or LPA are independent of each other, but both of them are required in order for AblPP to induce the HEK293-AblPP cells to detach from the supporting matrix.

Ephrin A1-induced PC3 cell roundup is dependent on Abl kinase

Using HEK293-AblPP cells, we identified two independent pathways that govern the roundup and detachment of cells following AblPP induction (Figure 2-6). We were next interested in determining whether these two pathways are required for cell detachment in other systems. Previous research has shown that ephrin A1 induces PC3 prostate cancer cells to round up and detach by inhibiting integrin affinity [38]. Ephrin A1 also can induce cell spreading in NIH3T3 cells [39], suggesting it has pleiotropic functions depending on cellular context. To test whether Abl was required for the ephrin A1 induced detachment of PC3 cells, we treated these cells with Fc-conjugated ephrin A1 in the absence or presence of the Abl kinase inhibitor STI571. Interestingly, we found that although ephrin A1 induced around 90% of PC3 cells to round up and detach within

10 minutes, inhibition of Abl kinase activity with STI571 largely blocked this phenotype, reducing the number of detached cells to around 30% (Figure 2-7A, 2-7B). Furthermore, ephrin A1 treatment caused endogenous Abl kinase to be tyrosine phosphorylated (Figure 2-7C). Time course experiments showed that Abl phosphorylation starts as early as 5 minutes after ephrin treatment, and goes away after 30 minutes, which correlated with the cell detachment phenotype and indicates that ephrin A1 can activate Abl kinase. Interestingly, we found that ephrin A1 treatment of PC3 cells also led to a decrease in Rap1-GTP levels and that STI571 treatment totally abrogated this effect (Figure 2-7D). Finally, we tested whether the Rho-ROCK1 pathway was also required for ephrin A1-induced cell detachment. By treating PC3 cells with Y27632 for 1 hour before addition of ephrin A1, we were able to completely rescue the ephrin A1-induced cell roundup and detachment (Figure 2-7E, 2-7F), suggesting that the Rho-ROCK1 pathway is also required for this process. Taken together, these data suggest that the two pathways we identified as being required for cell detachment in HEK293-AblPP cells are also required for the ephrin A1-induced detachment of PC3 cells.

DISCUSSION

Activation of Abl kinase sends a negative feedback to integrin inactivation

After integrin activation, the Abl tyrosine kinase is activated and the activation of Abl kinase regulates cytoskeletal rearrangement. Previously, it has been proposed that fibronectin engagement of integrins activates the kinase activity of Abl roughly three to

five fold. It was also shown that in 10T1/2 fibroblasts, after fibronectin stimulation, part of the nuclear Abl translocates transiently to focal adhesions [10, 40]. It is possible that this part of Abl plays a role in activating the cytoplasmic c-Abl *in trans*. In the present study, we present data showing that Abl can, in turn, function to directly regulate integrin activity, suggesting there may be a negative feedback pathway involved in integrin regulation in this setting. We show that this signal is likely transmitted through a CrkII-C3G-Rap1 pathway to send an inside-out signal to decrease integrin affinity.

The processes of cell rounding and detachment are both of critical importance *in vivo* as they are required for events such as mitosis or metastasis. Interestingly, a previous study has shown that high Rho activity contributes to cell rounding and a more rigid cell cortex [41]. It would be interesting to determine if Abl activation also has an effect on this process. We also showed that ephrin A1 induced PC3 prostate cancer cells to round up and that Abl activation played a role in this phenotype. Consistent with this observation, unligated integrin molecules could induce both apoptosis and metastasis in a neuroblastoma cell line, depending on the status of caspase-8 [42]. Previous research has already shown that Abl is also both pro- and anti-apoptotic. Here we propose that Abl can be pro-apoptotic by inducing integrin unligation, and can also induce cells to detach from ECM and change the microenvironment, thus favoring cell survival.

Cytoplasmic Abl regulates cell death

Abl tyrosine kinase is distributed in both the nucleus and cytoplasm. Nuclear Abl plays a role in transcriptional regulation, particularly in response to DNA damage.

Nuclear Abl is also involved in apoptosis in part due to its ability to prolong the half-life of the pro-apoptotic p73, a family member of p53 [8]. Nuclear Abl is also activated by tumor necrosis factor [43], suggesting that nuclear Abl is involved in regulating cell death in response to both genomic stress and death receptor-induced apoptosis. In contrast, cytoplasmic Abl largely regulates cytoskeletal rearrangement and is activated by growth factors and cell adhesion [12].

Although it is well-established that the nuclear pool of Abl is required for the induction of Abl kinase-induced cell death, recent research has suggested that cytoplasmic Abl also plays a role in this process. In a system in which Abl is activated by induced dimerization, we found that although the nuclear pool of Abl is required for cell death, the cytoplasmic pool of Abl collaborates once the apoptosis program is initiated. Furthermore, we found that cytoplasmic Abl can sensitize cells to TNF-induced apoptosis (Huang and Wang, unpublished results). Our discovery here that activated Abl is able to negatively regulate integrin activation, via inside-out signaling through Rap1 may explain this paradoxical phenomenon. It has been shown that the unligated integrin can lead to caspase-8 activation [42, 44]. AblPP is localized in both the nucleus and the cytoplasm (data not shown), and our data clearly suggested that AblPP can lead to a decrease in the affinity of integrins for fibronectin (Figure 2-2). It is worthwhile to check whether the caspase-8 activity is increased after AblPP expression. Of course, since integrin regulates focal adhesions, and thus affects the expression of genes involved in apoptosis [4, 45], cytoplasmic Abl may also collaborate with nuclear Abl in inducing apoptosis through an integrin-regulated pathway. Nevertheless, integrin might be an intermediate factor in the cell death pathways regulated by Abl kinase.

Rho-ROCK1 pathway might be general requirement for cell detachment

Here we have shown that in two different systems (i. e. AblPP-induced HEK293 cells and ephrin A1-treated PC3 cells), the Rho-ROCK1 pathway is required for the process of cell detachment. The Rho-ROCK1 pathway has been shown to generate stress fibers and focal adhesions, and thus a decrease in Rho activity would be expected when cells round up and detach. Indeed, it has been shown that the inhibition of Rho in cells such as fibroblasts decreases adhesion, causing a retraction of lamellae and a rounding of the cell body [25]. However, paradoxically, in mitotic cells, high Rho activity contributes to cell rounding and a more rigid cell cortex [41]. Furthermore, in leukocytes, which lack both stress fibers and focal adhesions, Rho appears to increase cell attachment, since inhibiting Rho activity elevates integrin-mediated adhesion in these systems [46]. In both systems we looked at, although Rho-ROCK1 activity is required for cell detachment, activation of the Rho pathway by itself, does not change the cell adhesion activity (Figure 2-4). Only when combined induction of Abl kinase activation and the resultant Rap1-regulated decrease s in integrin affinity, could inhibition of Rho-ROCK1 induce cell detachment. Since both HEK293 cells and PC3 cells are epithelial cells, it is possible that epithelial cells and fibroblasts have different mechanisms regulating their attachment to the ECM. This seems reasonable considering they have different ECMs *in vivo*. We also found that the Rap1-induced decrease in integrin affinity is independent of the Rho-ROCK1 pathway. However, although we did not detect any direct link between Abl-

induced Rap1 inactivation and LPA-induced Rho-ROCK1 activity, it is still possible that Abl has some other effects on Rho or ROCK1 by different modifications.

EXPERIMENTAL PROCEDURES

Generation of inducible cell lines – HEK293-AblPP, HEK293-Abl, and HEK293-AblKD cell lines were generated by using the Flp-In^{TM} system from Invitrogen (Carlsbad, CA). Briefly, the *Abl* gene was cloned into the pcDNA5-FRT-TO plasmid; an HA tag was also attached at the C-terminus of *Abl* gene. Then 0.2 μg of pcDNA5-FRT-TO-Abl, pcDNA5-FRT-TO-AblPP, or pcDNA5-FRT-TO-AblKD, together with 1.8 μg of the Flp recombinase expression vector pOG44 were co-transfected into the HEK293-FRT cell line, which contains a single integrated FRT (FLP Recombination Target) site and stably expresses the Tet repressor. The cells were then subjected to selection with 200 μg/ml of hygromycin and 15 μg/ml of blasticidin for 15 days. Single clonies were then picked, amplified, and screened for induction efficiency.

Cell culture - The inducible cell lines were cultured in DMEM media containing 10% FBS, 100 U penicillin/ streptomycin and 0.05% β-mercaptoethanol. Cells were routinely treated with 2 μg/ml of doxycycline at 37ºC for protein induction. The PC3 cell line was cultured in RPMI1640 media containing 10% FBS and 100 U penicillin/ streptomycin.

Antibodies and Chemicals - Mouse anti-Abl monoclonal antibody 8E9 was generated in our lab; mouse anti-HA was from Covance (Madison, WI); rabbit anti-

ROCK1, rabbit anti-Rap1, rabbit anti-RhoA, rabbit anti-C3G antibodies were from Santa Cruz Biotech (Santa Cruz, CA); rabbit anti-CrkII221Y was from Cell Signaling Company (Danvers, MA); mouse anti-β1-integrin antibody P4C10 was from Upstate (Lake Placid, NY); mouse anti-CrkII was from BD Biosciences (San Jose, CA); mouse anti-actin, doxycycline, and lysophosphatidic acid (LPA) were from Sigma (St Louis, MO); FITC-conjugated phalloidin was from Molecular Probes (Eugene, OR); STI571 was from Novartis; Fc-conjugated-ephrin A1 was from R & D systems (Minneapolis, MN); the conformation-specific anti-integrin antibody B44 was from Chemicon (Tamecula, CA).

Western blot - Whole cell lysates were prepared in RIPA buffer (50 mM Tris-HCl [pH 7.4], 150 mM NaCl, 1% NP-40, 0.25% sodium deoxycholate, 0.1% SDS, 0.5 mM EDTA, 1 mM EGTA, 1 mM DTT) plus protease inhibitor (from Sigma); 100 μg of total protein was resolved by SDS-PAGE, transferred onto PVDF or nitrocellulose membranes, blocked in 5% nonfat dry milk/TBST (20 mM Tris-HCl [pH 7.5], 150 mM NaCl, 0.05% Tween-20) and incubated with primary antibodies overnight at 4°C. Membranes were washed 3 × 10 minutes in TBST and incubated with HRP-conjugated secondary antibodies for 2 hours at room temperature. After 3 × 10 minutes washing, membranes were incubated with enhanced ECL reagent or Femto Max Sensitivity Substrate from Pierce (Rockford, IL) for 1 minute and exposed to X-ray films.

Cell adhesion assay - Plates (96-well) were coated with fibronectin from Sigma at concentrations of 0.1 to 20 μg/ml. Cells were brought into suspension by trpsinization, then seeded at 1 x 10^4 cells per well, and allowed to adhere for 2 hours at 37°C. Wells were then washed twice with serum-free DMEM/0.1% BSA, and adherent cells were fixed with 5% glutaraldehyde and then stained with crystal violet (0.1%). After extensive

washing to remove the free dye, the cell-bound crystal violet was extracted with 0.5% Triton X-100, and absorbance was measured at 595 nm.

Integrin activity assay – HEK293-AblPP or HEK293-AblKD cells were analyzed by flow cytometry. Cells were stained with antibody B44, which recognizes an epitope present on active integrins, immediately upon harvest via a 10 minute incubation at room temperature in either PBS/3% BSA (top panel), or PBS/3% BSA supplemented with 200 mM Mn^{2+} to activate integrins. Negative controls were treated with only a secondary antibody, while positive controls were labelled with monoclonal antibody P4C10 or JB1 which binds integrins irrespective of activation state. The relative activation index was defined as (F – Fo)/(Fmax – Fo), where F is the MFI of B44 binding, Fo is the MFI of negative control, and Fmax is the MFI of B44 binding in the presence of Mn^{2+}.

Fluorescence Microscope - At various time points, the HEK293-AblPP or HEK293-AblKD cells were fixed with 4% paraformaldehyde / phosphate buffered saline (PBS) for 15 minutes, permeabilized in 0.3% Triton X-100 / PBS, and then stained with Alexa 546-conjugated phalloidin (Molecular Probes, Eugene, OR). Fluorescent images were captured with a CCD camera.

Cell detachment assay - HEK293-AblPP or HEK293-AblKD cells were cultured overnight, changed to serum-free media and cultured for 2 more hours. Cells were then treated with 2 μg/ml doxycycline for 2 hours to induce AblPP or AblKD expression. After that, cells were fixed with 4% paraformaldehyde for 15 minutes, washed with PBS, and observed under a phase contrast microscope.

Pulldown assay of activated small GTPase - the HEK293-AblPP or HEK293-AblKD cells were treated with 2 μg/ml doxycycline for 2 hours to induce AblPP or

AblKD expression. Cells were lysed and Rap1-GTP was pulled-down by using bacteria-purified glutathione S-transferase (GST)-RalBD (RalGDS-binding domain) [47]. Rho-GTP was pulled-down with bacteria-purified GST-Rho-BD (Rhotekin Rho-binding domain) [48].

Immunoprecipitation – Cells were lysed in Co-IP lysis buffer (50 mM Tris-HCl [pH 7.4], 150 mM NaCl, 1% NP-40, 0.25% sodium deoxycholate, 0.5 mM EDTA, 1 mM EGTA, 1 mM DTT) plus protease inhibitor cocktail (from Sigma, St Louis, MS); 1 mg of whole cell lysates were incubated with 5 μg of anti-Abl monoclonal antibody 8E9 for overnight. The immunoprecipitates were resolved by SDS-PAGE and target proteins were detected by immunoblotting.

siRNA experiments - Sense and antisense RNA oligos corresponding to the target sequence for human *ROCK1* (GGUGAUUGGUAGAGGUGCA), and for *LacZ* (AACGTACGCGGAATACTTCGA) were synthesized and annealed by Ambion. The uniqueness of each individual target sequence was confirmed by a BLAST search of mouse genomic plus transcript database. Transfection of synthetic siRNA was performed using the Lipofectamine2000 reagent (from Invitrogen, Carlsbad, CA) with standard procedures. 48 hours after transfection, cells were collected and target protein levels were analyzed. Cotransfection of Cy3-labeled siRNA duplexes (from Molecular Probes, Engene, OR) were performed to determine transfection efficiency when necessary.

ACKNOWLEDGEMENT

We thank Dr. Sanford Shattil for the Rap1GAP, Rap1V14, and pGEX-RalRBD constructs. Dr. Elena Pasquale for the CrkII221F construct. We thank Scott Stuart for critical reading of the manuscript. This work is supported by grants NIH CA43054 and HL57900 to JYJW.

Chapter 2, in part, is being prepared for publication of the material as it may appear in "Abl tyrosine kinase induces cell detachment through Rap1-induced integrin inactivation and requires Rho activation, Xiaodong Huang, Diana Wu, Dwayne G. Stupack, and Jean Y. J. Wang, 2007 (in submission)". The dissertation author was the primary investigator and author of this paper.

Figure 2-1: AblPP induction causes the host HEK293-AblPP cells to detach from supporting matrix, and is kinase activity dependent.
A. AblPP can be quickly and tightly induced. The host HEK293-AblPP cells were treated with 2 μg/ml doxycycline for different time points. The cells were then collected, whole cell lysates were subjected to SDS-PAGE separation and AblPP protein was detected with an anti-HA antibodiy.
B. AblPP induction causes host HEK293-AblPP cells to detach from the supporting matrix. Host HEK293-AblPP cells were seeded on poly-L-lysine-coated coverslips and cultured overnight. AblPP protein was induced by 2 μg/ml doxycycline for 2 hours in the presence or absence of 5 μg/ml STI571. The cells were then fixed and observed under a phase contrast microscope.
C. Blocking Abl kinase activity prevents the detachment of HEK293-AblPP cells. HEK293-AblPP cells were treated with2 μg/ml doxycycline for 2 or 24 hours, in the absence or presence of 5 μM STI571. Detached cells were counted as in 1B. The histogram shows normalized average values ± s.e.m. from three independent experiments.
D. AblPP-induced cell detachment occurs at earlier time points than cell death. HEK293-AblPP cells were treated with 2 μg/ml doxycycline for different lengths of time. Floating cells and attached cells were collected and counted separately. The dead cells in both pools were also counted by using the trypan blue exclusion method.
E. The inducible expression of wild type Abl, AblPP, and AblKD. HEK293-Abl, HEK293-AblPP, and HEK293-AblKD cells were treated with 2 μg/ml doxycycline for 5 hours. The induced Abl, AblPP, and AblKD protein were detected by using an anti-HA antibody.
F. Abl kinase activity is required for detachment of HEK293-AblPP cells. HEK293-Abl, HEK293-AblPP, and HEK293-AblKD cells were treated with 2 μg/ml doxycycline for 2 hours. The detached cells were counted as in 1B. The histogram shows normalized average values ± s.e.m. from three independent experiments.

2-1A)

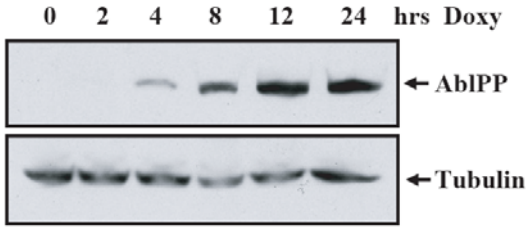

2-1B)

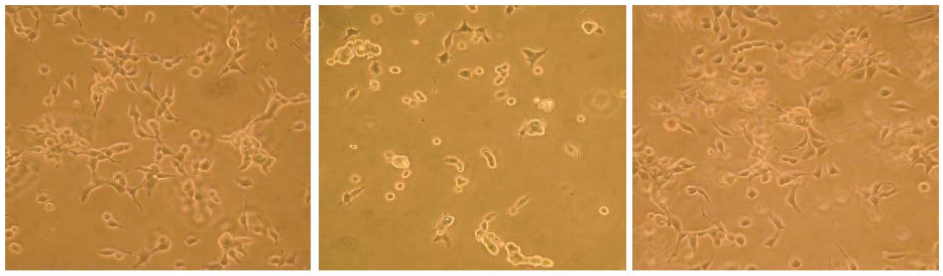

-Doxy **+Doxy** **+Doxy +STI571**

2-1C)

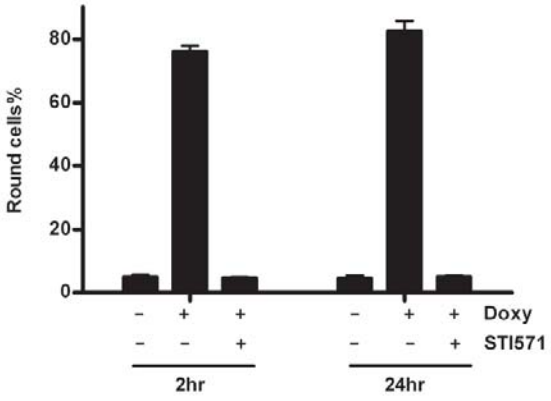

2-1D)

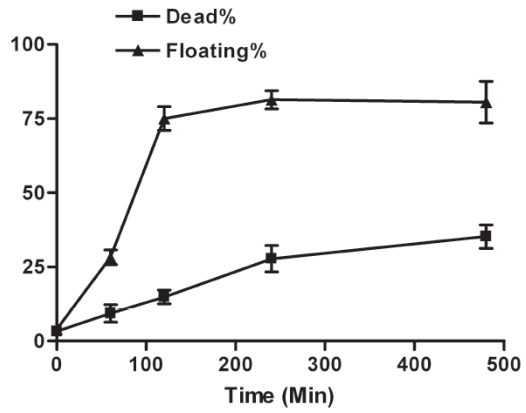

2-1E)

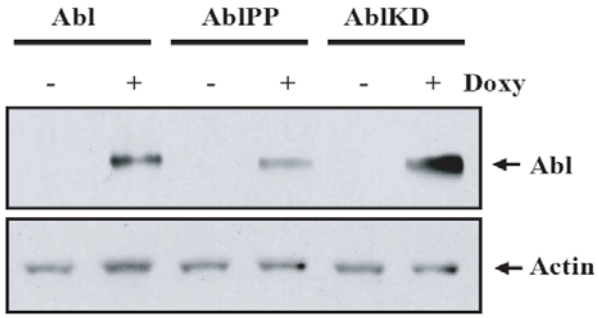

2-1F)

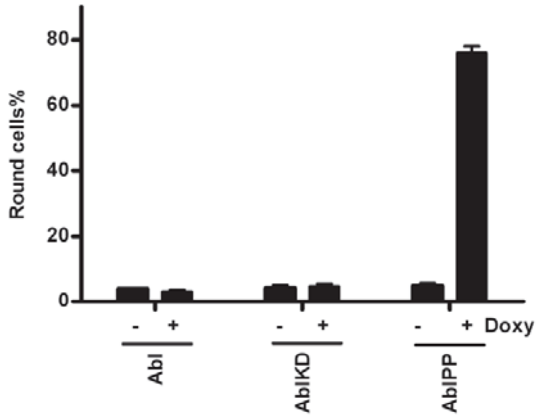

Figure 2-1 continued

Figure 2-2: AblPP expression inactivates integrins.
A. and B. The activated Abl kinase caused a decrease in cell adhesion. HEK293-AblKD and HEK293-AblPP cells were treated with 2 μg/ml doxycycline for 2 hours. Cell adhesion was measured as described in experimental procedures. The data were from three technical repeats.
C. and D. AblPP, but not AblKD caused the affinity of β1 integrins to drop. HEK293-AblKD and HEK293-AblPP cells were treated with 2 μg/ml doxycycline for 2 hours, in the absence or presence of 5 μg/ml of STI571. Integrin affinity was measured as described in experimental procedures.
E. The average level of β1 integrin activation is lower after AblPP induction in HEK293-AblPP cells. The histogram shows normalized average values ± s.e.m. (quantified from FACS) from three technical repeats. The integrin affinity measurement was performed as described in experimental procedures.

2-2A)

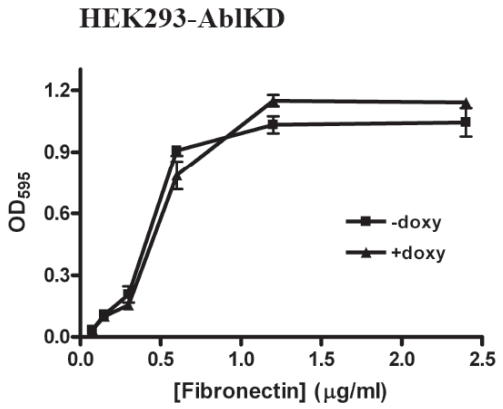
HEK293-AblKD
1.2
0.9
0.6
0.3
0.0
OD595
-doxy
+doxy
0.0
0.5
1.0
1.5
2.0
2.5
[Fibronectin] (μg/ml)

2-2B)

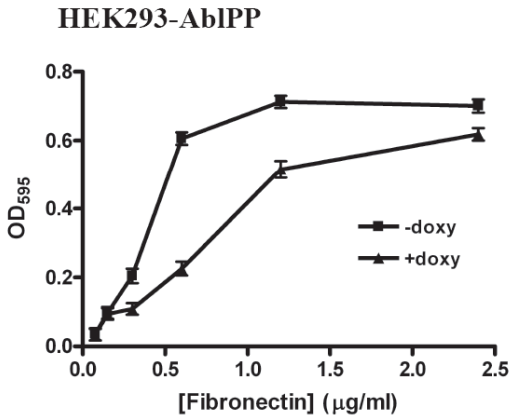
HEK293-AblPP
0.8
0.6
0.4
0.2
0.0
OD595
-doxy
+doxy
0.0
0.5
1.0
1.5
2.0
2.5
[Fibronectin] (μg/ml)

2-2C)

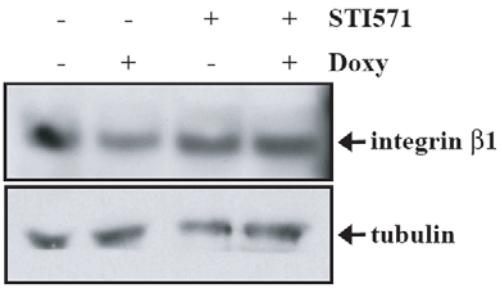
- - + + STI571
- + - + Doxy
integrin β1
tubulin

2-2D)

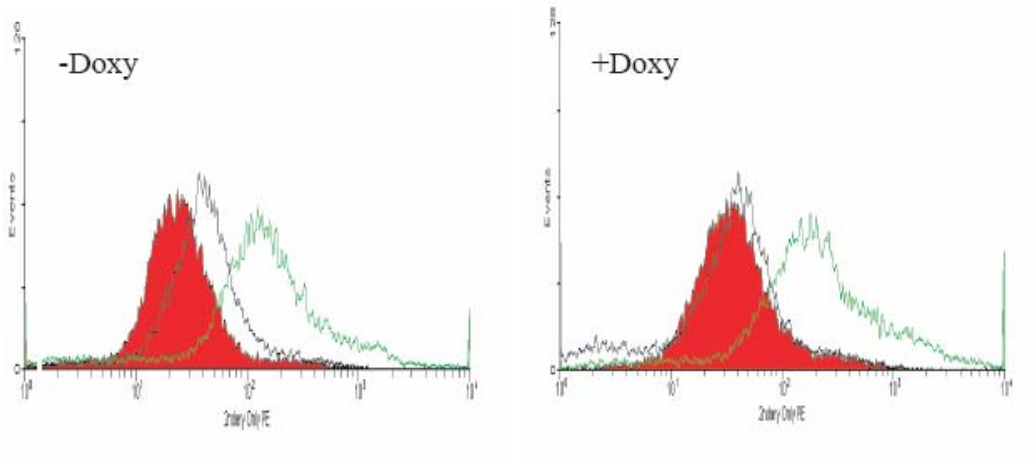

2-2E)

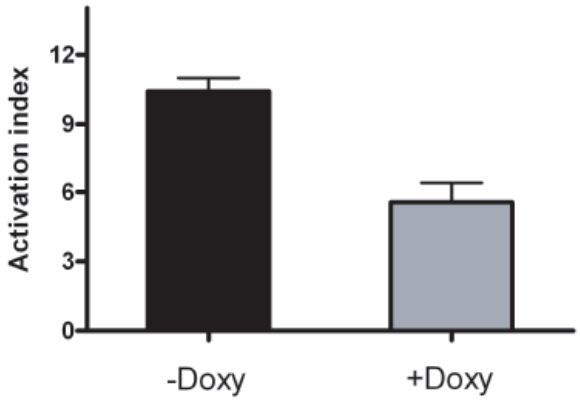

Figure 2-2 continued

Figure 2-3: Activation of Abl kinase disrupts CrkII-C3G complex, thus causes Rap1-GTP level to go down.

A. Active Abl kinase caused Rap1-GTP levels to go down. HEK293-AblPP cells were treated with 2 μg/ml doxycycline for 2 hours. Rap1-GTP levels were measured as described in experimental procedures.

B. The average level of Rap1-GTP dropped after AblPP expression in HEK293-AblPP cells. The histogram shows normalized average values ± s.e.m. (quantified from immunoblots) from three independent experiments.

C. A constitutively active Rap1 mutant (Rap1V12) abrogated AblPP-induced cell detachment. HEK293-AblPP cells were transfected with 2 μg of GFP, Rap1GAP, or Rap1V12 respectively for 48 hours. The cells were then treated with 2 μg/ml doxycycline for 2 hours. Detached cells were counted as described in experimental procedures.

D. Active Abl kinase phosphorylates CrkII on Tyr221. HEK293-AblPP cells were treated with 2 μg/ml doxycycline for 2 hours. Whole cell lysates were probed with an antibody recognizing phosphorylated Tyr221 of CrkII and then reprobed with an antibody to CrkII.

E. CrkII forms a complex with C3G and this complex was disrupted by AblPP induction. HEK293-AblPP cells were treated with 2 μg/ml doxycycline for 2 hours. Western blots of CrkII immunoprecipitates were probed with anti-HA or anti-C3G antibodies. Whole cell lysates were probed with the same antibodies to be used as loading controls.

F. CrkIIY221F, the dominant negative form of CrkII, abrogated AblPP-induced detachment of HEK293-AblPP cells. HEK293-AblPP cells were transfected with 2 μg of CrkIIY221F plasmid for 48 hours. The cells were then subjected to treatment with 2 μg/ml doxycycline for 2 hours. Detached cells were counted as described in experimental procedures. The histogram shows normalized average values ± s.e.m. from three independent experiments.

G. CrkIIY221F, the dominant negative form of CrkII, abrogated AblPP-induced decrease of Rap1-GTP levels. HEK293-AblPP cells were transfected with 2 μg of CrkIIY221F plasmid for 48 hours. The cells were then subjected to treatment with 2 μg/ml doxycycline for 2 hours. Rap1-GTP levels were measured as described in experimental procedures.

2-3A)

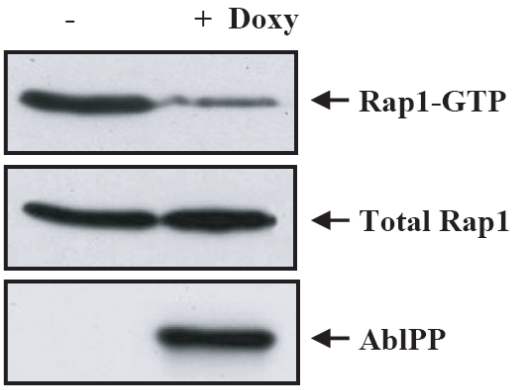
- + Doxy
Rap1-GTP
Total Rap1
AblPP

2-3B)

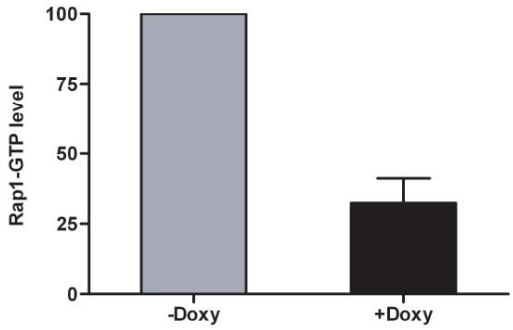
100
75
50
25
0
Rap1-GTP level
-Doxy
+Doxy

2-3C)

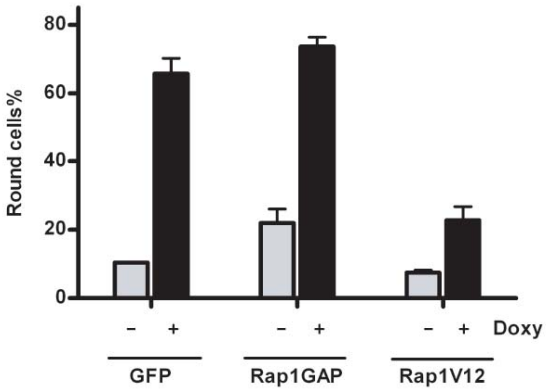
80
60
40
20
0
Round cells%
- + - + - + Doxy
GFP
Rap1GAP
Rap1V12

2-3D)

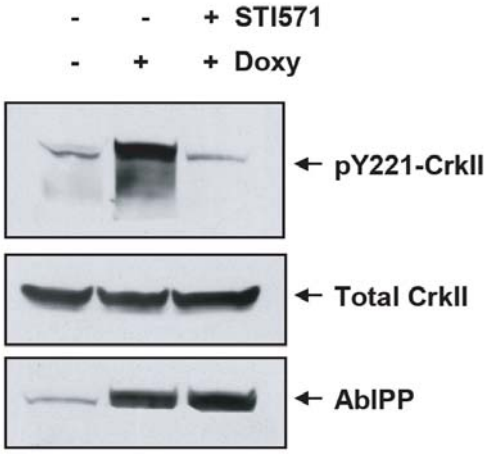

2-3E)

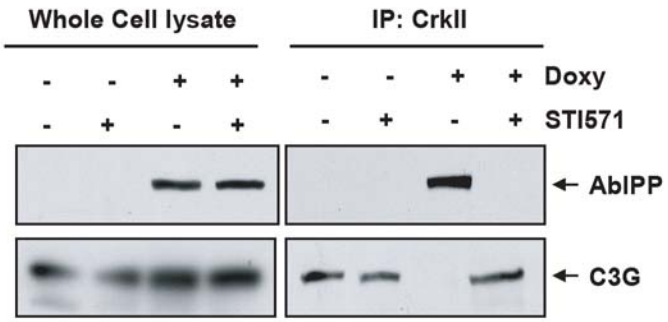

Figure 2-3 continued

2-3F)

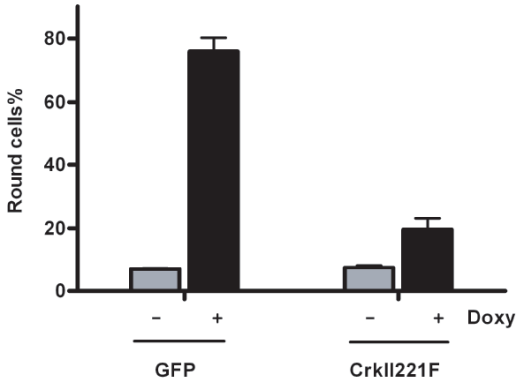

2-3G)

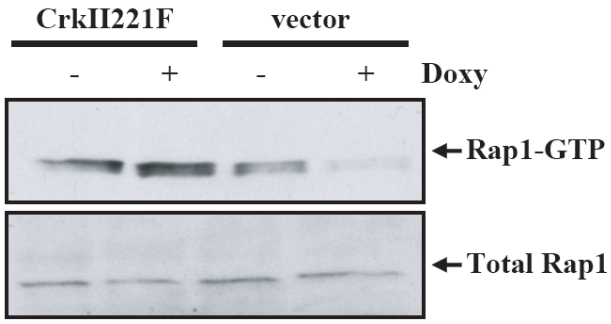

Figure 2-3 continued

Figure 2-4: The Rho-ROCK1 pathway was required in order for HEK293-AblPP cells to detach after Abl activation.
A. Induction of AblPP induced the host HEK293-AblPP cells to detach from supporting matrix in complete media, but not in serum-free media. HEK293-AblPP cells were cultured overnight; the media were then changed to fresh DMEM media in the presence or absence of serum. The cells were then treated with 2 μg/ml doxycycline for 2 hours. Cells were fixed and observed under phase contrast microscope.
B. The average level of cell detachment of HEK293-AblPP cells in DMEM media, in the presence or absence of serum. The histogram shows normalized average values ± s.e.m. from three independent experiments.
C. Presence of growth factors and Abl activation were both required to induce the host HEK293-AblPP cells to detach from the supporting matrix. HEK293-AblPP cells were treated with 2 μg/ml doxycycline for 2 hours in serum free media, in the presence or absence of 1 μg/ml LPA. Cells were then fixed and stained with FITC-conjugated phalloidin. Actin morphology was observed under fluorescence microscope.
D. The average level of cell detachment of HEK293-AblPP cells in serum-free DMEM media, in the presence or absence of serum or LPA. The experiment was performed as 2-4B. The histogram shows normalized average values ± s.e.m. from three independent experiments.
E. Rho activity is required for activated Abl to induce cells to detach. HEK293-AblPP cells were transfected with 2 μg of the constitutively activated Rho mutant, RhoV14, or the dominant negative Rho mutant, RhoN19 constructs for 48 hours. Cells were then treated with 2 μg/ml doxycycline for 2 hours. The detached cells were counted as described in experimental procedures. The histogram shows normalized average values ± s.e.m. from three independent experiments.
F. A specific inhibitor of ROCK1, Y27632 can completely block AblPP-induced HEK293-AblPP cell detachment from the supporting matrix. HEK293-AblPP cells were pre-treated with 20 nM Y27632 for 1 hour and then treated with 2 μg/ml doxycycline for 2 hours. The detached cells were counted as described in experimental procedure.
G. Knockdown of the ROCK1 protein. HEK293-AblPP cells were transfected with control-siRNA *(LacZ)* or *ROCK1*-siRNA. At 48 hours post transfection, both pools of the cells were treated with or without 2 μg/ml doxycycline for 2 hours. Whole cell lysates were then collected and probed with anti-ROCK1 antibodies; anti-actin blot was used as loading control.
H. Knockdown of ROCK1 inhibited AblPP-induced HEK293-AblPP cell detachment. At 48 hours post transfection with the indicated siRNA, HEK293-AblPP cells were treated with 2 μg/ml doxycycline for 2 hours. The detached cells were counted as described in experimental procedure. The histogram shows normalized average values ± s.e.m. from three independent experiments.

2-4A)

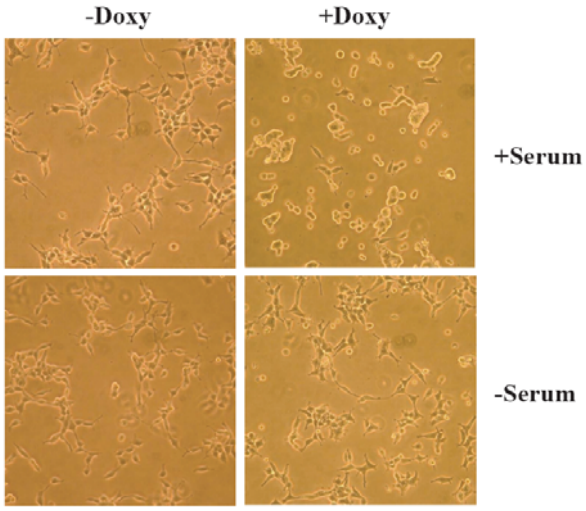
-Doxy
+Doxy
+Serum
-Serum

2-4B)

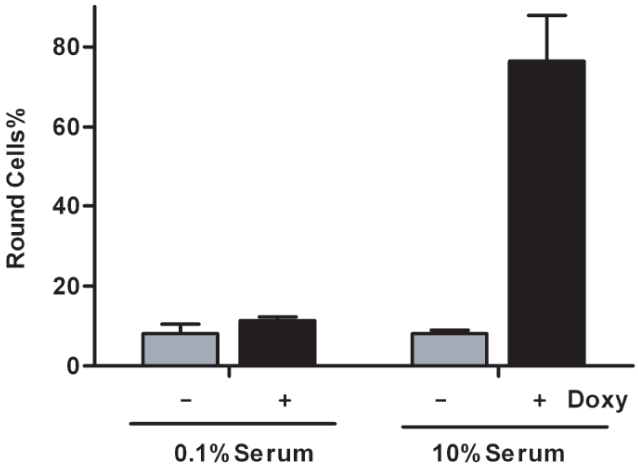
Round Cells%
80
60
40
20
0
-
+
-
+ Doxy
0.1% Serum
10% Serum

2-4C)

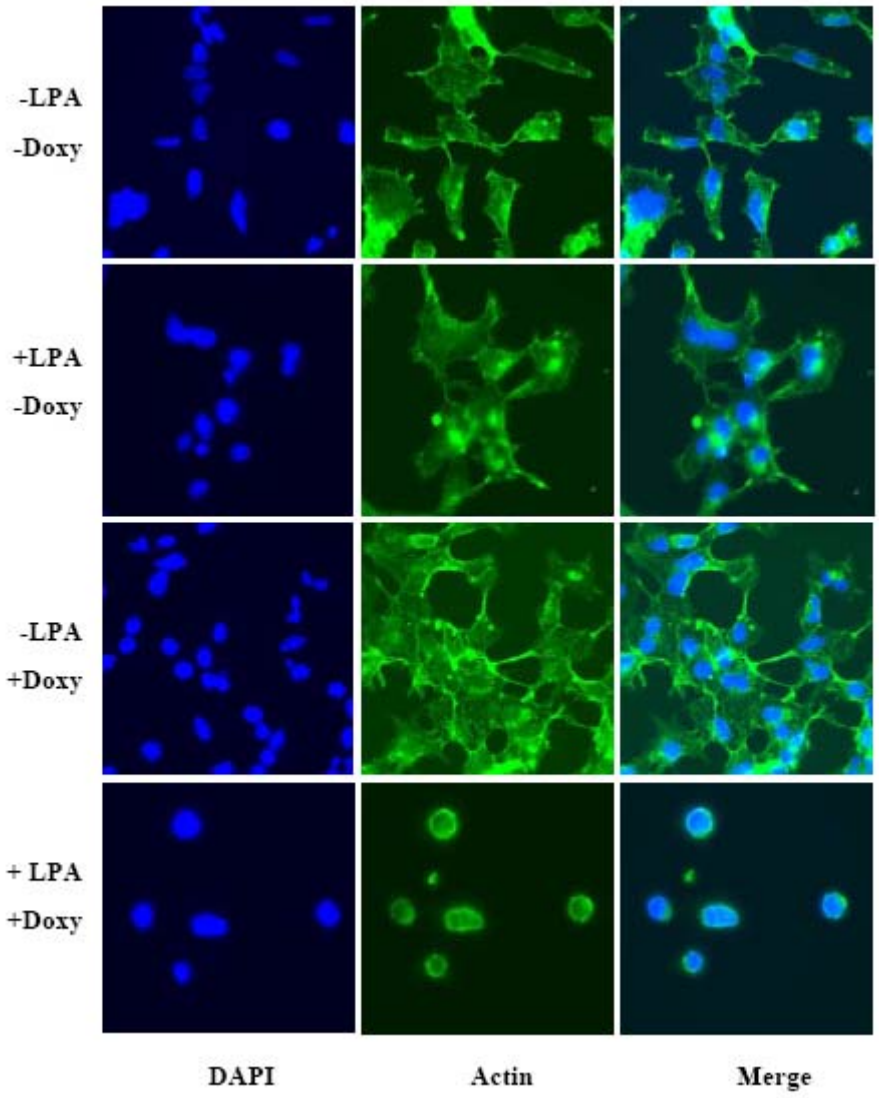

Figue 2-4 continued

2-4D)

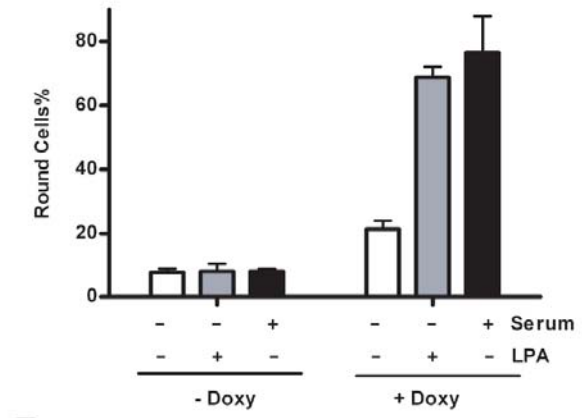

2-4E)

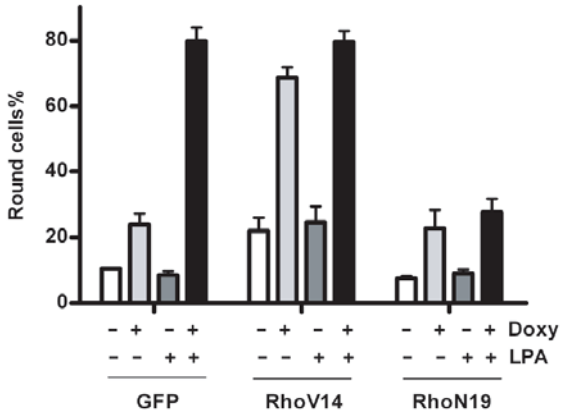

Figure 2-4 continued

2-4F)

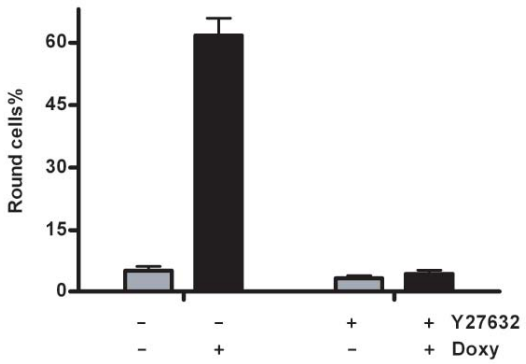

2-4G)

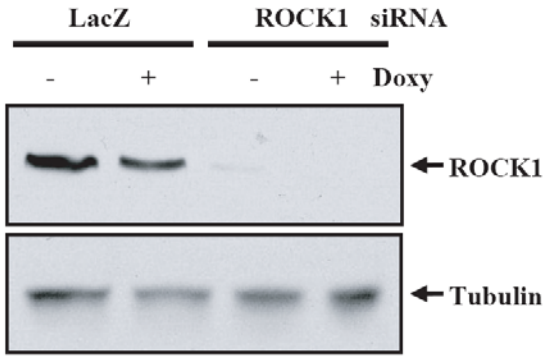

2-4H)

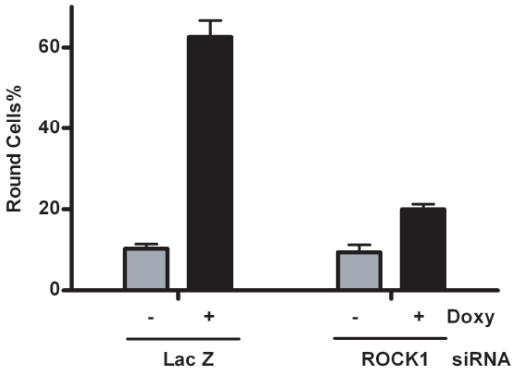

Figue 2-4 continued

Figure 2-5: The pathways induced by Abl activation and LPA are independent of each other.
A. and B. HEK293-AblPP cells were cultured overnight and then were kept in complete media (lanes 3, 4, CM, complete media) or subjected to serum starvation (lanes 1, 2, SFM, serum-free media) for 12 hours. The cells were then treated with or without 2 μg/ml doxycycline for 2 hours. The serum-starved cells (lanes5-8) were also subject to LPA treatment (lanes 6, 8) for 5 minutes with (lanes 7, 8) or without AblPP (lanes 5, 6) by treating with 2 μg/ml doxycycline for 2 hours. Rap1-GTP (A) or RhoA-GTP (B) were then pulled down from whole cell lysates as described in experimental procedures. Whole cell lysates were also resolved and immunoblotted with antibodies to Rap1 or RhoA as loading controls.

2-5A)

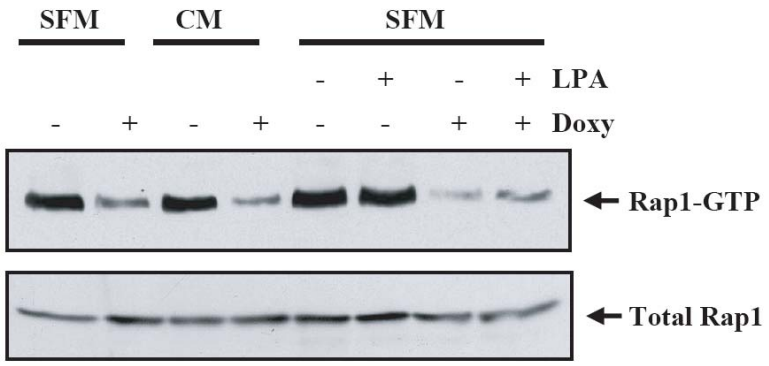
SFM
CM
SFM
- + - + LPA
- + - + - - + + Doxy
Rap1-GTP
Total Rap1

2-5B)

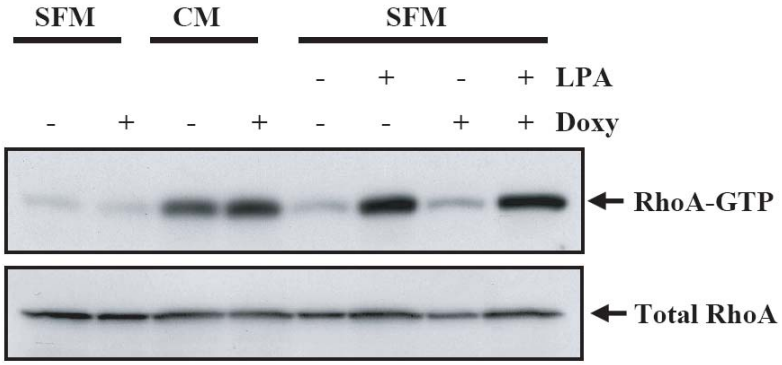
SFM
CM
SFM
- + - + LPA
- + - + - - + + Doxy
RhoA-GTP
Total RhoA

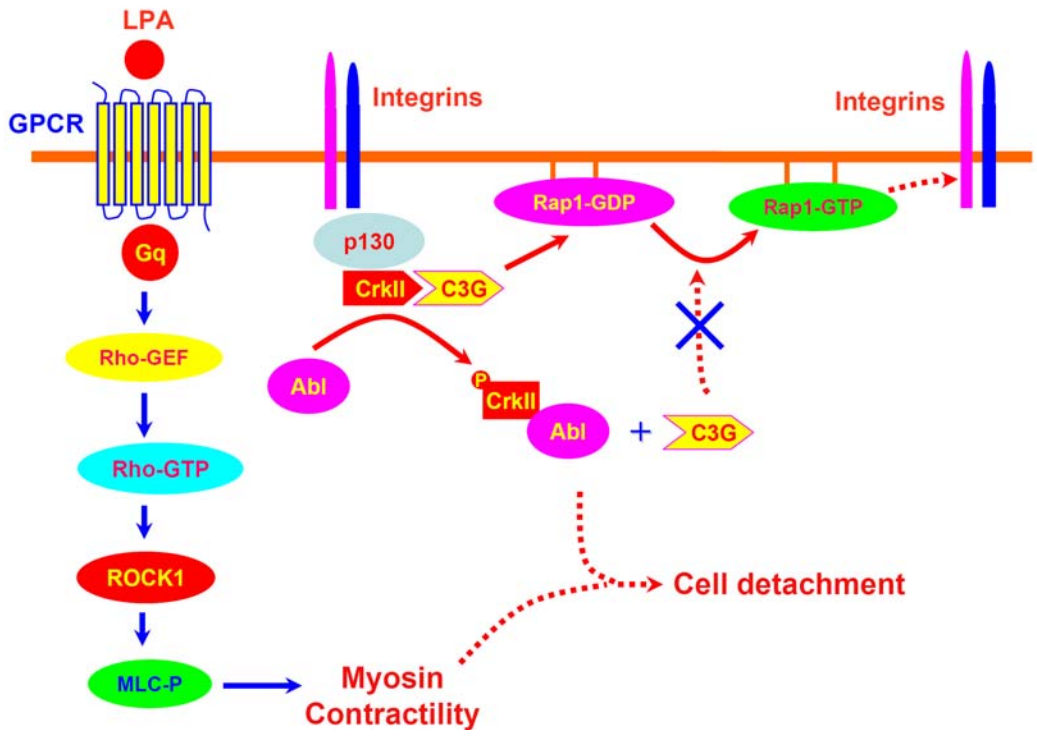

Figure 2-6: Two independent pathways are both required for activated Abl kinase to induce cells to detach.
Activation of the Abl kinase disrupts the complex between CrkII and C3G. The disruption of this complex disables the GEF activity of C3G. Without the GEF activity of C3G, Rap1 remains GDP-bound, and thus inactivated. This inactivation of Rap1 causes β1 integrin affinity to drop. At the same time, growth factors or LPA activate the Rho-ROCK pathway to generate myosin contractility. Only when both pathways exist, are HEK293-AblPP cells able to detach from the supporting matrix.

Figure 2-7: Ephrin A1-induced PC3 cell detachment also caused Rap1-GTP level to go down and requires ROCK1 activity.
A. STI571 partially blocked ephrin A1-induced PC3 cell detachment. PC3 cells were treated with 2 μg/ml ephrin A1 for 10 minutes, in the absence or presence of 5 μg/ml STI571. The cells were then fixed and observed under a phase contrast microscope.
B. The average level of detached PC3 cells was reduced by pretreatment with 5 μg/ml STI571 in PC3 cells. The histogram shows normalized average values ± s.e.m. from three independent experiments.
C. Endogenous c-Abl was phosphorylated within 15 minutes after treatment of PC3 cells with 2 μg/ml ephrin A1. After 15 minutes of treatment with ephrin A1, either in the absence or presence of 5 μg/ml STI571, PC3 cells were collected. Western blots of Abl immunoprecipitates were probed with the anti-phospho-tyrosine antibody 4G10. Whole cell lysates were probed with an anti-Abl antibody as loading control.
D. Time course experiment of c-Abl phosphorylation after treatment of PC3 cells with 2 μg/ml ephrin A1. PC3 cells were treated with ephrin A1 for different lengths of time. Western blots of Abl immunoprecipitates were probed with the anti-phospho-tyrosine antibody 4G10.
E. Ephrin A1 treatment led to a reduction in Rap1-GTP levels, but could be rescued by pre-treatment with 5 μg/ml STI571. PC3 cells were subjected to ephrin A1 treatment for 15 minutes, and Rap1-GTP was pulled-down and detected as described in experimental procedures.
F. ROCK1 activity was also required for ephrin A1-induced cell detachment. PC3 cells were treated with 2 μg/ml ephrin A1 for 15 minutes, either in the absence or presence of 20 nM Y27632, a specific ROCK1 inhibitor. The cells were then fixed and observed under a phase contrast microscope.
G. The average level of detached PC3 cells was reduced after pretreatment with a ROCK1 specific inhibitor, Y27632 in PC3 cells. The histogram shows normalized average values ± s.e.m. from three independent experiments.

2-7A)

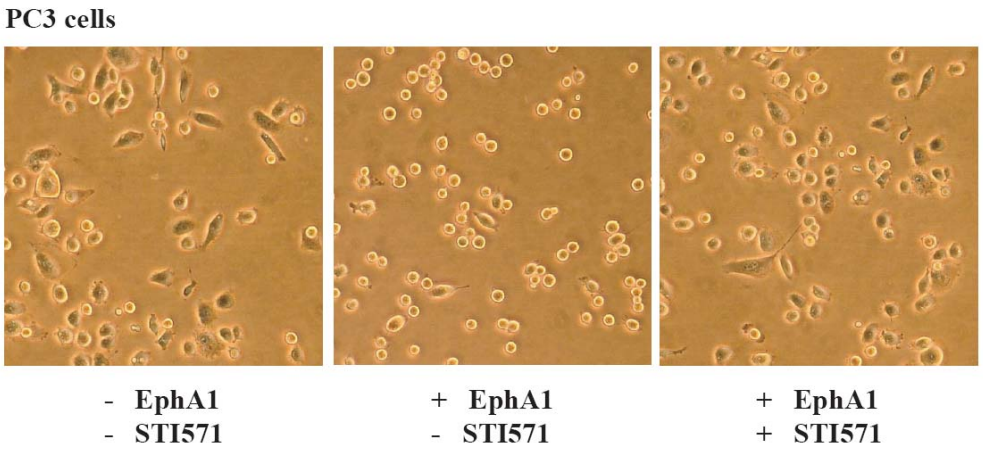
PC3 cells
- EphA1
- STI571
+ EphA1
- STI571
+ EphA1
+ STI571

2-7B)

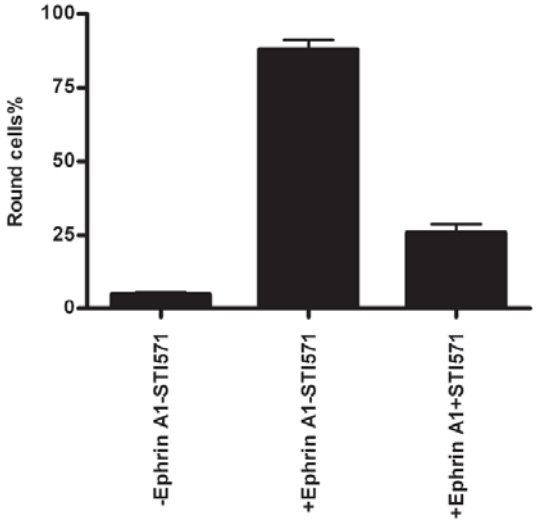
Round cells%
100
75
50
25
0
-Ephrin A1-STI571
+Ephrin A1-STI571
+Ephrin A1+STI571

2-7C)

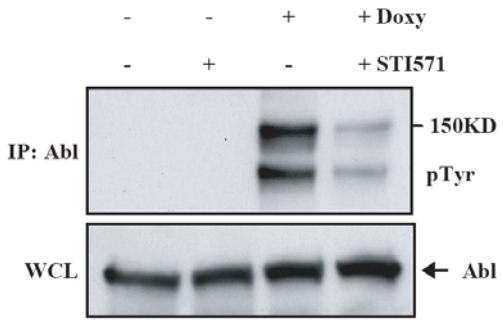

2-7D)

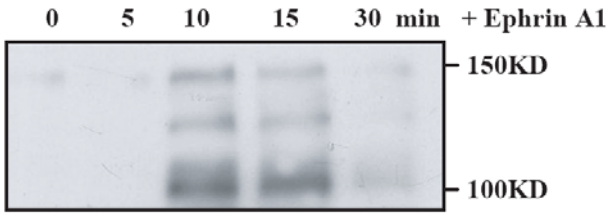

2-7E)

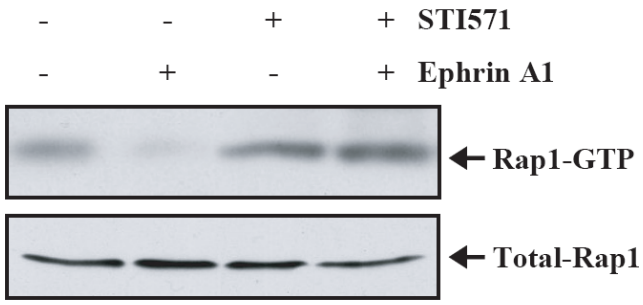

Figure 2-7 continued

2-7F)

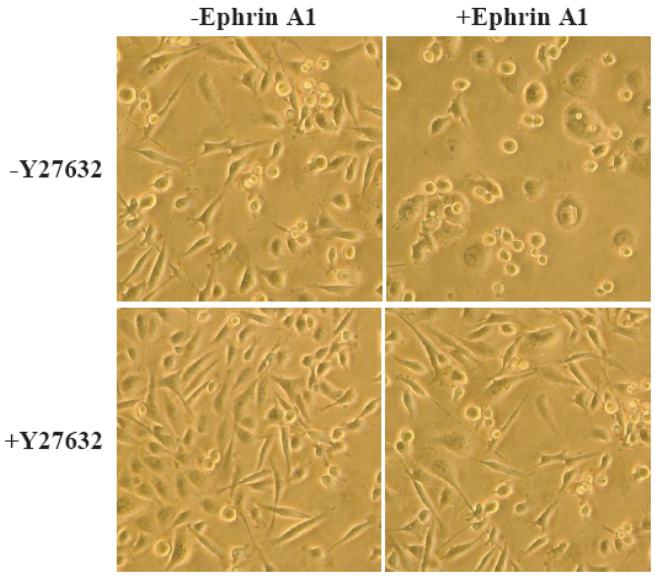

2-7G)

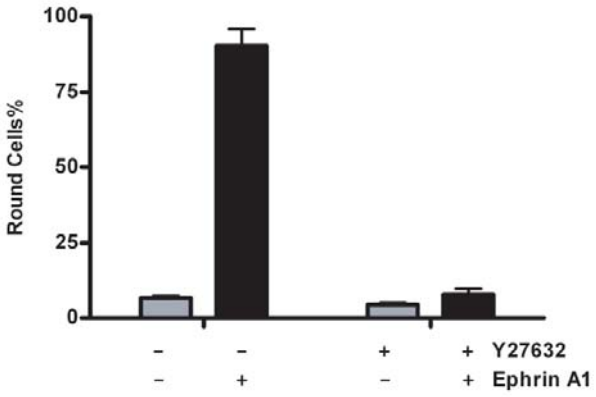

Figure 2-7 continued

REFERENCES

1. Ginsberg, M.H., A. Partridge, and S.J. Shattil, *Integrin regulation.* Curr Opin Cell Biol, 2005. **17**(5): p. 509-16.

2. Hynes, R.O., *Integrins: bidirectional, allosteric signaling machines.* Cell, 2002. **110**(6): p. 673-87.

3. Hynes, R.O., *Integrins: a family of cell surface receptors.* Cell, 1987. **48**(4): p. 549-54.

4. Frisch, S.M. and R.A. Screaton, *Anoikis mechanisms.* Curr Opin Cell Biol, 2001. **13**(5): p. 555-62.

5. Schwartz, M.A. and M.H. Ginsberg, *Networks and crosstalk: integrin signalling spreads.* Nat Cell Biol, 2002. **4**(4): p. E65-8.

6. Wang, J.Y., *Controlling Abl: auto-inhibition and co-inhibition?* Nat Cell Biol, 2004. **6**(1): p. 3-7.

7. Woodring, P.J., T. Hunter, and J.Y. Wang, *Inhibition of c-Abl tyrosine kinase activity by filamentous actin.* J Biol Chem, 2001. **276**(29): p. 27104-10.

8. Gong, J.G., et al., *The tyrosine kinase c-Abl regulates p73 in apoptotic response to cisplatin-induced DNA damage.* Nature, 1999. **399**(6738): p. 806-9.

9. Preyer, M., C.W. Shu, and J.Y. Wang, *Delayed activation of Bax by DNA damage in embryonic stem cells with knock-in mutations of the Abl nuclear localization signals.* Cell Death Differ, 2007. **14**(6): p. 1139-48.

10. Lewis, J.M., et al., *Integrin regulation of c-Abl tyrosine kinase activity and cytoplasmic-nuclear transport.* Proc Natl Acad Sci U S A, 1996. **93**(26): p. 15174-9.

11. Plattner, R., et al., *c-Abl is activated by growth factors and Src family kinases and has a role in the cellular response to PDGF.* Genes Dev, 1999. **13**(18): p. 2400-11.

12. Woodring, P.J., T. Hunter, and J.Y. Wang, *Regulation of F-actin-dependent processes by the Abl family of tyrosine kinases.* J Cell Sci, 2003. **116**(Pt 13): p. 2613-26.

13. Bos, J.L., J. de Rooij, and K.A. Reedquist, *Rap1 signalling: adhering to new models.* Nat Rev Mol Cell Biol, 2001. **2**(5): p. 369-77.

14. Bos, J.L., et al., *In search of a function for the Ras-like GTPase Rap1.* FEBS Lett, 1997. **410**(1): p. 59-62.

15. Gotoh, T., et al., *Identification of Rap1 as a target for the Crk SH3 domain-binding guanine nucleotide-releasing factor C3G.* Mol Cell Biol, 1995. **15**(12): p. 6746-53.

16. de Rooij, J., et al., *Epac is a Rap1 guanine-nucleotide-exchange factor directly activated by cyclic AMP.* Nature, 1998. **396**(6710): p. 474-7.

17. Kawasaki, H., et al., *A family of cAMP-binding proteins that directly activate Rap1.* Science, 1998. **282**(5397): p. 2275-9.

18. Polakis, P.G., et al., *Purification of a plasma membrane-associated GTPase-activating protein specific for rap1/Krev-1 from HL60 cells.* Proc Natl Acad Sci U S A, 1991. **88**(1): p. 239-43.

19. Herrmann, C., et al., *Differential interaction of the ras family GTP-binding proteins H-Ras, Rap1A, and R-Ras with the putative effector molecules Raf kinase and Ral-guanine nucleotide exchange factor.* J Biol Chem, 1996. **271**(12): p. 6794-800.

20. Cook, S.J., et al., *RapV12 antagonizes Ras-dependent activation of ERK1 and ERK2 by LPA and EGF in Rat-1 fibroblasts.* Embo J, 1993. **12**(9): p. 3475-85.

21. Zwartkruis, F.J., et al., *Extracellular signal-regulated activation of Rap1 fails to interfere in Ras effector signalling.* Embo J, 1998. **17**(20): p. 5905-12.

22. Reedquist, K.A., et al., *The small GTPase, Rap1, mediates CD31-induced integrin adhesion.* J Cell Biol, 2000. **148**(6): p. 1151-8.

23. Katagiri, K., et al., *Rap1 is a potent activation signal for leukocyte function-associated antigen 1 distinct from protein kinase C and phosphatidylinositol-3-OH kinase.* Mol Cell Biol, 2000. **20**(6): p. 1956-69.

24. Caron, E., A.J. Self, and A. Hall, *The GTPase Rap1 controls functional activation of macrophage integrin alphaMbeta2 by LPS and other inflammatory mediators.* Curr Biol, 2000. **10**(16): p. 974-8.

25. Chrzanowska-Wodnicka, M. and K. Burridge, *Rho-stimulated contractility drives the formation of stress fibers and focal adhesions.* J Cell Biol, 1996. **133**(6): p. 1403-15.

26. Burridge, K. and K. Wennerberg, *Rho and Rac take center stage.* Cell, 2004. **116**(2): p. 167-79.

27. Kimura, K., et al., *Regulation of myosin phosphatase by Rho and Rho-associated kinase (Rho-kinase).* Science, 1996. **273**(5272): p. 245-8.

28. Riveline, D., et al., *Focal contacts as mechanosensors: externally applied local mechanical force induces growth of focal contacts by an mDia1-dependent and ROCK-independent mechanism.* J Cell Biol, 2001. **153**(6): p. 1175-86.

29. Watanabe, N., et al., *Cooperation between mDia1 and ROCK in Rho-induced actin reorganization.* Nat Cell Biol, 1999. **1**(3): p. 136-43.

30. Li, F. and H.N. Higgs, *The mouse Formin mDia1 is a potent actin nucleation factor regulated by autoinhibition.* Curr Biol, 2003. **13**(15): p. 1335-40.

31. Barila, D., et al., *A nuclear tyrosine phosphorylation circuit: c-Jun as an activator and substrate of c-Abl and JNK.* Embo J, 2000. **19**(2): p. 273-81.

32. Welch, P.J. and J.Y. Wang, *Abrogation of retinoblastoma protein function by c-Abl through tyrosine kinase-dependent and -independent mechanisms.* Mol Cell Biol, 1995. **15**(10): p. 5542-51.

33. Ohba, Y., et al., *Requirement for C3G-dependent Rap1 activation for cell adhesion and embryogenesis.* Embo J, 2001. **20**(13): p. 3333-41.

34. Kimura, K., et al., *Regulation of the association of adducin with actin filaments by Rho-associated kinase (Rho-kinase) and myosin phosphatase.* J Biol Chem, 1998. **273**(10): p. 5542-8.

35. Hart, M.J., et al., *Direct stimulation of the guanine nucleotide exchange activity of p115 RhoGEF by Galpha13.* Science, 1998. **280**(5372): p. 2112-4.

36. Kozasa, T., et al., *p115 RhoGEF, a GTPase activating protein for Galpha12 and Galpha13.* Science, 1998. **280**(5372): p. 2109-11.

37. Hernandez, S.E., et al., *How do Abl family kinases regulate cell shape and movement?* Trends Cell Biol, 2004. **14**(1): p. 36-44.

38. Miao, H., et al., *Activation of EphA2 kinase suppresses integrin function and causes focal-adhesion-kinase dephosphorylation.* Nat Cell Biol, 2000. **2**(2): p. 62-9.

39. Carter, N., et al., *EphrinA1-induced cytoskeletal re-organization requires FAK and p130(cas).* Nat Cell Biol, 2002. **4**(8): p. 565-73.

40. Lewis, J.M. and M.A. Schwartz, *Integrins regulate the association and phosphorylation of paxillin by c-Abl.* J Biol Chem, 1998. **273**(23): p. 14225-30.

41. Maddox, A.S. and K. Burridge, *RhoA is required for cortical retraction and rigidity during mitotic cell rounding.* J Cell Biol, 2003. **160**(2): p. 255-65.

42. Stupack, D.G., et al., *Potentiation of neuroblastoma metastasis by loss of caspase-8.* Nature, 2006. **439**(7072): p. 95-9.

43. Dan, S., et al., *Activation of c-Abl tyrosine kinase requires caspase activation and is not involved in JNK/SAPK activation during apoptosis of human monocytic leukemia U937 cells.* Oncogene, 1999. **18**(6): p. 1277-83.

44. Stupack, D.G., et al., *Apoptosis of adherent cells by recruitment of caspase-8 to unligated integrins.* J Cell Biol, 2001. **155**(3): p. 459-70.

45. Schwartz, M.A. and R.K. Assoian, *Integrins and cell proliferation: regulation of cyclin-dependent kinases via cytoplasmic signaling pathways.* J Cell Sci, 2001. **114**(Pt 14): p. 2553-60.

46. Worthylake, R.A. and K. Burridge, *Leukocyte transendothelial migration: orchestrating the underlying molecular machinery.* Curr Opin Cell Biol, 2001. **13**(5): p. 569-77.

47. Bertoni, A., et al., *Relationships between Rap1b, affinity modulation of integrin alpha IIbbeta 3, and the actin cytoskeleton.* J Biol Chem, 2002. **277**(28): p. 25715-21.

48. Hall, A. and C.D. Nobes, *Rho GTPases: molecular switches that control the organization and dynamics of the actin cytoskeleton.* Philos Trans R Soc Lond B Biol Sci, 2000. **355**(1399): p. 965-70.

CHAPTER 3

Systems analysis of quantitative shRNA-library screens indentifies novel regulators of cell adhesion

ABSTRACT

High throughput screens with RNA interference technology enable loss-of-function analysis of gene activities in mammalian cells. Previously, several lentivirus-based shRNA libraries have been used to identify gene functions through clonal and qualitative analyses. However, because of the relatively high noise levels and the fact that not all shRNAs are functional, these screens can be difficult to analyze. To deal with these issues we developed a new analytical strategy that combines the quantitative data with biological knowledge, i.e. Gene Ontology and pathway information, to increase the power of this technique. Using this strategy we identified 16 candidate shRNA-target genes associated with cell detachment induced by a deregulated c-Abl tyrosine kinase. Included in this set of genes was IL6ST, a cellular membrane protein that we have confirmed as being involved in c-Abl-induced cell detachment through independent shRNA experiments. Our results suggest that the power of genome-wide quantitative shRNA screens can be significantly increased when analyzed using a systems biology-based approach to identify functional gene networks.

INTRODUCTION

RNA interference with small interfering RNAs (siRNA) and short hairpin RNAs (shRNA) has proven to be a powerful tool for genetic synthetic lethality studies, especially for diploid mammalian cells [1]. Short double-stranded RNAs between 19-29

base pairs can efficiently silence gene expression by mediating the sequence-specific degradation of target mRNAs [2] and leading to suppression of endogenous gene expression [3]. With whole genome sequences available for humans and many other model organisms, it is now possible to use shRNA libraries to perform genome-wide screens that examine the contribution of every gene to a specific biological process, by creating RNA interfering libraries to perturb the function of all known genes [4-7]. Among the current methods for large-scale shRNA library screens, one of the most efficient techniques uses lentivirus to transfer the whole shRNA library to the cell population of interest. The relative abundance of shRNAs can then be evaluated before and after treatment of cells by oligo-microarray.

However, there are some obstacles that must be overcome in order to extract reliable data from such a screen. For instance, although some shRNAs have been reported to down-regulate genes efficiently and specifically, there is currently no large scale shRNA library that has been thoroughly validated to be specific for the genes targeted. In addition, it is possible that some of the shRNAs might be lost in the study or simply be lethal to the cells, which would preclude them from providing useful data. Furthermore, the shRNAs recovered from a given population of cells must be amplified before being measured by microarray and it is likely that this amplification step will not be uniform across replicates. Finally, the commercial microarrays used to analyze shRNA abundance in these screens were originally designed to measure large mRNA transcripts rather than shorter shRNA molecules. The ability to extract statistically significant results from these microarrays came in part from the fact that most of these arrays were designed using multiple short oligo probes to measure one mRNA. However, the size of the shRNA

limits the readout for any given shRNA to only a single probe, reducing the statistical power of this method. While the inclusion of multiple shRNAs for each gene of interest helps to address this problem, this is still limited by the efficacy of each of the individual shRNAs. Collectively, these obstacles make the signal-to-noise ratio in current shRNA screening experiments very low compared to traditional microarray studies. To facilitate a reliable result from this type of experiments, we developed a method that makes use of the Gene Ontology (GO) information. This methodology allows us to increase the statistical power by grouping shRNAs by the functional category of their target genes.

GO terms are a summary of biological information about genes. It was organized into a hierarchy under one of the three root categories: Biological Process, Cellular Component, or Molecular Functions. Each of these three categories gives rise to a hierarchy of subgroups in which the biological process or function that the genes contribute to becomes more specific. By grouping genes into functional categories and doing statistical inference on sets of genes sharing similar functions, rather than on the individual genes themselves, we can greatly reduce the noise level and increase the statistical power. In addition, we drastically reduce the problem of off-target effects, as it is unlikely that multiple shRNAs will all have a similar off-target effect on a specific GO group.

In addition to Gene Ontology analysis, we also conducted pathway analysis based on gene interaction information retrieved from literatures. Network analysis has been shown to be a powerful tool to understand biological responses by providing a global view of gene products and their relationships [8]. Using these two bioinformatics methods, we have taken data from an shRNA screen of genes involved in Abl-induced

cell detachment and identified a new pathway regulating this process. The *c-Abl* gene encodes a ubiquitously expressed non-receptor tyrosine kinase that can be activated by various extracellular stimuli [9, 10], including growth factors and ECM proteins to regulate distinct F-actin structures [11]. Thus, the Abl kinase has been shown to play a role in a number of actin-dependent processes such as cell spreading, cell migration, membrane ruffling, neurite extension, and focal adhesion formation [11-13].

While all this research has established a definitive role for c-Abl in cytoskeletal rearrangement, the investigations of the mechanisms governing these processes are still in their early stages [11, 14]. To further understand the pathways involved in these processes, we built an HEK293 cell line expressing a constitutively activate Abl protein (AblPP) under the control of a TET-on promoter. Induction of Abl in this system induced host cells to detach from the supporting matrix. To identify the genes involved in this process of cell detachment, we infected these cells with an shRNA library targeting 8,500 human genes and screened for shRNAs that were present in differential amount before and after Abl induction. Using GO terms to identify groups of genes affected by Abl induction, and network analysis to identify the most likely connection between these genes and Abl, we were able to identify new Abl-dependent pathways of cytoskeletal rearrangement. As a proof of principle, we have experimentally confirmed one of the putative effectors, the membrane protein IL6ST. Taken together, these results show the power of using systems biology approach to extract meaningful results from shRNA screening studies.

MATERIALS AND METHODS

Cell culture **-** HEK293 cells expressing AblPP under the control of TET-regulated promoter (TET-on system) were generated as described (Huang et al., in preparation). These cells were cultured in DMEM media containing 10% FBS, penicillin/streptomycin and 0.1% β-mercaptoethanol. Cells were routinely treated with 2 μg/ml doxycycline at 37ºC to induce cell detachment unless noted otherwise.

Lentirirus production and infection of AblPP cells **-** Lentiviral particles were generated by transient transfection of 293FT cells by IL6ST shRNAs (from Sigma) and VSV-G-expression plasmids. The supernatants were collected 48 hours after transfection. Stable cell lines expressing IL6ST shRNAs were generated by transduction with the retroviral supernatants in the presence of 8 μg/ml polybrene, with transduced cells selected for resistance to puromycin (2.0 μg/ml).

shRNA screen, provirus recovery, DNA microarray **-** The lentiviral shRNA library used was 8.5K human GeneNet^{TM} shRNA library constructed in pFIV-H1-puro vector, consisting of 42,500 shRNAs directed against 8,500 human genes. The infection of AblPP cells by this library was performed by following the standard protocol from GeneNet^{TM} (http://www.systembio.com/). Briefly, 1×10^6 AblPP cells were infected with the lentiviral shRNA library at an MOI of 0.5. One day after infection, the cells were selected with 2 μg/ml puromycin. Selected cells were subjected to two rounds of AblPP-induced cell detachment by treatment with 2 μg/ml doxycycline for 16 hours. The screened cells were amplified; total RNA was extracted and was reverse transcribed to cDNA. The proviral sequence in the remaining attached colonies was obtained by two

rounds of PCR. In the first round of PCR, the template used was cDNA and the primers were (forward: 5'-AATGTCTTTGGATTTGGGAATCTTA-3'; reverse: 5'-AAAAGGGTGGACTGGGATGAGTA-3'). During the second round of PCR two nested primers were used (forward: 5'-ATCGTCAATCACCTTCCTGTCAGA-3', and this primer has biotin residues at the 5' end; reverse: 5'-AATAGAAAGAATGCTTATGGACGCTA-3'). The amplified sequences of shRNA targets were used for hybridization with Affymetrix Human Genome Focus Arrays using standard protocols. Three biological repeats were performed, for both the surviving population and control population of cells.

Western Blot - Whole cell lysates were prepared in RIPA buffer (50 mM Tris-HCl [pH 7.4], 150 mM NaCl, 1% NP-40, 0.25% sodium deoxycholate, 0.1% SDS, 0.5 mM EDTA, 1 mM EGTA, 1 mM DTT) plus protease inhibitor (from Sigma); 50-100 μg of total protein were resolved by SDS-PAGE, transferred onto PVDF membranes, blocked in 5% nonfat dry milk/TBST (20 mM Tris-HCl [pH 7.5], 150 mM NaCl, 0.05% Tween-20) and incubated with primary antibodies overnight at 4°C. Membranes were washed 3 × 10 minutes in TBST and incubated with HRP-conjugated secondary antibodies for 1-3 hours at room temperature. After 3 × 10 minutes washing, membranes were incubated with enhanced ECL reagent (from Pierce) for 1 minute and exposed to X-ray films. Anti-pTyr antibody 4G10 and anti-Abl antibody 8E9 were both prepared from our lab.

Cell detachment assay - AblPP cells were seeded on 12-well plate coated with poly-L-lysine and cultured in 37°C for overnight. The cells were treated with 2 μg/ml doxycycline for different time and were fixed with 4% paraformaldehyde for 15 minutes,

washed with PBS and observed under phase-contrast microscope. The bright and round cells were treated as positive cells. In each assay, at least 300 cells were counted.

Data analysis - The shRNA levels of the 3 pre- and post- AblPP induction experiments were normalized by quartiles, and then log2 transformed using R language (http://cran.r-project.org/) and BioConductor packages (http://www.bioconductor.org/). In order to identify high- and low- abundant shRNAs, the shRNA levels of pre- induction were fitted by a Gaussian-Mixture model using EM algorithm and the probability of each shRNA belonging to high abundance group was calculated.

To be more robust to get rid of the possible noise in the data, while selecting the shRNAs that were enriched after selection we used the minimum of the log ratios among the 3 repeats. Then for each gene we selected one shRNA that has the maximum ratio as representative. To select shRNAs that were depleted after selection we calculated the pre-/post- ratio and repeated the above procedure. To be robust to the experimental and biological noises in the data, we used only the rank of the log ratios of genes. To calculate the p-value of genes being significantly enriched or depleted in the study, we used paired t-statistics to compare the shRNA abundance in pre- and post- induction.

Rank sum statistics of Gene Ontology - We used Gene Ontology (GO) to group genes based on their functional category and selected significant GO terms that are associated with cell detachment. The GO terms that are too general containing more than 500 genes or too specialized containing less than 2 genes were ignored. For the rest of the GO terms, we calculated the sum of rank of the genes that belong to the GO term, and compared that to the rank of 1000 randomly selected gene sets with the same number of genes to calculate the Z-score and corresponding P-value.

Protein interaction analysis - We constructed human protein interaction network from documented molecular interactions retrieved from Biomolecular Object Network Databank (BOND: http://bond.unleashedinformatics.com/) and Human Protein Reference Database (HPRD: http://www.hprd.org/) [15] and visualized by Cytoscape software V2.4 (http://www.cytoscape.org/). While building the interaction network, we kept only the protein-protein interactions since the cell detachment is a quick process regulated by only protein-protein interactions without gene transcription and translation involved. To find the shortest pathways to connect given genes in the protein interaction network, we first located the biggest connected component in the whole human protein network which contains 9150 genes and 35969 interactions, and ignored the remaining less connected genes. Then we assigned a weight to the edges connecting these genes by the sum of clustering coefficient of the 2 genes each edge connects [16]. Finally, the shortest path between a pair of given genes were found by the Dijkstra's shortest paths algorithm [17].

RESULTS AND DISCUSSION

shRNA library screening of AblPP-induced HEK293 cell detachment

Normally, the c-Abl tyrosine kinase is held in an inactive conformation in the absence of activation signals. The disruption of the inactive conformation can be achieved by substituting two proline residues for two glutamate residues in the linker region between the SH2 and catalytic domains (P242E/P249E). This mutant confers constitutive kinase activity to c-Abl [18]. We placed this Abl mutant under the control of

TET-regulated promoter (TET-on system) and stably transfected this construct into HEK293 cells (referred to AblPP cells from this point on). Upon AblPP expression, around 80% of the host cells detached from the supporting matrix in about 2 hours (Huang, X., *et al.*, in preparation).

To investigate the mechanism of Abl-induced cell detachment, we infected the AblPP cells with an 8.5K human GeneNet^{TM} shRNA library, which contains 43,828 shRNAs targeting 8,750 human genes (Figure 3-1A), with each gene being targeted by 4-5 shRNAs. The shRNAs in this library were designed based on the Affymetrix Human Genome Focus Array and therefore the relative abundance of each shRNA can be measured by the intensity of the signal from the corresponding probe on this array. AblPP cells infected with this library were first selected with puromycin to eliminate uninfected cells. The remaining cells were then subjected to two rounds of AblPP induction and cells that did not detach in response to AblPP induction were collected (Figure 3-1B). The insensitivity of these cells to AblPP induction was neither due to a loss of AblPP expression nor due to a loss of Abl kinase activity (Figure 3-1C). We then recovered the proviruses in the surviving cells and measured the abundance of shRNA. We performed 3 biological repeats.

Rank-based Gene Ontology analysis

The raw data of shRNA abundance before and after AblPP induction were quantile normalized and log transformed. The histogram of shRNA abundance prior to AblPP induction shows that many shRNAs had very low abundance even before AblPP

was induced. We reasoned that some of these shRNAs might have been lost during expansion of the culture, or might be lethal to the host cells. To filter out these shRNAs, we fitted the data of uninduced samples by a Gaussian Mixture model and selected 13,140 shRNAs that were highly abundant in all 3 replicates (with posterior probability above 0.99) for further analysis.

When analyzed in the same manner as a traditional mRNA microarray (for example, calculating the p-value for shRNAs by paired t-statistics and adjust the p-value to control False Discovery Rate (FDR)), we were unable to identify any shRNA from this library as being significantly different after AblPP induction. There are a number of possible reasons for this. First, the experimental protocols that were optimized to measure gene expression level might not be the best to measure the relative abundance of PCR product in our shRNA study. Second, Affymetrix microarrays were designed using 11-16 pairs of short oligo-probes to measure the expression level of one gene, thus the noise level can be repressed by averaging across multiple probes, whereas each shRNA sequence in our study can only be measured by one single probe. This severely limits the statistical power. And furthermore the shRNAs in the library are not functionally verified, some of them may not be able to down-regulate the gene of interest or may have off-target effects that may mislead results. Thus, in order to extract information form this shRNA screen data, we designed a new analysis method.

We designed a rank-based GO analysis method that is similar to the Gene Set Enrichment Analysis (GSEA) method [19], which resorts to Gene Ontology information to group shRNAs based on the known functions of their target genes (see Materials and Methods for details). By analyzing the collective data for a group of genes, rather than

any single gene alone, we effectively increased the statistical power of our analysis. In our analysis of these functional categories, we were able to find groups of genes significantly enriched or depleted after AblPP induction.

Specifically, shRNAs were assigned to their target genes based on Affymetrix annotations, and for each gene the shRNA with the maximum fold change after AblPP induction was used as the representative. To be robust, we used only the rank of the log ratio of genes. We grouped genes by their Gene Ontology categories, and for each GO category we calculated the mean rank of the fold change of genes, and compared this to a random set of genes to determine the p-value (see Materials and Methods for details). With criterion of a p-value below 0.01, we selected 7 GO terms in the category of Biological Process (BP), 2 GO terms in the category of Cellular Component (CC) and 9 GO terms in the category of Molecular Function (MF) whose constituent genes were significantly enriched after selection. We also selected 9 GO terms in BP, 2 GO terms in CC, and 9 GO terms in MF whose genes were significantly depleted. These GO terms are listed in Table 3-1 together with their *p*-values. Among these GO terms, some are known to be related to cell adhesion, such as transmembrane receptor protein tyrosine kinase signaling pathway (BP), negative regulation of cell proliferation (BP), extracellular matrix (CC), and collagen binding (MF).

Pathway analysis

Of the 8,500 genes targeted by the shRNA library, a total of 833 genes belonged to at least one of the significantly enriched or depleted GO terms. We built a human

protein interaction network based on the Biomolecular Object Network Database (BOND) and Human Protein Reference Database (HPRD), and mapped these genes into the network (Figure 3-2A). For these enriched and depleted genes, we then used paired t-statistics to compare their relative abundance before and after AblPP induction. There are 14 genes significantly enriched and 7 genes significantly depleted with p-value below 0.01 (Table 3-2 and 3-3), out of them 11 enriched and 5 depleted genes were also in the gene interaction network. We then tried to find shortest paths to connect each pair of the 16 significantly enriched or depleted genes to construct a Shortest Path Network (SPN) (Figure 3-2B). From this SPN, we further identified 7 hub genes with connectivity greater than 5 (Table 3-4) [20, 21]. In an independent candidate-approach study, we have identified ROCK1 to be required for Abl-induced detachment (Huang X., *et al.*, in preparation). We also integrated c-Abl and ROCK1 into this shortest path network.

IL6ST is an effector in AblPP-induced cell detachment pathway

Among the candidate genes, we found IL6ST, which has been shown to regulate cell-cell adhesion in a cadherin-dependent manner in cultured cardiomyocytes [22]. To validate the function of IL6ST in our study, we designed new shRNA sequences and infected AblPP cells with a lentiviral vector expressing these shRNAs. Quantitative PCR results indicated that the mRNA level of IL6ST was significantly reduced (Figure 3-3A). The AblPP cells depleted of IL6ST were resistant to AblPP-induced cell detachment (Figure 3-3B), and this phenotype was not due to either loss of AblPP expression or

phosphorylation in AblPP cells (Figure 3-3C), suggesting that IL6ST was a *bona fide* effector in Abl kinase-induced cell detachment pathway.

CONCLUSION

In this study, we combined qualitative shRNA screening experiment with the current literature knowledge, including Gene Ontology and gene-interaction networks, to identify gene networks that are associated with cell adhesion. By grouping genes based on their GO category and conducting statistical analysis of sets of genes instead of each individual one, we show that the experimental noise of this type of shRNA screen can be effectively reduced allowing for biologically relevant discoveries to be made. By mapping the identified genes onto the protein interaction network and performing topological analyses of the network architecture, we discovered not only genes that are significantly modulated, but also how these genes are inter-connected and how they might influence entire regulatory pathways.

ACKNOWLEDGEMENT

We thank UCSD GeneChip core for conducting the microarray hybridization and scanning, Scott Stuart for reading the manuscript. This work was partially supported by ACS-IRG #70-002, NCI Special Cancer Center Support Grant CA23100-22 to X. L., NIH CA43054 and HL57900 to J. Y. J. W..

Chapter 3, in part, is being submitted of the material as it may appear in "Systems Analysis of Quantitative shRNA-Library Screens Identifies Novel Regulators of Cell Adhesion, Xiaodong Huang, Jean Y. J. Wang, and Xin Lu, 2007 (in submission)". The author of the dissertation is the primary investigator and author of this paper.

Figure 3-1: shRNA library screening of Abl kinase-induced cell de-adhesion.

A. Schematic outline of the experimental setup for the identification of effectors in Abl-induced cell detachment. Briefly, we infected 1 million AblPP cells with the lentiviral library at an MOI of 0.5. One day after infection, the cells were selected with 2 μg/ml puromycin. Selected cells were subjected to two rounds of AblPP-induced cell detachment by treatment with 2 μg/ml doxycycline for 16 hours. The proviral sequence from the remaining attached cells were extracted and amplified; their relative abundance was analyzed using the Affymetrix Human Genome Focus Array.
B. Percentage of detached cells after each round of AblPP induction. AblPP cells before and after shRNA library transduction were subjected to AblPP-induced cell detachment. Following the 2^{nd} round of AblPP induction, AblPP cells did not detach.
C. AblPP was induced to similar levels and exhibited similar kinase activity during each round of AblPP induction. NI, non-infected; 1^{st}, after 1^{st} round of selection; 2^{nd}, after 2^{nd} round of selection.

3-1A)

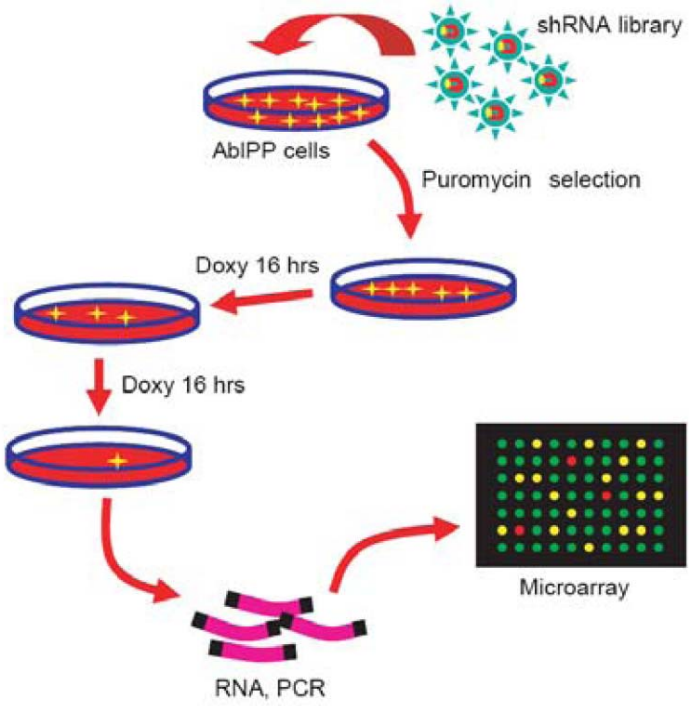
shRNA library
AblPP cells
Puromycin selection
Doxy 16 hrs
Doxy 16 hrs
Microarray
RNA, PCR

3-1B)

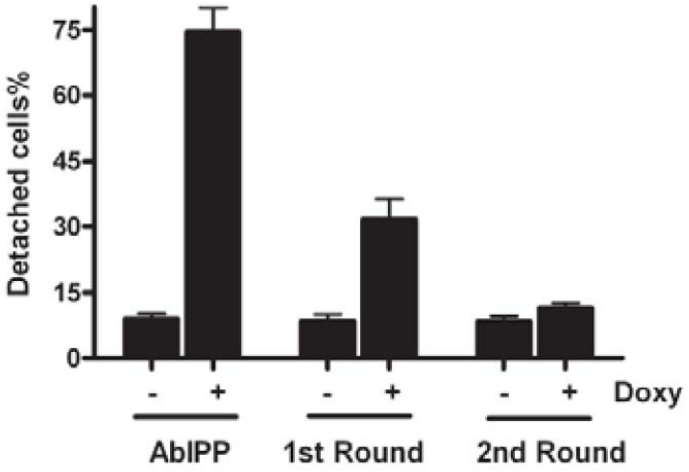

3-1C)

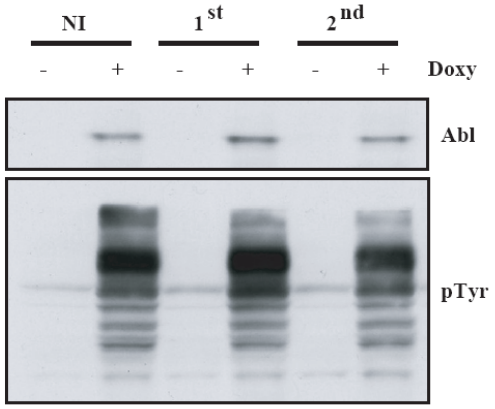

Figure 3-1 continued

Figure 3-2: The human gene interaction network and the shortest path network connecting the 16 significantly enriched or depleted target genes.
A. Human gene interaction network. Nodes represent genes and lines connecting nodes represent gene interactions. Red and blue spots high-lighted represent genes belong to significantly enriched or depleted GO terms with a p-value of rank sum statistics below 0.01.
B. The shortest path network connecting all 16 significantly enriched or depleted genes. Red and blue spots represent genes significantly enriched or depleted. Green diamonds represent hub genes with connectivity greater than 5. Black triangles represent pathways connecting Abl and ROCK1 into this network.

3-2A)

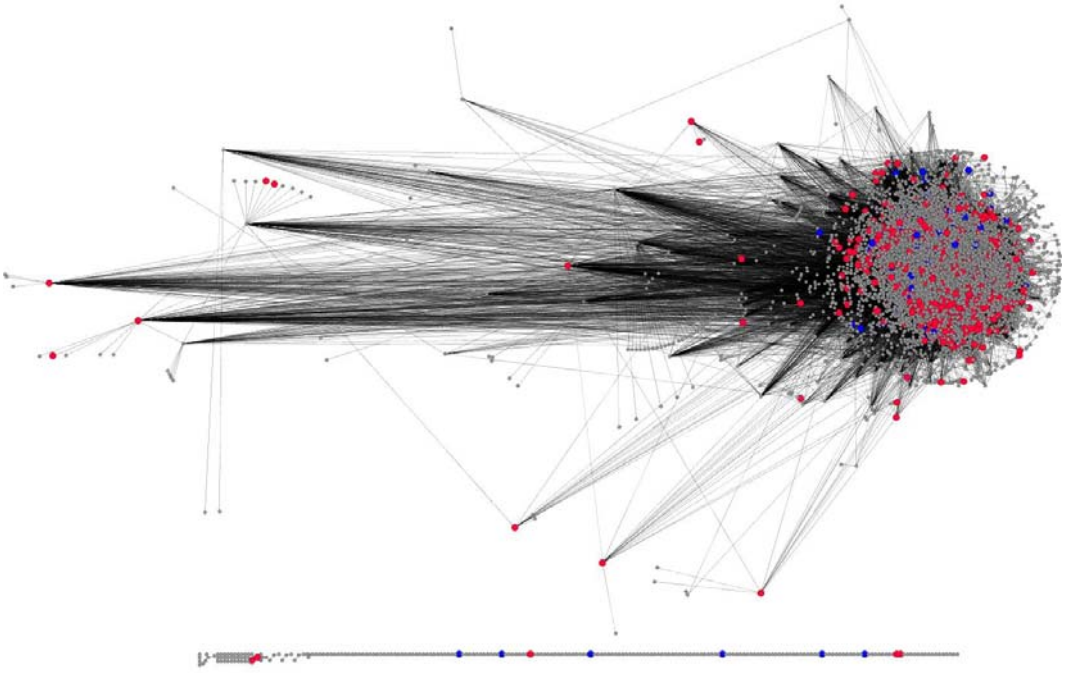

3-2B)

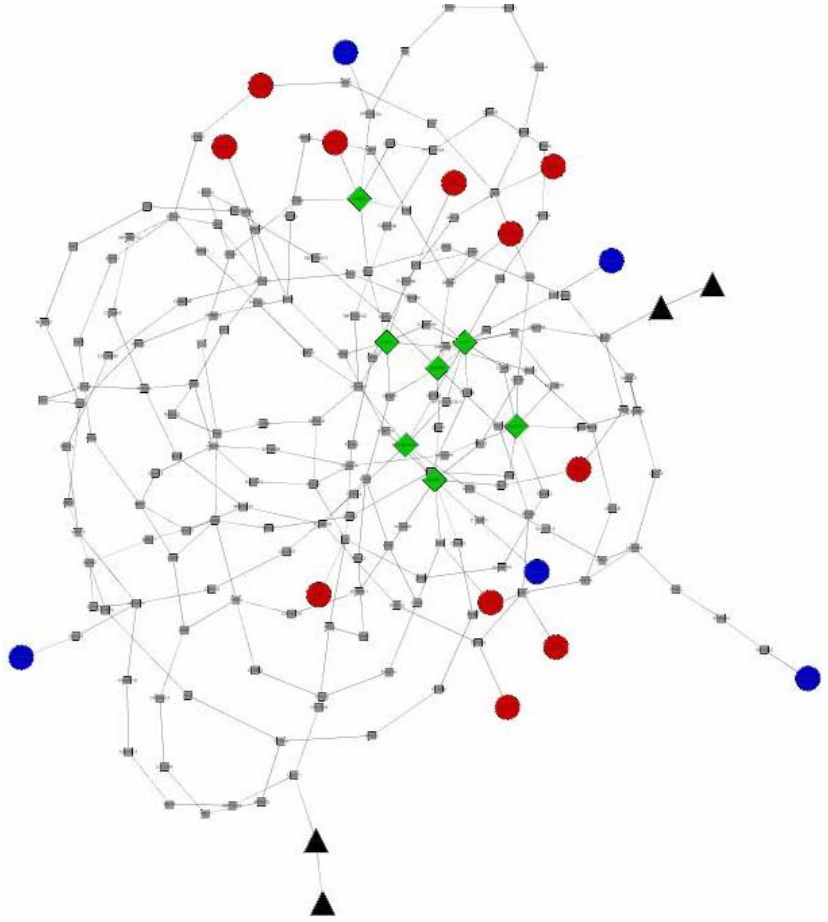

Figure 3-2 continued

Figure 3-3: IL6ST rescued AblPP-induced cell de-adhesion.
A. Relative abundance of IL6ST mRNA level in AblPP cells infected by IL6ST shRNA or control shRNA was measured by quantitative PCR. The mRNA level from AblPP cells infected by control shRNA was set as 100.
B. AblPP was induced in AblPP cells infected by IL6ST shRNA or control shRNA by doxycycline addition and cell detachment assay was measured at 4 hours.
C. The knockdown of IL6ST did not affect the expression of AblPP or its kinase activity.

3-3A)

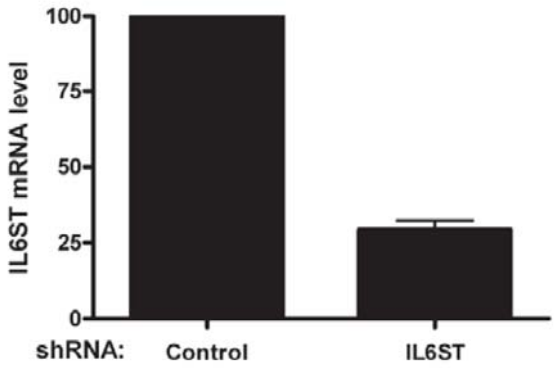
100
75
50
25
0
IL6ST mRNA level
shRNA:
Control
IL6ST

3-3B)

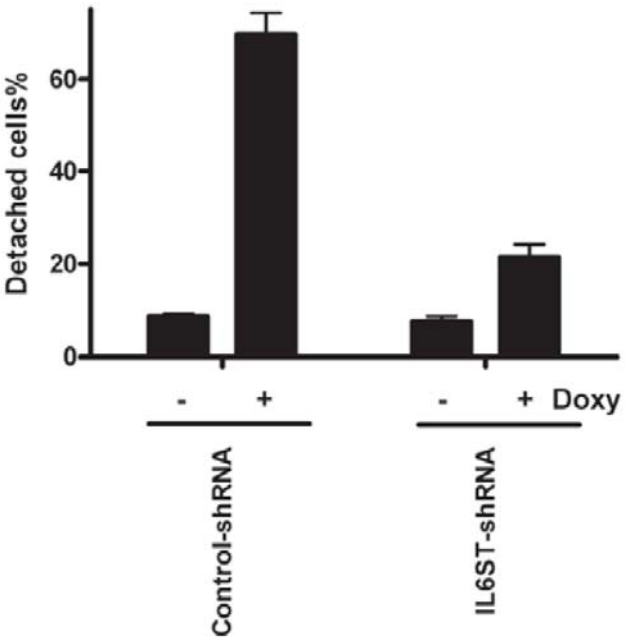
60
40
20
0
Detached cells%
-
+
-
+ Doxy
Control-shRNA
IL6ST-shRNA

3-3C)

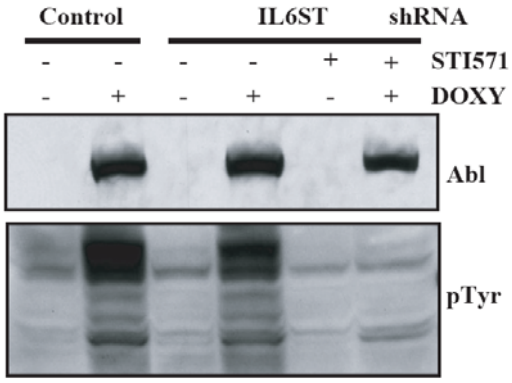

Figure 3-3 continued

Table 3-1: Significantly enriched or depleted GO terms.

Enriched GO terms

Category	GO.ID	GO.Term	P value
BP	7169	transmembrane receptor protein tyrosine kinase signaling pathway	0.000108
	6069	ethanol oxidation	0.004402
	30183	B cell differentiation	0.004668
	8285	negative regulation of cell proliferation	0.004690
	6641	triacylglycerol metabolism	0.005847
	42592	Homeostasis	0.009063
	6631	fatty acid metabolism	0.009442
CC	118	histone deacetylase complex	0.001873
	5578	extracellular matrix (sensu Metazoa)	0.008284
MF	16566	specific transcriptional repressor activity	0.001047
	15248	sterol transporter activity	0.004570
	4024	alcohol dehydrogenase activity, zinc-dependent	0.004699
	4407	histone deacetylase activity	0.006790
	4300	enoyl-CoA hydratase activity	0.008276
	3700	transcription factor activity	0.008297
	8484	sulfuric ester hydrolase activity	0.008613
	5518	collagen binding	0.009071
	4924	oncostatin-M receptor activity	0.009582

Table 3-1 continued

Depleted GO terms

Category	GO.ID	GO.Term	P value
BP	6959	humoral immune response	0.000405
	6356	regulation of transcription from RNA polymerase I promoter	0.002046
	15986	ATP synthesis coupled proton transport	0.004346
	1701	embryonic development (sensu Mammalia)	0.004439
	30187	melatonin biosynthesis	0.006552
	6906	vesicle fusion	0.007231
	7286	spermatid development	0.008267
	31424	Keratinization	0.008692
	17148	negative regulation of protein biosynthesis	0.009817
CC	16469.00	proton-transporting two-sector ATPase complex	0.002401
	19898.00	extrinsic to membrane	0.006794
MF	16165	lipoxygenase activity	0.000954
	4111	creatine kinase activity	0.003959
	46933	hydrogen-transporting ATP synthase activity, rotational mechanism	0.004516
	46961	hydrogen-transporting ATPase activity, rotational mechanism	0.004516
	4983	neuropeptide Y receptor activity	0.004746
	8048	calcium sensitive guanylate cyclase activator activity	0.005498
	17096	acetylserotonin O-methyltransferase activity	0.006552
	4857	enzyme inhibitor activity	0.007804
	15232	heme transporter activity	0.009458

Table 3-2: Target genes that shRNA were significantly enriched.

Gene	P-value	T-statistics	Entrez Gene ID
EDN2	0.0011	20.9528	1907
ARNTL2	0.0020	15.7851	56938
ZNF232	0.0030	12.7514	7775
ADH5	0.0040	11.1071	128
COL15A1	0.0043	10.7380	1306
EMP3	0.0071	8.2852	2014
MYT2	0.0072	8.2309	8827d
ZNF219	0.0079	7.8689	51222
IL6ST	0.0080	7.8232	3572
MEOX2	0.0080	7.8013	4223
EPHB4	0.0092	7.2683	2050
KLF10	0.0093	7.2104	7071
TFEC	0.0097	7.0622	22797
NPC1	0.0098	7.0363	4864

Table 3-3: Target genes that shRNA were significantly depleted.

Gene	P-value	T-statistics	Entrez Gene ID
ABCB7	0.0019	-16.2715	22
RFXANK	0.0027	-13.5118	8625
CD28	0.0031	-12.5570	940
ASMT	0.0035	-11.8293	438
PPYR1	0.0039	-11.2743	5540
CKB	0.0053	-9.6779	1152
SPOCK3	0.0066	-8.6420	50859

Table 3-4: The hub genes identified from the shortest path network connecting significantly enriched or depleted shRNA target genes.

Entrez Gene ID	Gene
22981	*RP4-691N24.1*
4188	*MDFI*
2130	*EWSR1*
57473	*GM632*
509	*ATP5C1* *
4110	*MAGEA11*
60	*ACTB*
6310	*ATXN1*
4088	*SMAD3*
5764	*PTN*

* The gene ATP5C1 belong to depleted GO terms, but was not significantly depleted in the study (p-value=0.21).

REFERENCES

1. Einav, Y., R. Agami, and D. Canaani, *shRNA-mediated RNA interference as a tool for genetic synthetic lethality screening in mouse embryo fibroblasts.* FEBS Lett, 2005. **579**(1): p. 199-202.

2. Elbashir, S.M., et al., *Duplexes of 21-nucleotide RNAs mediate RNA interference in cultured mammalian cells.* Nature, 2001. **411**(6836): p. 494-8.

3. Tuschl, T., *Expanding small RNA interference.* Nat Biotechnol, 2002. **20**(5): p. 446-8.

4. Tsuji, A.B., et al., *A fast, simple method for screening radiation susceptibility genes by RNA interference.* Biochem Biophys Res Commun, 2005. **333**(4): p. 1370-7.

5. Bernards, R., T.R. Brummelkamp, and R.L. Beijersbergen, *shRNA libraries and their use in cancer genetics.* Nat Methods, 2006. **3**(9): p. 701-6.

6. Guo, Q., et al., *A randomized lentivirus shRNA library construction.* Biochem Biophys Res Commun, 2007. **358**(1): p. 272-6.

7. Hoyer, D., *RNA interference for studying the molecular basis of neuropsychiatric disorders.* Curr Opin Drug Discov Devel, 2007. **10**(2): p. 122-9.

8. Sharan, R. and T. Ideker, *Modeling cellular machinery through biological network comparison.* Nat Biotechnol, 2006. **24**(4): p. 427-33.

9. Lewis, J.M., et al., *Integrin regulation of c-Abl tyrosine kinase activity and cytoplasmic-nuclear transport.* Proc Natl Acad Sci U S A, 1996. **93**(26): p. 15174-9.

10. Renshaw, M.W., J.M. Lewis, and M.A. Schwartz, *The c-Abl tyrosine kinase contributes to the transient activation of MAP kinase in cells plated on fibronectin.* Oncogene, 2000. **19**(28): p. 3216-9.

11. Woodring, P.J., T. Hunter, and J.Y. Wang, *Regulation of F-actin-dependent processes by the Abl family of tyrosine kinases.* J Cell Sci, 2003. **116**(Pt 13): p. 2613-26.

12. Lewis, J.M. and M.A. Schwartz, *Integrins regulate the association and phosphorylation of paxillin by c-Abl.* J Biol Chem, 1998. **273**(23): p. 14225-30.

13. Mayer, B.J., H. Hirai, and R. Sakai, *Evidence that SH2 domains promote processive phosphorylation by protein-tyrosine kinases.* Curr Biol, 1995. **5**(3): p. 296-305.

14. Plattner, R., et al., *c-Abl is activated by growth factors and Src family kinases and has a role in the cellular response to PDGF.* Genes Dev, 1999. **13**(18): p. 2400-11.

15. Muller, H., et al., *E2Fs regulate the expression of genes involved in differentiation, development, proliferation, and apoptosis.* Genes Dev, 2001. **15**(3): p. 267-85.

16. Lu, X., et al., *Hubs in biological interaction networks exhibit low changes in expression in experimental asthma.* Mol Syst Biol, 2007. **3**: p. 98.

17. Dijkstra, E.W., *A note on two problems in connexion with graphs.* Numerische Mathematik, 1959. **1**: p. S. 269–271.

18. Barila, D., et al., *A nuclear tyrosine phosphorylation circuit: c-Jun as an activator and substrate of c-Abl and JNK.* Embo J, 2000. **19**(2): p. 273-81.

19. Subramanian, A., et al., *Gene set enrichment analysis: a knowledge-based approach for interpreting genome-wide expression profiles.* Proc Natl Acad Sci U S A, 2005. **102**(43): p. 15545-50.

20. Han, J.D., et al., *Evidence for dynamically organized modularity in the yeast protein-protein interaction network.* Nature, 2004. **430**(6995): p. 88-93.

21. Patil, A. and H. Nakamura, *Disordered domains and high surface charge confer hubs with the ability to interact with multiple proteins in interaction networks.* FEBS Lett, 2006. **580**(8): p. 2041-5.

22. Fujio, Y., et al., *Signals through gp130 upregulate Wnt5a and contribute to cell adhesion in cardiac myocytes.* FEBS Lett, 2004. **573**(1-3): p. 202-6.

CHAPTER 4

Nuclear and Cytoplasmic Abl Contribute to Cell Death through Different Mechanisms

ABSTRACT

Abl is a non-receptor tyrosine kinase that shuttles between the nucleus and cytoplasm because it contains three nuclear localization signals (NLS) and one nuclear export signal (NES). In the nucleus, the Abl tyrosine kinase is activated by DNA damage or tumor necrosis factor (TNF) to induce cell death. To examine the mechanism by which Abl regulates cell death, we employed dimerization as a means to control Abl activity by fusing the FK506-binding protein (FKBP) to the N-terminus of Abl. The FKBP-Abl can be stably expressed at levels comparable to the endogenous Abl in $p21^{-/-}$ cells. Additionally, expression of the adenoviral E1A protein sensitizes these cells to death induced by the dimerization of FKBP-Abl detected by caspase activation and DNA fragmentation. Mutational inactivation of the Abl NLS abrogated cell death, whereas FKBP-Abl was more efficient than FKBP-AblNuk, a nuclear-exclusive Abl, in inducing cell death. Furthermore, entrapment of FKBP-Abl in the nucleus by leptomycin B (LMB) compromised the efficiency of apoptosis, suggesting that while the nuclear pool is required for Abl-induced cell death, the cytoplasmic pool contributes once the apoptosis program is initiated. Activation of FKBP-Abl, FKBP-AblNuk, and FKBP-AblμNLS, synergized with TNF to kill cells. The sensitization of TNF-induced cell death by nuclear Abl is correlated with activation of caspase-2.

INTRODUCTION

Recently, a number of reports have shown c-Abl tyrosine kinase is involved in apoptosis after its kinase activity is activated by physiological or pharmacological stimulations. DNA damage inducers, such as cisplatin [1], IR [2], and etoposide [3] can all activate c-Abl tyrosine kinase. c-Abl is also activated in mouse fibroblasts and thymocytes after tumor necrosis factor (TNF) treatment [4]. The ability of Abl kinase to activate apoptosis is best illustrated by entrapping BCR-Abl in the nucleus [5]. Normally, the BCR-Abl protein is localized exclusively to the cytoplasm and it has been shown to inhibit apoptosis by activating PI3 kinase, Akt, and by other mechanisms [6-8]. The mechanism that imposes the cytoplasmic localization of BCR-Abl is not fully understood. However, by treating fibroblasts with both LMB to block nuclear export and with STI571, a selective inhibitor of Abl kinase activity, BCR-Abl can be accumulated in the nucleus. The nuclear BCR-Abl kinase can be re-activated by washing away STI571 or through the metabolic decay of STI571. This re-activation of kinase activity can induce the activation of caspases and DNA laddering, the classic phenotypes of apoptotic cells [5].

Although the pathway of Abl-induced apoptosis is largely unknown, several lines of evidence have suggested that members of p53 family are involved in this process. The tumor suppressor gene p53 plays a critical role in the cellular response to DNA damage. It is inhibited and destabilized by Mdm2. Two mechanisms have been reported regarding the functional interaction between Abl and p53. The C-terminal region of Abl appears to be able to bind p53 and this interaction can enhance the transcription of p53-dependent promoters [9, 10]. However, it was shown that c-Abl can activate transcription in general

by phosphorylating the RNA polymerase C-terminal-domain (CTD) and stimulating promoter escape [11, 12]. Therefore, the transcription enhancement of p53 by Abl may not be restricted to p53-regulated promoters. Goldberg *et al.* have proposed an alternative way that c-Abl affects p53 function. They found when activated, c-Abl phosphorylates human Mdm2 (HDM2) at tyrosine394. This phosphorylation impairs the inhibition of p53 by Mdm2 and p53 is released, thus inducing cells to undergo apoptosis. Therefore, c-Abl may exert a positive effect on p53 by antagonizing Mdm2 [13].

p73 and p63 are homologs of p53. The notion that p63 and p73 also function as tumor suppressors is supported by several lines of evidence suggesting they are involved in apoptosis after cellular stress. p73 was phosphorylated and stabilized after c-Abl activation induced by genotoxic stress [1, 14, 15]. Furthermore, a dimerizable AblNuk-FK506-binding protein (FKBP) has been shown to stay in the nucleus, and the activation of kinase activity by dimerizer addition can induce $p53^{-/-}$, but not $p73^{-/-}$ fibroblasts to undergo apoptosis [16]. Recently, it has been shown that in mouse thymocytes, c-Abl and p73 are required for TNF-induced apoptosis, while p53 is not necessary [4]. This further supports the notion that p73 is an effector in c-Abl-induced apoptosis.

How p73 transduces the apoptosis signals remains an open question. The most straightforward hypothesis is that p73 can bind the promoters of p53-regulated genes and activate their transcription. Jost *et al.* have shown that ectopically expressed p73 can bind to p53 DNA-binding sites and transactivate p53-responsive genes, such as p21, PUMA, BAX, and NOXA [17]. Recently, it has been shown that p73 elicits apoptosis via the mitochondrial pathway using PUMA and Bax as mediators [18]. However, in TNF-induced apoptosis, although c-Abl and p73 are necessary, new protein synthesis is not

required, suggesting p73 might also regulate apoptosis by a transcription-independent pathway. Chipuk *et al.* have shown that p53 can directly activate BAX in a transcription-independent way, and this can mediate mitochondrial membrane permeabilization and induce cells to undergo apoptosis [19]. Interestingly, p73 can also shuttle between the nucleus and the cytoplasm [20]. Whether p73 can regulate apoptosis in cytoplasm is still unknown.

There is also evidence suggesting that the stress-activated kinases: JNK and p38 are possible effectors in the Abl-induced apoptosis pathway [21, 22]. An early report by Kharbanda *et al.* has suggested that IR-induced activation of JNK is dependent on c-Abl function [22]. However, this conclusion could not be further supported by subsequent studies [3, 23]. In a recent paper, Borges and Wang have shown that c-Abl is not required for IR to induce apoptosis while ATM and p53 are both required in developing mouse retina [24]. Perhaps the functional interaction of c-Abl and the stress-activated kinases might only be important in some cell types under some specific stress conditions to cause apoptosis.

Here we used a synthetic chemical, AP20187 (dimerizer), to control Abl kinase activity and found that while the nuclear pool is required for Abl-induced cell death, the cytoplasmic pool of Abl contributes once the apoptosis program is initiated. We also found that dimerization of FKBP-Abl, FKBP-AblNuk, or FKBP-AblμNLS, can synergistically sensitize TNF-induced cell death. Furthermore, we found that caspase-2 activation might be the reason that nuclear Abl sensitizes TNF-induced apoptosis.

EXPERIMENTAL PROCEDURES

Generation of p21E cell line - Retrovirus expressing E1A was generated by using the Phoenix retroviral expression system (Orbigen, San Diego, CA). *p21*$^{-/-}$ Mouse embryonic fibroblasts (MEFs) were infected with retrovirus expressing E1A, and the cells were automatically immortalized. The expression of E1A was confirmed by immunoblotting.

Cell culture - *p21E* cells expressing FKBP-Abl, FKBP-AblNuk, or FKBP-Abl were cultured with high-glucose (4.5-g/liter) DMEM media supplemented with penicillin G (100 U/ml), streptomycin (100 μg/ml), 10% fetal bovine serum, and L-glutamine (2 mM).

Apoptosis induction and assay - Dimerizer (AP20187) was obtained from ARIAD (Cambridge, MA). *p21E* cells were routinely treated with 50 nM dimerizer to induce cell death unless noted otherwise. Recombinant mouse TNF-α was obtained from R&D Systems (Minneapolis, MN). In general, cells were treated with 10 ng/ml of TNF-α. Apoptosis was determined by morphological characterization. Briefly, cells were fixed with 4% paraformaldehyde and permeabilized with 0.3% Triton X-100 followed by incubation with Hoechst 33258 (Molecular Probes, Carlsbad, CA) for 1 minute. Dead cells were identified by characteristic condensed nuclear staining.

Immunofluorescence - Cells were fixed in 4% paraformaldehyde, permeabilized in 0.3% Triton X-100, blocked in 10% normal goat serum, and then stained with monoclonal anti-HA followed by Alexa 568-conjugated secondary antibody (Molecular Probes, Eugene, OR). Fluorescent images were captured with a CCD camera.

Immunoprecipitation , Immunoblotting, and Antibodies - Whole cell lysates were prepared in RIPA buffer (50 mM Tris-HCl [pH 7.4], 150 mM NaCl, 1% NP-40, 0.25% sodium deoxycholate, 0.1% SDS, 0.5 mM EDTA, 1 mM EGTA, 1 mM DTT) plus protease inhibitor (Sigma, St Louis, MS), and 10 mM sodium vanadate. 50-100 μg of total protein were resolved by SDS-PAGE, transferred onto PVDF membranes, blocked in 5% nonfat dry milk/TBST (20 mM Tris-HCl [pH 7.5], 150 mM NaCl, 0.05% Tween-20) and incubated with primary antibodies overnight at 4°C. Membranes were washed 3 × 10 minutes in TBST and incubated with HRP-conjugated secondary antibodies for 1-3 hours at room temperature. After 3 × 10 minutes washing, membranes were incubated with enhanced ECL reagent (Pierce, Rockford, IL) for 1 minute and exposed to X-ray films. To detect phosphor-Abl induced by dimerizer treatment, 5 μg anti-HA (Covance, Madison, WI) was mixed with 1 mg whole cell lysates, the immune complex collected on protein A-sepharose, resolved by SDS-PAGE and then immunoblotted with anti-pTyr antibody (Upstate Biotechnology, Lake Placid, NY). The other antibodies used were as follows: anti-Abl, 8E9 (BD Biosciences, San Diego, CA); anti-tubulin (Santa Cruz Biotechnology, Santa Cruz, CA); rabbit polyclonal anti-procaspase-3 antibody, and mouse monoclonal anti-caspase-2 antibody were kind gifts from Yuri Lazebnik (Cold Spring Harbor Laboratory).

Caspase-2 pulldown assay - We adopted the method described by Tu et al. to label activated caspase-2 in cells. Briefly, *p21E* cells expressing FKBP-Abl, FKBP-AblNuk, or FKBP-μNLS were pre-incubated with 50 μM biotin-VAD-FMK, with or without 50 nM dimerizer, after 1 hour of incubation at 37ºC, 10 ng/ml mTNF was added. Cells were harvested 5 hours later, lysed in 0.5 ml RIPA buffer, 1 mg of total proteins

were incubated with 50 µl streptavidin/Sepharose beads (Amersham) at 4ºC overnight. The beads were washed with RIPA buffer, boiled in 25 µl of 3 × SDS sample buffer and the supernatant was resolved by SDS-PAGE and caspase-2 was detected by immunoblotting.

TUNEL – TUNEL kit was from Roche Applied Sciences (Indianapolis, IN) and the experiments were performed following the protocol from the kit. Briefly, cells were fixed in 4% paraformaldehyde for 10 minutes; permeabilized in 0.3% Triton X-100 for 5 minutes; and incubated with TUNEL reaction reagents for 1 hour at 37°C. Nuclei were counterstained with Hoechst 33258 (Molecular Probes).

RESULTS AND DISCUSSION

Dimerization of FKBP-Abl induces *p21E* cells to undergo apoptosis

Abl is activated in human leukemias by the fusion of BCR or Tel sequences to the Abl N-terminus, both of which can lead to dimer or tetramer formations. McWhirter and Wang have shown that BCR activates Abl through its coiled-coil domain by inducing tetramer formation [25]. Based on this evidence, we built a construct in which an FKBP (FK506 binding protein) domain is attached to the N-terminus of Abl to form the chimeric FKBP-Abl, we also put an HA tag in the C-terminus of the protein for easy detection (Figure 4-1A). A chemical inducer of dimerization, AP20187, or ‘dimerizer’, is a cell-permeant organic molecule with two separate motifs that each bind with subnanomolar affinity to FKBP domain [26]. Previous research has shown that the

localization of Abl protein plays an important role in Abl-induced apoptosis [16, 27]. Therefore, we also made FKBP-AblNuk, in which the leucine residues in the NES were mutated to alanines, abating its nuclear export function and introduced three NLSs from SV40 large T antigen for better nuclear entry efficiency [16]. We also built FKBP-AblμNLS, which has the normal NES but no functional NLS (Figure 4-1A).

To choose a suitable cell line to analyze the pathway of Abl-induced apoptosis, we started by using fibroblasts with different genetic backgrounds. We noticed transient transfection of FKBP-Abl could induce apoptosis in E1A-transfomed *p21*$^{-/-}$ fibroblasts (*p21E*) (Figure 4-1B). Thus, we introduced the FKBP-Abl, FKBP-AblNuk, or FKBP-AblμNLS cassette into an MSCV-based retroviral vector for the production of retroviruses, which were used to infect *p21E* cells and to establish polyclonal cell lines. The chimeric Abl expression level was comparable to that of the endogenous Abl in these *p21E* MEFs (Figure 4-1C). By applying 50 nM dimerizer at 12 hours after seeding the *p21E* cells expressing FKBP-Abl, FKBP-AblNuk, or FKBP-AblμNLS, the Abl kinase activity was detected within 2 hours after dimerizer addition (Figure 4-1D), although a low background could also be detected. Interestingly, we found apoptotic cells could be observed as early as 6 hours after dimerizer addition by using TUNEL method (Figure 4-1E). About 25% of cells became TUNEL positive at 12 hours after dimerizer addition (Figure 4-1F).

Localization of Abl affected the apoptosis efficiency

Abl protein contains three NLSs, each of which can independently direct Abl into the nucleus [28]. Abl can also undergo nuclear export as it contains a NES at its C-terminus [29]. In proliferating fibroblasts, Abl is evenly distributed in the cytoplasm and the nucleus. To test the effect of localization of Abl on Abl-induced cell death, we compared the apoptosis efficiency of FKBP-Abl, FKBP-AblNuk, and FKBP-AblμNLS after dimerizer addition. First we checked the localization of the expressed chimerical proteins in *p21E* cells. As expected, FKBP-Abl is evenly distributed in both the nucleus and the cytoplasm, while FKBP-AblNuk is exclusively localized in the nucleus and most of FKBP-AblμNLS is in the cytoplasm (Figure 4-2A). We compared the apoptosis efficiency of these three versions of Abl by adding 50 nM dimerizer to activate Abl kinase activity. The dimerizer treatment at this concentration did not cause any detectable change of localization of these three versions of chimeric Abl protein (data not shown). Interestingly, we found while FKBP-AblNuk can induce about 10-15% cells to undergo apoptosis in about 12 hours after dimerizer addition, FKBP-Abl had better efficiency to induce *p21E* cells to undergo apoptosis. On the contrary, activation of FKBP-AblμNLS had no effect in inducing cells to undergo apoptosis (Figure 4-2B). Furthermore, we found dimerizer addition could induce caspase-3 cleavage in *p21E* cells expressing FKBP-Abl or FKBP-AblNuk, but not in *p21E* cells expressing FKBP-AblμNLS (Figure 4-2C), suggesting that activation of the nuclear pool is required for Abl-induced cell death.

Cytoplasmic Abl collaborates once apoptosis is initiated by nuclear Abl

Leptomycin B (LMB) is a drug which can inhibit nuclear export by binding to exportin-1 [30]. Previous results have shown LMB inhibits nuclear Abl from translocating to the cytoplasm [29]. By pre-treating *p21E* fibroblasts expressing FKBP-Abl, FKBP-AblNuk, and FKBP-AblμNLS with 10 nM of LMB, we found the FKBP-Abl protein was entrapped in the nucleus, while the localization of FKBP-AblNuk and FKBP-AblμNLS were not affected (Figure 4-3A and data not shown). Although 10 nM of LMB alone did not induce all those cell lines to undergo apoptosis (data not shown), LMB treatment correlated with a lower level of apoptosis induced by activation of FKBP-Abl with 50 nM of dimerizer (Figure 4-3B). In other words, the apoptosis efficiency of activating FKBP-Abl was partly inhibited by LMB treatment but the apoptotic efficiency of FKBP-AblNuk was not affected (Figure 4-3B). The *p21E* cells expressing FKBP-AblμNLS were not affected by LMB treatment since the majority of the FKBP-AblμNLS protein was still localized to the cytoplasm and did not induce cells to undergo apoptosis (Data not shown). These results suggest that nuclear export of the Abl protein contributed to the induction of apoptosis.

Upon inducing kinase activation with the chemical dimerizer in the *p21E* background, FKBP-Abl has better apoptosis efficiency than the nuclear-exclusive FKBP-AblNuk, and FKBP-AblμNLS could not induce cells to undergo apoptosis. Since the protein expression level and auto-phosphorylation of the three proteins were almost at the same level (Figure 4-1C, 1D), we excluded the possibility of differential expression or activation. Vigneri and Wang have shown that BCR-Abl can induce cells to undergo apoptosis once the protein is trapped in the nucleus [5]. Our results are consistent with this observation. Since the localization of Abl in both the nucleus and the cytoplasm

caused Abl to have better apoptotic efficiency, it suggested that although activation of nuclear localization of Abl kinase is necessary for initiation of Abl-induced apoptosis, presence of Abl in both compartments leads to a higher level of death.

The better killing efficiency of FKBP-Abl over that of -AblNuk can be explained by two possibilities: (1) To induce apoptosis, Abl needs to be present in both compartments; (2) Abl needs to be activated in the nucleus and exported to cytoplasm for better apoptotic efficiency. To distinguish between these two possibilities, the *FKBP-AblNuk* gene cassette was introduced into MSCV-puromycin-based retroviral vector, and *FKBP-AblμNLS* was introduced into MSCV-hygromycin-based retroviral vector for the production of recombinant retroviruses, and we infected *p21E* cells with these two different types of retrovirus. By selecting with hygromycin and puromycin at the same time, we generated a cell line that expressed both FKBP-AblNuk and FKBP-AblμNLS, but neither of these two chimeric proteins could shuttle between the nucleus and the cytoplasm. Interestingly, we found activation of these two chimeric Abl proteins at the same time in *p21E* cells had greater apoptosis efficiency than activating FKBP-AblNuk alone, and it had an almost equivalent efficiency as activation of FKBP-Abl (Figure 4-3C). This cell line had FKBP-AblNuk in nucleus and FKBP-AblμNLS in cytoplasm, suggesting that the presence of Abl in both the nucleus and the cytoplasm could increase the apoptotic induction by Abl kinase, but shuttling between nucleus and cytoplasm *per se* was not required.

Activation of Abl synergizes with TNF to kill cells

It has been shown that tumor necrosis factor (TNF) activates c-Abl kinase in U937 cells and inhibition of Abl kinase can block the apoptosis program [3]. Recently, Chau *et al.* have shown that activation of c-Abl and p73 are required for TNF-induced cell death in mouse embryonic fibroblasts and thymocytes [4]. To find out whether the localization of Abl also plays a role in TNF-induced cell death, we compared the apoptosis efficiency by activation of FKBP-Abl, FKBP-AblNuk, and FKBP-AblμNLS combined with TNF treatment. We found that although murine TNF (mTNF) alone or dimerizer alone treatment could only induce a low level of *p21E* cells expressing FKBP-Abl to undergo apoptosis in 12 hours, FKBP-Abl activation by dimerizer treatment synergistically sensitized mTNF to induce *p21E* cells to undergo apoptosis (Figure 4-5A, 4-5B). Furthermore, we found activation of FKBP-AblNuk or FKBP-AblμNLS could also sensitize TNF-induced cell death, although the efficiency was not as good as activation of FKBP-Abl (Figure 4-5B). This suggests that both the nuclear and the cytoplasmic pool of Abl protein have a role in sensitizing TNF-induced cell death.

Interestingly, we found in *p21E* background, a capase-2 specific inhibitor, z-VDVAD-fmk could completely and partially inhibit the sensitization induced by activation of FKBP-AblNuk or FKBP-Abl to TNF-induced cell death, respectively (Figure 4-5C). We also found that caspase-2 was cleaved after mTNF treatment, combined with activation of FKBP-Abl, or FKBP-AblNuk, but was not cleaved when combined with FKBP-AblμNLS activation (Figure 4-5D). To further prove this, we employed an *in vivo* labeling method to label the activated caspase-2, and we found caspase-2 was activated after TNF treatment, combined with activation of FKBP-Abl, and FKBP-AblNuk, but not FKBP-AblμNLS (Figure 4-5E). This suggests that the

activation of the nuclear, but not the cytoplasmic pool of Abl might sensitize apoptosis induced by TNF treatment through activation of caspase-2.

It has been shown that cytoplasmic Abl is activated by growth factors such as PDGF and EGF [31], or integrins binding with proteins within the extracellular matrix (ECM) [32]. We have found activation of cytoplasmic Abl can send an inside-out signal back to integrin and cause integrin affinity to go down. Unligated integrin molecules activate caspase-8 and induce cells to die [33]. Whether the cytoplasmic Abl sensitizes TNF-induced cell death through inactivating of integrins in *p21E* cells remains unknown at this stage.

Figure 4-1: Activation of FKBP-Abl in E1A-immortalized *p21*$^{-/-}$ mouse embryonic fibroblasts (*p21E*) can induce apoptosis.

A. Diagrams of FKBP-Abl, FKBP-AblNuk, and FKBP-AblμNLS. An FKBP domain was attached at the N-terminus of the constructs, and a HA tag was attached to the C-terminus of the gene. FKBP-AblNuk had three additional NLSs from SV40 large T antigen and the NES of Abl was mutated. In FKBP-AblμNLS, the 3 NLSs of Abl were mutated and were no longer functional. NLS, nuclear localization signal; NES, nuclear export signal; FKBP, FK506 binding domain [26].

B. Activation of FKBP-Abl in *p21E* cells could induce apoptosis in transient transfection experiment. Apoptosis was determined by counting condensed nuclei. Results were based on 3 independent experiments, and each time, at least 100 GFP positive cells were counted.

C. Expression of FKBP-Abl, FKBP-AblNuk, and FKBP-AblμNLS in *p21E* cells. The indicated cell lines were harvested and whole cell lysates were resolved by SDS-PAGE and immunoblotted with anti-Abl antibodies. Lane 1, FKBP; lane 2, FKBP-Abl; lane 3, FKBP-AblNuk; lane 4, FKBP-AblμNLS.

D. Activation of FKBP-Abl, FKBP-AblNuk, and FKBP-AblμNLS in *p21E* cells with dimerizer addition. The indicated cell lines were detached, held in serum-free DMEM media, and then treated with 50 nM dimerizer or vehicle (0.1% ethanol) for 2 hours. Whole cell lysates were then obtained for immunoprecipitation with an HA antibody, and immunoblotting with an antibody recognizing phosphorylated tyrosine.

E. Activation of FKBP-Abl by dimerizer treatment induced *p21E* cells to become TUNEL positive. *p21E* cells expressing FKBP-Abl were treated with 50 nM dimerizer for different times. Apoptotic cells were detected by using TUNEL staining as described in Experimental Procedures.

F. Time course of *p21E* cell death induced by FKBP-Abl activation by 50 nM AP20187. The apoptotic cells appeared at as early as 4 hours after AP20187 addition. At 12 hours after dimerizer addition, about 25% cells were TUNEL positive.

4-1A)

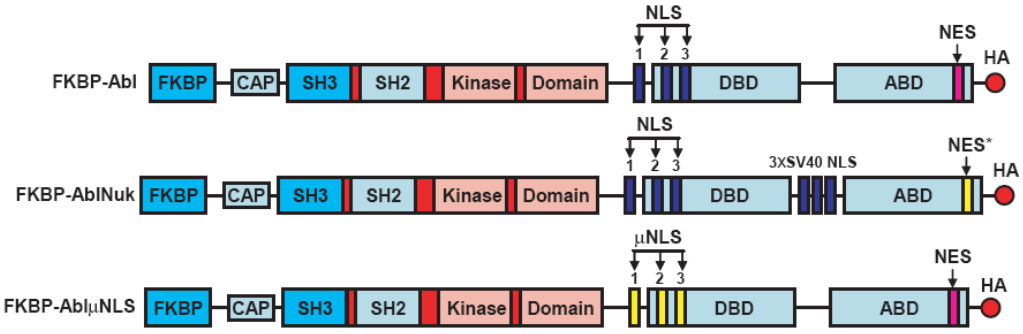
FKBP-Abl
FKBP
CAP
SH3
SH2
Kinase
Domain
NLS
1 2 3
DBD
ABD
NES
HA
FKBP-AblNuk
NES*
3XSV40 NLS
FKBP-AblμNLS
μNLS

4-1B)

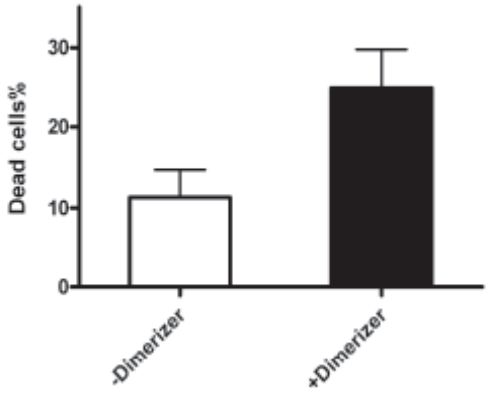
Dead cells%
30
20
10
0
-Dimerizer
+Dimerizer

4-1C)

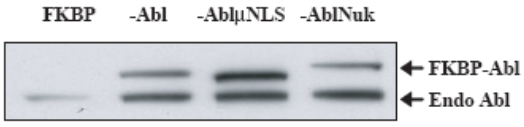

4-1D)

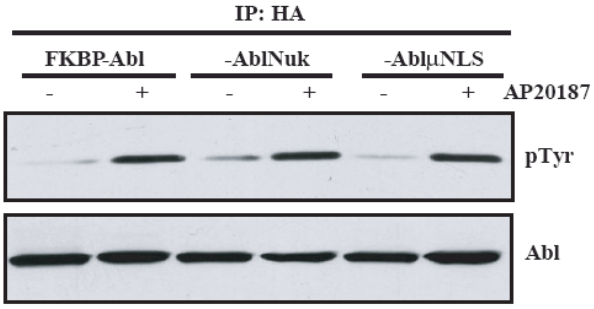

Figure 4-1 continued

4-1E)

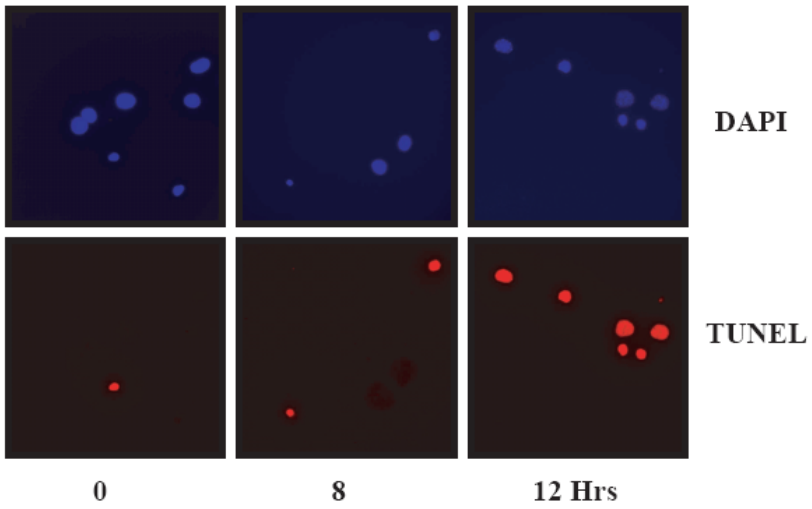

4-1F)

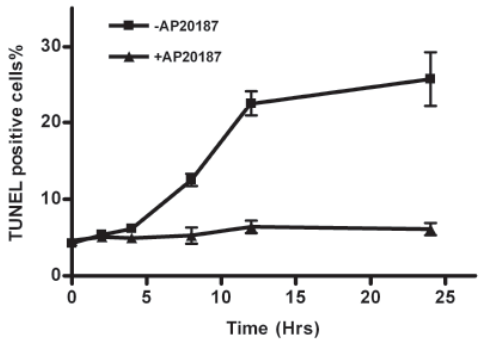

Figure 4-1 continued

Figure 4-2: Nuclear localization was required for Abl to initiate apoptosis.
A. Localization of FKBP-Abl, FKBP-AblNuk, and FKBP-AblμNLS in *p21E* cells. FKBP-Abl was evenly distributed in both the nucleus and the cytoplasm; FKBP-AblNuk was exclusively localized in the nucleus, and FKBP-AblμNLS was exclusively localized in the cytoplasm. Anti-HA was used to detect FKBP-Abl, FKBP-AblNuk, and FKBP-AblμNLS. Hoechst was used for nuclear staining.
B. Abl localization had an important effect in apoptosis efficiency. Although activation of FKBP-Abl and FKBP-AblNuk by dimerizer could both induce *p21E* cells to undergo apoptosis, they had different efficiency. On the contrary, activation of FKBP-AblμNLS did not induce *p21E* cells to undergo apoptosis.
C. Activation of FKBP-Abl and FKBP-AblNuk, but not FKBP-AblμNLS could induce caspase-3 cleavage in *p21E* cells. The three different cell lines were treated with 50 nM AP20187 for 12 hours; whole cell lysates were then resolved with SDS-PAGE and immunoblotted with an anti-procaspase-3 antibody.

4-2A)

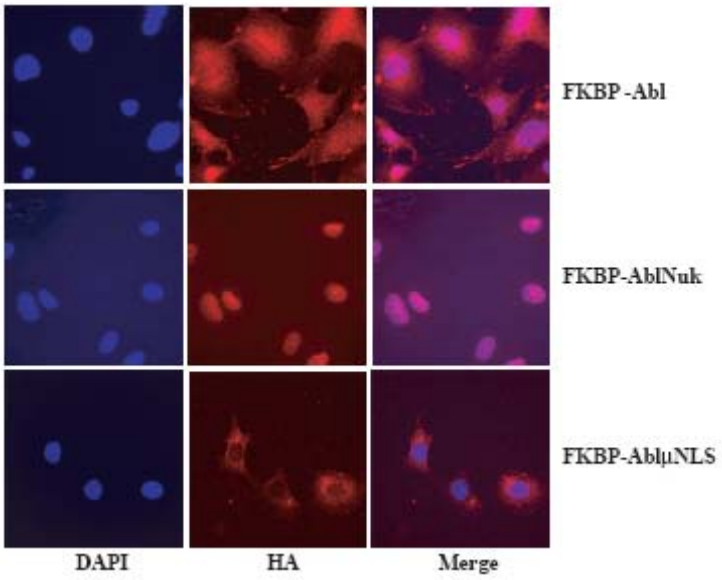
FKBP-Abl
FKBP-AblNuk
FKBP-AblμNLS
DAPI
HA
Merge

4-2B)

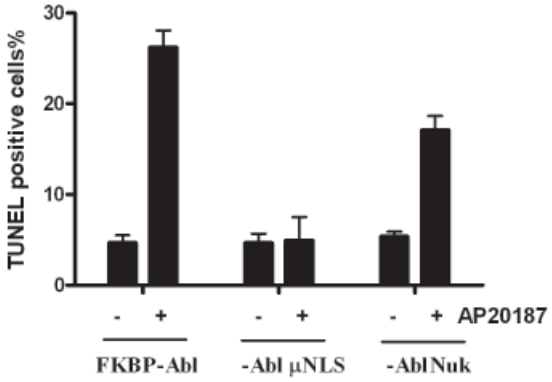
TUNEL positive cells%
30
20
10
0
- + - + - + AP20187
FKBP-Abl
-Abl μNLS
-Abl Nuk

4-2C)

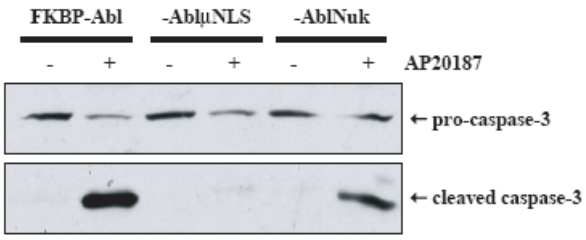

Figure 4-2 continued

Figure 4-3: Entrapment of FKBP-Abl into nucleus compromised its apoptosis efficiency.
A. LMB entrapped FKBP-Abl into the nucleus, but did not change the localization of FKBP-AblNuk. *p21E* cells expressing FKBP-Abl or FKBP-AblNuk were treated with 10 nM LMB for 2 hours and the localization of FKBP-Abl or FKBP-AblNuk was detected by using anti-HA antibody.
B. Entrapment of FKBP-Abl into the nucleus compromised the apoptosis efficiency after activation of FKBP-Abl; *p21E* cells expressing FKBP-Abl or FKBP-AblNuk were treated with 10 nM LMB for 2 hours and then treated with 50 nM dimerizer for 12 hours. The dead cells were detected by using TUNEL staining.
C. Activation of the co-expressed FKBP-AblNuk and FKBP-AblμNLS proteins increased the apoptosis efficiency to about the same level as activation of the FKBP-Abl protein. *p21E* cells were infected with retrovirus expressing FKBP-AblNuk in a puromycin-resistant vector, and FKBP-AblμNLS in a hygromycin-resistant vector. The cells were treated with 50 nM dimerizer for 12 hours. The dead cells were detected by using TUNEL staining.

4-3A)

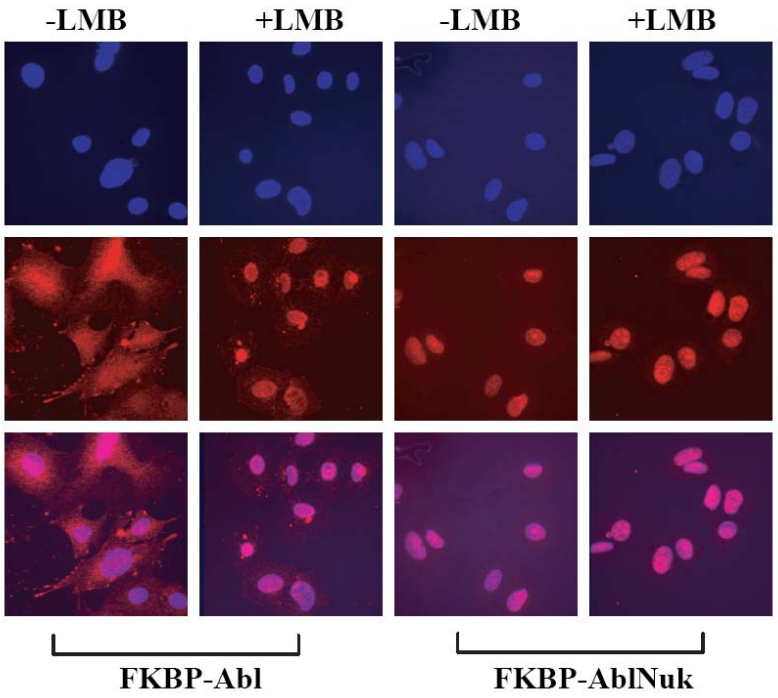
-LMB
+LMB
-LMB
+LMB
FKBP-Abl
FKBP-AblNuk

4-3B)

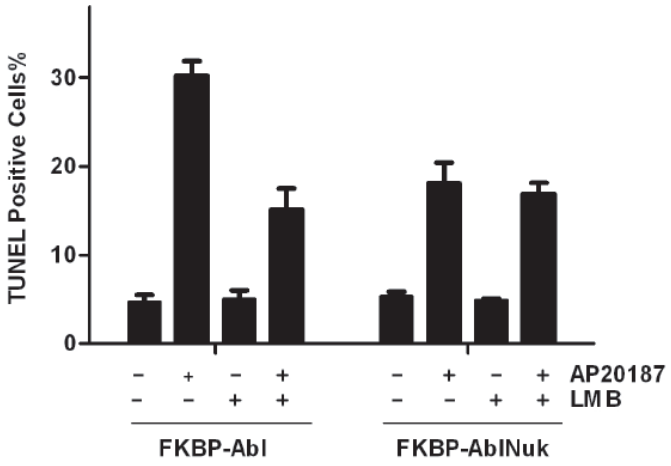
TUNEL Positive Cells%
30
20
10
0
AP20187
LMB
FKBP-Abl
FKBP-AblNuk

4-3C)

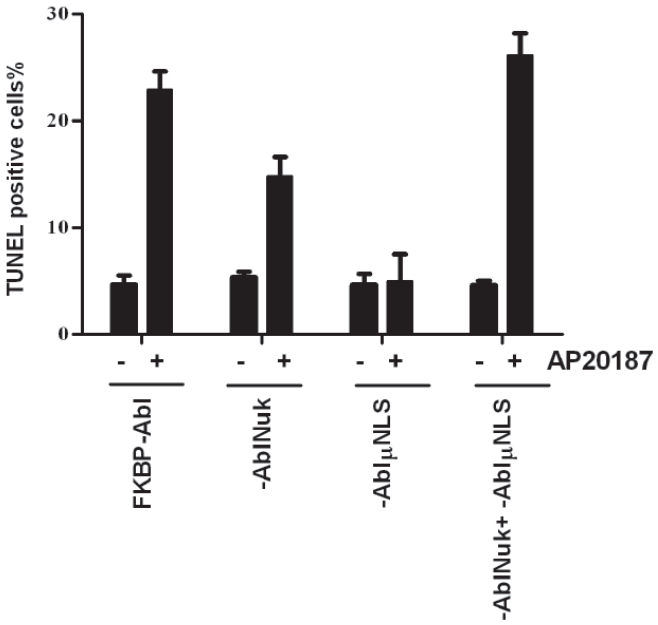

Figure 4-3 continued

Figure 4-4: Activation of FKBP-Abl, FKBP-AblNuk, and FKBP--AblμNLS synergistically sensitized TNF-induced apoptosis in p21E cells.
A. Activation of FKBP-Abl sensitized TNF-induced apoptosis in the *p21E* background. *p21E* cells expressing FKBP-Abl or FKBP were treated with 10 ng/ml mTNF for 8 hours. Apoptotic cells were detected by using TUNEL staining.
B. Activation of FKBP-Abl, FKBP-AblNuk, and FKBP-AblμNLS all sensitized *p21E* cells to TNF-induced apoptosis. *p21E* cells expressing FKBP-Abl, FKBP-AblNuk, or FKBP-AblμNLS were treated with 10 ng/ml mTNF for different lengths of time, in the absence or presence of 50 nM dimerizer. Apoptotic cells were detected by using TUNEL staining.
C. z-VDVAD, a specific caspase-2 inhibitor, inhibited sensitization of TNF-induced apoptosis in *p21E* cells by activation of FKBP-Abl, FKBP-AblNuk, but not activation of FKBP-AblμNLS. *p21E* cells expressing FKBP-Abl, FKBP-AblNuk, or FKBP-AblμNLS were pretreated with or without 50 μM z-VDVAD for 1 hour, and then treated with 10 ng/ml mTNF for 8 hours plus 50 nM dimerizer. Apoptotic cells were detected by using TUNEL staining.
D. Caspase-2 was cleaved in *p21E* cells after mTNF treatment, combined with activation of FKBP-Abl, FKBP-AblNuk, but not activation of FKBP-AblμNLS. *p21E* cells expressing FKBP-Abl, FKBP-AblNuk, or FKBP-AblμNLS were treated with 10 ng/ml mTNF, in the absence or presence of 50 nM AP20187 for 8 hours. The whole cell lysates were resolved by SDS-PAGE and immunoblotted with an antibody against caspase-2.
E. Biotinylation of caspase-2 in *p21E* cells after activation of FKBP-Abl, FKBP-AblNuk, or FKBP-AblμNLS. *p21E* cells expressing the indicated chimeric Abl protein were collected at 5 hours after mTNF treatment, in the absence or presence of 50 nM AP20187, whole cell lysates (1 mg total protein) were incubated with streptavidin beads and caspase-2 was detected in the bound fractions by immunoblotting. The constitutively biotinylated acetyl-CoA-transferase protein was used as a pulldown efficiency control.

4-4A)

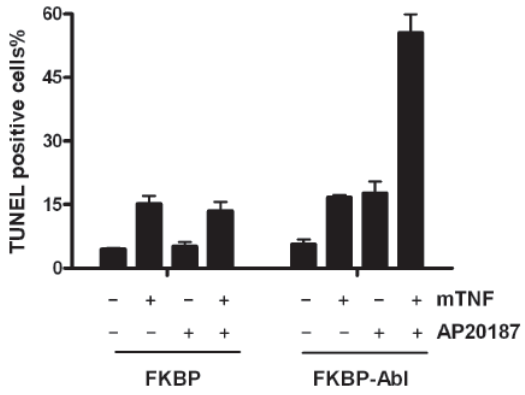
TUNEL positive cells%
60
45
30
15
0
− + − + − + − + mTNF
− − + + − − + + AP20187
FKBP
FKBP-Abl

4-4B)

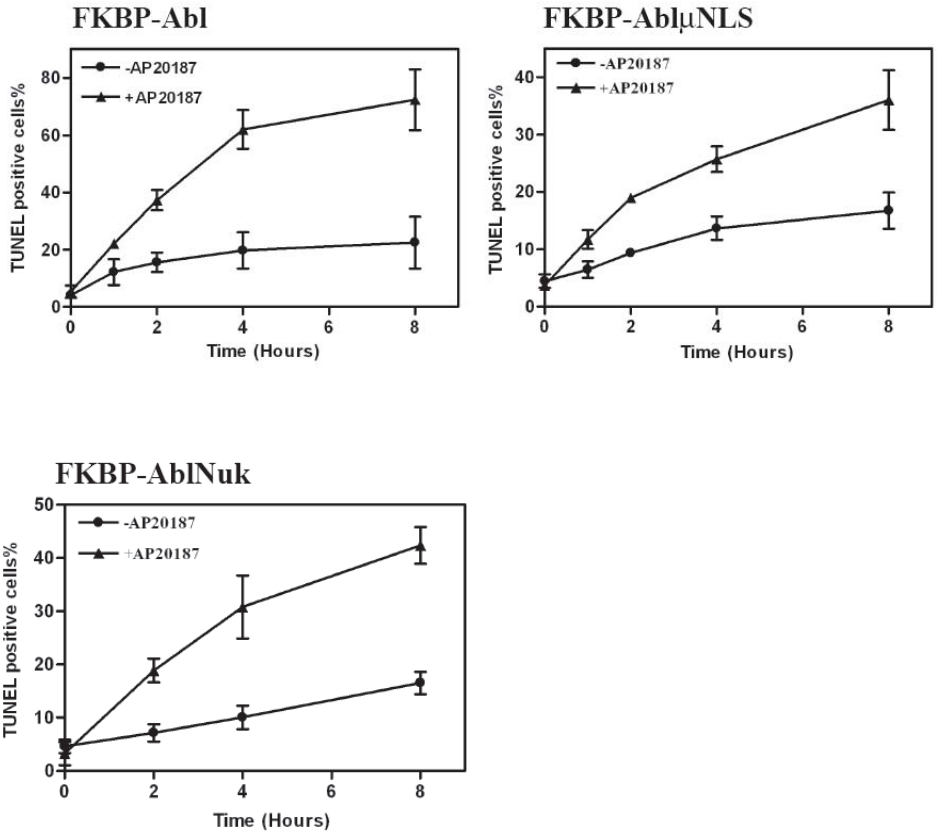
FKBP-Abl
-AP20187
+AP20187
TUNEL positive cells%
Time (Hours)
FKBP-AblμNLS
-AP20187
+AP20187
TUNEL positive cells%
Time (Hours)
FKBP-AblNuk
-AP20187
+AP20187
TUNEL positive cells%
Time (Hours)

4-4C)

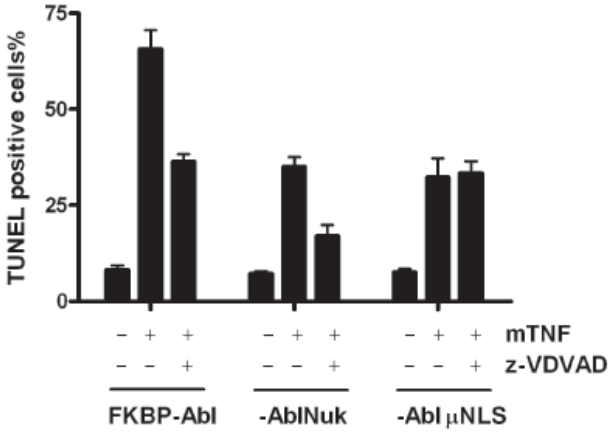

4-4D)

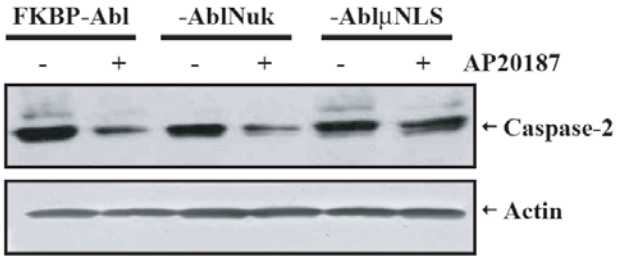

4-4E)

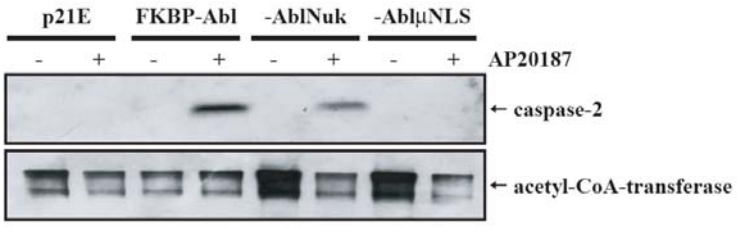

Figure 4-4 continued

REFERENCES

1. Gong, J.G., et al., *The tyrosine kinase c-Abl regulates p73 in apoptotic response to cisplatin-induced DNA damage.* Nature, 1999. **399**(6738): p. 806-9.

2. Baskaran, R., et al., *Ataxia telangiectasia mutant protein activates c-Abl tyrosine kinase in response to ionizing radiation.* Nature, 1997. **387**(6632): p. 516-9.

3. Dan, S., et al., *Activation of c-Abl tyrosine kinase requires caspase activation and is not involved in JNK/SAPK activation during apoptosis of human monocytic leukemia U937 cells.* Oncogene, 1999. **18**(6): p. 1277-83.

4. Chau, B.N., et al., *Tumor necrosis factor alpha-induced apoptosis requires p73 and c-ABL activation downstream of RB degradation.* Mol Cell Biol, 2004. **24**(10): p. 4438-47.

5. Vigneri, P. and J.Y. Wang, *Induction of apoptosis in chronic myelogenous leukemia cells through nuclear entrapment of BCR-ABL tyrosine kinase.* Nat Med, 2001. **7**(2): p. 228-34.

6. Amarante-Mendes, G.P., et al., *Bcr-Abl exerts its antiapoptotic effect against diverse apoptotic stimuli through blockage of mitochondrial release of cytochrome C and activation of caspase-3.* Blood, 1998. **91**(5): p. 1700-5.

7. McGahon, A.J., et al., *Regulation of the Fas apoptotic cell death pathway by Abl.* J Biol Chem, 1995. **270**(38): p. 22625-31.

8. Skorski, T., et al., *Transformation of hematopoietic cells by BCR/ABL requires activation of a PI-3k/Akt-dependent pathway.* Embo J, 1997. **16**(20): p. 6151-61.

9. Nie, Y., et al., *Stimulation of p53 DNA binding by c-Abl requires the p53 C terminus and tetramerization.* Mol Cell Biol, 2000. **20**(3): p. 741-8.

10. Yuan, Z.M., et al., *Genotoxic drugs induce interaction of the c-Abl tyrosine kinase and the tumor suppressor protein p53.* J Biol Chem, 1996. **271**(43): p. 26457-60.

11. Welch, P.J. and J.Y. Wang, *A C-terminal protein-binding domain in the retinoblastoma protein regulates nuclear c-Abl tyrosine kinase in the cell cycle.* Cell, 1993. **75**(4): p. 779-90.

12. Baskaran, R., G.G. Chiang, and J.Y. Wang, *Identification of a binding site in c-Ab1 tyrosine kinase for the C-terminal repeated domain of RNA polymerase II.* Mol Cell Biol, 1996. **16**(7): p. 3361-9.

13. Goldberg, Z., et al., *Tyrosine phosphorylation of Mdm2 by c-Abl: implications for p53 regulation.* Embo J, 2002. **21**(14): p. 3715-27.

14. Agami, R., et al., *Interaction of c-Abl and p73alpha and their collaboration to induce apoptosis.* Nature, 1999. **399**(6738): p. 809-13.

15. Yuan, Z.M., et al., *p73 is regulated by tyrosine kinase c-Abl in the apoptotic response to DNA damage.* Nature, 1999. **399**(6738): p. 814-7.

16. Vella, V., et al., *Exclusion of c-Abl from the nucleus restrains the p73 tumor suppression function.* J Biol Chem, 2003. **278**(27): p. 25151-7.

17. Jost, C.A., M.C. Marin, and W.G. Kaelin, Jr., *p73 is a simian [correction of human] p53-related protein that can induce apoptosis.* Nature, 1997. **389**(6647): p. 191-4.

18. Melino, G., et al., *p73 Induces apoptosis via PUMA transactivation and Bax mitochondrial translocation.* J Biol Chem, 2004. **279**(9): p. 8076-83.

19. Chipuk, J.E., et al., *Direct activation of Bax by p53 mediates mitochondrial membrane permeabilization and apoptosis.* Science, 2004. **303**(5660): p. 1010-4.

20. Inoue, T., et al., *Nuclear import and export signals in control of the p53-related protein p73.* J Biol Chem, 2002. **277**(17): p. 15053-60.

21. Barila, D., et al., *A nuclear tyrosine phosphorylation circuit: c-Jun as an activator and substrate of c-Abl and JNK.* Embo J, 2000. **19**(2): p. 273-81.

22. Kharbanda, S., et al., *c-Abl activation regulates induction of the SEK1/stress-activated protein kinase pathway in the cellular response to 1-beta-D-arabinofuranosylcytosine.* J Biol Chem, 1995. **270**(51): p. 30278-81.

23. Liu, Z.G., et al., *Three distinct signalling responses by murine fibroblasts to genotoxic stress.* Nature, 1996. **384**(6606): p. 273-6.

24. Borges, H.L., et al., *Radiation-induced apoptosis in developing mouse retina exhibits dose-dependent requirement for ATM phosphorylation of p53.* Cell Death Differ, 2004. **11**(5): p. 494-502.

25. McWhirter, J.R. and J.Y. Wang, *Activation of tyrosinase kinase and microfilament-binding functions of c-abl by bcr sequences in bcr/abl fusion proteins.* Mol Cell Biol, 1991. **11**(3): p. 1553-65.

26. Clackson, T., et al., *Redesigning an FKBP-ligand interface to generate chemical dimerizers with novel specificity.* Proc Natl Acad Sci U S A, 1998. **95**(18): p. 10437-42.

27. Preyer, M., C.W. Shu, and J.Y. Wang, *Delayed activation of Bax by DNA damage in embryonic stem cells with knock-in mutations of the Abl nuclear localization signals.* Cell Death Differ, 2007. **14**(6): p. 1139-48.

28. Wen, S.T., P.K. Jackson, and R.A. Van Etten, *The cytostatic function of c-Abl is controlled by multiple nuclear localization signals and requires the p53 and Rb tumor suppressor gene products.* Embo J, 1996. **15**(7): p. 1583-95.

29. Taagepera, S., et al., *Nuclear-cytoplasmic shuttling of C-ABL tyrosine kinase.* Proc Natl Acad Sci U S A, 1998. **95**(13): p. 7457-62.

30. Fornerod, M., et al., *CRM1 is an export receptor for leucine-rich nuclear export signals.* Cell, 1997. **90**(6): p. 1051-60.

31. Plattner, R., et al., *c-Abl is activated by growth factors and Src family kinases and has a role in the cellular response to PDGF.* Genes Dev, 1999. **13**(18): p. 2400-11.

32. Lewis, J.M., et al., *Integrin regulation of c-Abl tyrosine kinase activity and cytoplasmic-nuclear transport.* Proc Natl Acad Sci U S A, 1996. **93**(26): p. 15174-9.

33. Stupack, D.G., et al., *Potentiation of neuroblastoma metastasis by loss of caspase-8.* Nature, 2006. **439**(7072): p. 95-9.

CHAPTER 5

Blockade of TNF-Induced Bid Cleavage by Caspase-Resistant Rb

ABSTRACT

Tumor necrosis factor-α (TNF) activates caspase-8 to cleave effector caspases or Bid, resulting in type-1 or type-2 apoptosis, respectively. We show here that TNF also induces caspase-8-dependent C-terminal cleavage of the retinoblastoma protein (Rb). Interestingly, fibroblasts from $Rb^{MI/MI}$ mice, in which the C-terminal caspase cleavage site is mutated, exhibit defect in Bid cleavage despite caspase-8 activation. Recent results suggest that TNF-receptor endocytosis is required for the activation of caspase-8. Consistent with this notion, inhibition of V-ATPase, which plays an essential role in acidification and degradation of endosomes, specifically restores Bid cleavage in $Rb^{MI/MI}$ cells. Inhibition of V-ATPase sensitizes $Rb^{MI/MI}$ but not wild-type fibroblasts to TNF-induced apoptosis, and stimulates inflammation-associated colonic apoptosis in $Rb^{MI/MI}$ but not wild-type mice. These results suggest that Rb cleavage is required for Bid cleavage in TNF-induced type-2 apoptosis and this requirement can be supplanted by the inhibition of V-ATPase.

INTRODUCTION

Tumor necrosis factor-α (TNF) is an inflammatory cytokine that orchestrates the systemic responses to infections and injuries. Discovered as an inducer of tumor necrosis, TNF also promotes tumor development particularly under conditions of chronic inflammation [1-3]. The tumor promoting activity of TNF is mediated through its activation of the NF-κB pathway, which stimulates the production of cytokines,

chemokines and apoptotic inhibitors [4, 5]. Nonetheless, the type-1 TNF receptor (TNFR1) contains a death domain (DD) that can induce the assembly of death-inducing signaling complex (DISC) to activate the initiator caspase-8, leading to the induction of apoptosis [6, 7]. TNFR1 also activates programmed necrosis that is independent of caspase activity but mediated by reactive oxygen species (ROS) [8-10]. The pro-death function of TNF is observed when the NF-κB pathway is inactivated. In *ex vivo* experiments, cycloheximide (CHX) is routinely used to divert TNF signal towards death by blocking the expression of NF-κB-induced genes, such as FLIP and mitochondrial superoxide dismutase (mSOD) that prevent the activation of caspase-8 and the generation of ROS, respectively [11, 12]. In cells defective in the NF-κB pathway, TNF alone (without CHX) is sufficient to induce cell death [13, 14]. In mice, TNF- and TNFR1-dependent cell death is observed in a variety of mouse tissues under conditions of acute inflammation [2, 5, 15]. The molecular mechanisms that govern the survival versus the death response to TNF are likely to be complex and have not been fully elucidated.

An important clue to how TNF differentially activates NF-κB or caspase-8 has come from recent studies showing TNFR1 endocytosis is a pre-requisite for DISC assembly [16, 17]. In the plasma membrane, activated TNFR1 is capable of stimulating the NF-κB pathway but it does not associate with FADD or caspase-8 [18, 19]. By contrast, two other DD-receptors, i.e., FAS/CD95 and DR5, do assemble DISC at the plasma membrane when activated by FAS-ligand or TRAIL, respectively [19]. In experiments conducted with a human fibrosarcoma cell line (HT1080) that expresses a degradation-resistant IκB-α to divert TNF signal towards caspase-8, Micheau and

Tschopp detected a cytosolic DISC complex containing TRADD, FADD and caspase-8 but free of TNFR1 [18]. Subsequent studies conducted with human U937 and mouse 3T3 cells detected TNFR1-associated TRADD-FADD-caspase-8 complex in the endosomal fraction [16]. Together, these results suggest that TNFR1 endocytosis and the release of DISC from the receptor-endosome may play a role in determining the cellular response to TNF.

The retinoblastoma susceptibility gene product, Rb, is a nuclear scaffolding protein with multiple protein-binding pockets [20-23]. Rb inhibits the transcription of E2F-regulated genes to block cell cycle progression. Because E2F also stimulates the expression of apoptotic factors, such as caspases and Apaf-1, inhibition of E2F by Rb confers apoptotic resistance in growth-arrested cells [24]. Upon stimulation with mitogenic factors, Rb is inactivated through phosphorylation by cyclin-dependent kinases to promote cell cycle entry and S-phase progression [25]. Upon exposure to death stimuli, Rb is cleaved by caspase at a predominant site, $DEAD^{886}G^{887}$, near the C-terminus of the protein [26-28]. Cleavage at this site generates a large fragment of Rb (RbΔI) that retains E2F-binding and transcription repression functions [26, 27, 29]. Thus, the C-terminal cleavage does not interfere with the anti-proliferative activity of Rb. We have mutated this C-terminal caspase cleavage site to $DEAA^{886}E^{887}$ in the mouse *Rb* gene to create the *Rb-MI* allele [30]. The *Rb-MI* allele confers resistance to inflammation-induced apoptosis in the mouse intestine, which is dependent on TNF (30). The *Rb-MI* allele also confers resistance to TNF-induced apoptosis in explanted thymocytes and in fibroblasts derived from the mouse embryos [30, 31]. Interestingly, however, *Rb-MI* does not protect fibroblasts from apoptosis induced by TRAIL (BN Chau and JYJ Wang, unpublished),

nor is it protective of hepatocyte apoptosis induced by the ligation of FAS receptor (T-T Chen and JYJ Wang, unpublished).

Death receptors such as FAS and TNFR1 stimulate apoptosis through two pathways, both activated by caspase-8 [4, 32]. In the type-1 pathway, initiator caspase-8 directly cleaves and activates effector caspases to induce apoptosis [33]. In the type-2 pathway, initiator caspase-8 cleaves Bid and the resulting tBid induces mitochondria outer membrane permeability to cause the release of pro-apoptotic factors leading to the activation of apoptosome and caspase-9 [33, 34]. We have previously shown that TNFR1-induced cytochrome c release is defective in *Rb-MI* fibroblasts [30]. In pursuing the mechanism underlying this defect, we have discovered that inhibition of vacuolar ATPase can restore TNFR1-induced type-2 apoptotic pathway in *Rb-MI* cells.

The vacuolar ATPase (V-ATPase) is a proton pump that is conserved in eukaryotic cells [35, 36]. Composed of a soluble V_1 complex that hydrolyzes ATP and an integral membrane V_0 complex that forms the proton channel, V-ATPase couples ATP hydrolysis to the translocation of protons from the cytosol to the lumen of late endosomes, multivesicular bodies and lysosomes [35, 37]. V-ATPase-dependent lumenal acidification provides the necessary condition for lysosomal degradative enzymes to perform their functions. Moreover, acidification is also required for endosomal trafficking [37, 38], best demonstrated by a recent report that V-ATPase allows the recruitment of Arf6 and ARNO to the endosomal membrane for sorting to the multivesicular body and lysosome [39]. We show here that TNFR1 activates the 43-kd endosomal caspase-8 in *Rb-MI* cells but Bid is not cleaved. However, Bid cleavage is rescued either by the knockdown of Rb-MI or by the inhibition of V-ATPase.

EXPERIMENTAL PROCEDURES

Cell culture - Fibroblasts derived from $Rb^{+/+}$ (*Rb-wt*) and $Rb^{MI/MI}$ *(Rb-MI)* mouse embryos were immortalized through the 3T3 passage protocol. The *Caspase-8*$^{-/-}$ and *Caspase-8*$^{+/+}$ MEFs [40] were gifts from Dr. David Wallach (Weizmann Institute, Israel). MEFs were cultured in DMEM media containing 10% FBS, penicillin/ streptomycin and 0.05% β-mercaptoethanol. Cells were routinely treated with 10 ng/ml recombinant human TNF (hTNF) plus 2.5 μg/ml cycloheximide (CHX) for 5 hours at 37ºC unless noted otherwise.

Antibodies and Chemicals - Rb antibodies used are rabbit anti-Rb (851) raised against the C-terminal fragment (residues 768–928) of Rb [20] and anti-Rb from Pharmingen (554136); rat anti-caspase-8 (1G12), rat anti-FADD (12E7) were from Alexis Biochemicals; rabbit anti-Smac was from Chemicon; goat anti-Bid, rabbit anti-Cox-IV were from Biovision; goat-anti-ATP6V1B1 (N-20), rabbit-anti-Mcl-1 (S-19), rabbit anti-TRADD (H-278) were from Santa Cruz Biotechnology; rabbit-anti-phospho-c-Jun, mouse anti-cleaved caspase-3 (5A1), rabbit anti-PARP1 were from Cell Signaling Technology; mouse-anti-cytochrome c antibody was from BD Bioscience; biotin-VAD-FMK was from Kamiya; caspase-8 fluorometric assay kit was from Biovision; caspase-3 fluorometric assay kit was from Molecular Probes; TUNEL staining kit was obtained from BD Biosciences; recombinant human and mouse TNF-α were from R & D Systems;

MG-132, cathepsin inhibitor z-YY-FMK were from Calbiochem; bafilomycin A1, concanamycin A, and FCCP were from Sigma.

Western blot - Whole cell lysates were prepared in RIPA buffer (50 mM Tris-HCl [pH 7.4], 150 mM NaCl, 1% NP-40, 0.25% sodium deoxycholate, 0.1% SDS, 0.5 mM EDTA, 1 mM EGTA, 1 mM DTT) plus protease inhibitor (from Sigma); 50-100 μg of total protein were resolved by SDS-PAGE, transferred onto PVDF membranes, blocked in 5% nonfat dry milk/TBST (20 mM Tris-HCl [pH 7.5], 150 mM NaCl, 0.05% Tween-20) and incubated with primary antibodies overnight at 4°C. Membranes were washed 3 × 10 minutes in TBST and incubated with HRP-conjugated secondary antibodies for 1-3 hours at room temperature. After 3 × 10 minutes washing, membranes were incubated with enhanced ECL reagent (from Pierce) for 1 minute and exposed to X-ray films. To detect Rb protein in MEFs, 5 μg anti-Rb (851) was mixed with 1 mg whole cell lysate, the immune complex collected on protein A-sepharose, resolved by SDS-PAGE and then immunoblotted with anti-Rb antibody from Pharmingen.

Propidium iodide uptake - Cells were trypsinized and re-suspended in 500 μl PBS containing 1 μg/ml propidium iodide (PI), incubated for 10 minutes at room temperature and immediately analyzed by flow cytometry, counting at least 10,000 events per sample. For each treatment condition, triplicate samples were analyzed from which the average percentage of PI positive cells was calculated.

DEVDase and IETDase assay - Cells were lysed in PIPES/CHAPS buffer (10 mM HEPES-KOH [pH 7.5], 10 mM KCl, 1.5 mM $MgCl_2$, 1 mM EDTA, 1 mM EGTA) and clarified by centrifugation. 100 μg of total protein was incubated with 50 μM Ac-DEVD-AMC or Ac-IETD-AFC for 60 minutes at 37°C. Fluorometric detection of AMC

and AFC was performed in triplicates by excitation at 360 nm/emission at 460 nm (AMC) or excitation at 400 nm/emission at 505 nm (AFC).

Cell fractionation - Cells were trypsinized, washed in PBS, re-suspended in mannitol/sucrose buffer (210 mM mannitol, 70 mM sucrose, 10 mM HEPES [pH 7.5], 0.5 mM EDTA) plus protease inhibitor and broken up by passage through a 22.5 gauge needle. Heavy membrane fractions (containing mitochondria) were pelleted by centrifugation. 100 μg of the supernatant was resolved on a 14% SDS-PAGE gel followed by immunoblotting with anti-cytochrome c or anti-Samc.

In vitro cytochrome c release assay - Freshly isolated liver mitochondria were combined with cytosolic extracts from untreated or TNF-treated *Rb-wt* or *Rb-MI* cells diluted in KCl buffer (125 mM KCl [pH 7.4], 10 mM HEPES-KOH, 5 mM Na_2HPO_4, 4 mM $MgCl_2$, 0.5 mM EGTA) and incubated for 45 minutes at 37°C under gentle agitation. Mitochondria were pelleted by centrifugation. The supernatants and the pellets were separately analyzed for cytochrome c and Cox-IV by immunoblotting.

In vivo affinity-labeling of Caspase-8 - We adopted the method described by Tu et al [41] to label activated caspase-8 in cells. Briefly, 1×10^7 cells were trypsinized, centrifuged, re-suspended in 4 ml of DMEM containing 10% FBS with 50 μM biotin-VAD-FMK, after 1 hour of incubation at 37ºC, 10 ng/ml hTNF plus CHX (2.5 μg/ml) were added. Cells were harvested at the indicated time, lysed in 0.5 ml RIPA buffer, 1 mg of total proteins were incubated with 50 μl streptavidin/Sepharose beads (Amersham) at 4ºC overnight. The beads were washed with RIPA buffer, boiled in 25 μl of 3 × SDS sample buffer and the supernatant was resolved by SDS-PAGE and caspase-8 was detected by immunoblotting.

Synchronization of endocytosis - *Rb-wt* or *Rb-MI* cells were first incubated with different doses of hTNF/CHX at 4°C for 90 minutes, then shifted to 37°C for different amounts of time. Cells were subjected to either cell death assay by PI uptake or DEVDase and IETDase assay.

DSS-induced colonic apoptosis in mice - $Rb^{+/+}$, $Rb^{+/MI}$, or $Rb^{MI/MI}$ mice were fed water containing 3% dextran sulfate sodium (DSS, M.W. =36,000-50,000 from Sigma). At 56 hour into DSS feeding, they were injected i.p. with either bafilomycin A1 at a concentration of 25 ng/g body weight or vehicle. Mice were sacrificed 16 hours later, colonic tissues were collected in a roll, fixed in 4% paraformaldehyde for 2 days, embedded into paraffin blocks, cut into 5 μm sections, de-paraffined and TUNEL labeled. Fluorescent images of labeled sections were captured by CCD camera; TUNEL-positive nuclei were counted in at least 25 crypts per tissue samples. All animal studies were approved by the University of California San Diego institutional animal care and use committee.

Lysosomal pH measurement –We adopted the method described by Trombetta et al [42] to measure the luminal pH of endosomes and lysosomes. Briefly, ten thousand *Rb-wt* or *Rb-MI* mouse fibroblasts were plated per well in a 96-well plate. After overnight culture, cells were loaded with the pH-sensitive FITC-dextran (Sigma) for 1 hour at 37ºC, followed by treatment with hTNF/CHX or bafilomycin A1 (200 nM) for 5 hours. At the end of the experiment, excess FITC-dextran was removed by extensive washing with DMEM media and the wells were replaced with phosphate buffered saline. The fluorescence emitted at 520 nm was recorded at two excitation wavelengths 450 and 490 nm using a SpectraMax Gemini fluorescence plate reader. The pH values were

determined by comparing the fluorescence signals to a standard curve constructed for FITC-dextran in phosphate/citrate buffers of different pH between 4.0 and 8.0.

DNA microarray - *Rb-MI* or *Rb-wt* cells were subjected to different treatments, then the total RNA was extracted and the cRNA probes were synthesized, labeled with biotin (for Affymetrix GeneChip® (MGU74A)), Cy5 or Cy3 (for Agilent mouse whole genome array (G4112A)). Array hybridization, data collection and analysis were conducted using protocols and programs supplied by the manufacturers and indicated in the Figures and Tables.

siRNA experiments - Sense and antisense RNA oligos corresponding to the target sequence for mouse *Rb* (GUUGAUAAUGCUAUGUCAA), mouse *ATP6V1B1* (TCCACCTCAGTCCTATATA) and for *LacZ* (AACGTACGCGGAATACTTCGA) were synthesized and annealed by Ambion. Uniqueness of individual target sequences was confirmed by a BLAST search of mouse genomic plus transcript database. Transfection of synthetic siRNA was performed using Lipofectamine reagent with standard procedures. 48 hours after transfection, cells were collected and target protein levels were analyzed. Cotransfection of Cy3-labeled siRNA duplexes were performed to determine transfection efficiency when necessary.

RESULTS

TNFR1-induced type-2 apoptotic pathway is blocked in *Rb-MI* cells

We have previously shown that *Rb-MI* mouse fibroblasts are resistant to apoptosis induced by the type-1 TNF receptor (TNFR1), which is activated by human TNF or an anti-TNFR1 agonist antibody [30]. Consistent with previous results, human TNF/CHX (hTNF, activates only the mouse TNFR1) or mouse TNF/CHX (mTNF, activates TNFR1 and R2) led to caspase activation measured by the cleavage of DEVD-AMC or IETD-AFC in *Rb-wt* cells (Figure 5-1A and 5-1B). In *Rb-MI* fibroblasts, mTNF/CHX but not hTNF/CHX caused caspase activation (Figure 5-1A and 5-1B). We also measured the IETDase activity, which is mostly mediated by caspase-8 [43], at several concentrations of mTNF and hTNF. With the *Rb-wt* cells, the half-maximum IETDase measured at 5 hours after stimulation was observed at approximately 10 ng/ml of either hTNF or mTNF, although the maximal levels of IETDase were higher in mTNF/CHX-treated *Rb-wt* cells. With the *Rb-MI* cells, the IETDase activity stimulated by mTNF/CHX was about two-fold lower than that found in *Rb-wt* cells at every mTNF concentration tested (Figure 5-1C). With hTNF, however, *Rb-MI* cells appeared non-responsive, with no detectable stimulation of IETDase at hTNF concentrations up to 80 ng/ml (Figure 5-1C).

We have previously shown that hTNF/CHX-induced cytochrome c release is defective in *Rb-MI* cells [30]. As shown in Figure 5-1D, cytosolic Smac and cytochrome c were detected in *Rb-wt* cells treated with hTNF/CHX or mTNF/CHX, but their release only occurred in mTNF/CHX-treated *Rb-MI* cells. Consistent with the role of Bid cleavage in TNF-induced cytochrome c release [34, 44], we observed Bid cleavage in *Rb-wt* cells treated with hTNF/CHX or mTNF/CHX, but Bid was only cleaved in mTNF/CHX-treated *Rb-MI* cells (Figure 5-1E). To further examine the cytochrome c release defect in *Rb-MI* cells, we prepared lysates from hTNF/CHX-treated *Rb-wt* and

Rb-MI cells and incubated them with liver mitochondria. Cytochrome c release activity was detected in lysates from hTNF/CHX-treated *Rb-wt* cells but not those from *Rb-MI* cells (Figure 5-1F). The lysates of *Rb-MI* cells, either before or after hTNF/CHX treatment, did not interfere with cytochrome c release induced by a recombinant NC-Bid [45] (Figure 5-1G), suggesting the defect is not caused by an inhibitor of tBid in *Rb-MI* lysates. In keeping with this conclusion, we found that hTNF/CHX induced similar modifications of Mcl-1, an inhibitor of cytochrome c release, in *Rb-wt* and *Rb-MI* cells (http://www.jbc.org/cgi/data/M702261200/DC1/1). We also prepared liver mitochondria from *Rb-MI* mice and found them to be competent in releasing cytochrome c in response to lysates from hTNF/CHX-treated *Rb-wt* fibroblasts (Figure 5-1H). Taken together, these results show that TNFR1-induced Bid cleavage is defective in *Rb-MI* cells and that the lack of tBid rather than the accumulation of inhibitors accounted for the cytochrome c release defect in hTNF/CHX-treated *Rb-MI* cells.

TNFR1-induced cleavage of Rb requires caspase-8

TNF-induced Bid cleavage is dependent on caspase-8 [34, 44]. Likewise, TNFR1-induced Rb cleavage is also dependent on caspase-8 (Figure 5-2 A-D). Treatment with hTNF/CHX did not cause the cleavage of Rb, PARP1 or caspase-3 in fibroblasts derived from caspase-8 knockout mouse (Figure 5-2B), nor did it activate the DEVDase or IETDase activity (Figure 5-2C and 5-2D). Cleavage of Rb, PARP1, caspase-3 and activation of DEVDase or IETDase in response to hTNF/CHX occurred in fibroblasts from *Caspase-8*$^{+/+}$ littermates (Figure 5-2 B-D). Since caspase-8 is required for TNFR1

to induce the cleavage of Rb and Bid, and since Bid cleavage is defective in *Rb-MI* cells, our results (Figures 5-1 and 5-2) suggest that Rb cleavage is required for Bid cleavage.

TNFR1-induced Bid cleavage is restored by the knockdown of Rb-MI

To demonstrate that the Rb-MI protein is required to prevent Bid cleavage, we used siRNA to knockdown its expression (Figure 5-2E). The knockdown of wild type Rb protein did not enhance hTNF/CHX-induced IETDase activity, Bid cleavage or cell death (Figure 5-2 F-H). In contrast, knockdown of Rb-MI restored hTNF/CHX-induced IETDase activity, Bid cleavage and cell death (Figure 5-2 F-H). These results suggest that Rb cleavage is sufficient to promote TNFR1-induced Bid cleavage, because the knockdown of Rb does not further enhance Bid cleavage. By contrast, the Rb-MI protein, which cannot be cleaved, blocks Bid cleavage. Furthermore, the Rb-MI protein must be present to prevent TNFR1 from inducing the cleavage of Bid, because Bid cleavage is restored with the knockdown of Rb-MI.

TNF-induced gene expression is similar in *Rb-wt* and *Rb-MI* cells

Given the established role of Rb in the regulation of gene expression, we performed microarray analyses to compare gene expression profiles of *Rb-MI* cells treated with hTNF/CHX versus mTNF/CHX. However, we did not detect any statistically significant differences despite the fact that mTNF/CHX, but not hTNF/CHX, induced Bid cleavage in *Rb-MI* cells (http://www.jbc.org/cgi/data/M702261200/DC1/1, and

http://www.jbc.org/cgi/data/M702261200/DC1/2). We also compared hTNF/CHX-induced gene expression changes in *Rb-wt* and *Rb-MI* cells and found a similar cohort of upregulated and downregulated genes in these two cell lines (http://www.jbc.org/cgi/data/M702261200/DC1/3). We have previously observed hTNF/CHX-induced IκB-α degradation in *Rb-wt* and *Rb-MI* cells [30], consistent with the similar upregulation of several known NF-κB regulated genes by TNF in these cells (http://www.jbc.org/cgi/data/M702261200/DC1/3). We also found that hTNF/CHX-induced phosphorylation of c-Jun was similar in *Rb-wt* and *Rb-MI* cells (http://www.jbc.org/cgi/data/M702261200/DC1/1). Thus, Rb-MI did not exert a detectable effect on TNF-induced gene expression, which is mediated by the TNFR1 at the plasma membrane. Moreover, Bid cleavage defect in *Rb-MI* cells is not likely to require new gene expression since it is observed in the presence of CHX.

Activation of caspase-8 in *Rb-MI* cells

We have previously observed the loss of full-length caspase-8, occurring between 12 to 24 hours after hTNF/CHX treatment in both *Rb-wt* and *Rb-MI* primary fibroblasts [30], indicating that caspase-8 activation is not impaired in *Rb-MI* cells. With the immortalized *Rb-wt* and *Rb-MI* fibroblasts, we could not detect any reduction in full-length caspase-8 at 5 hours after hTNF/CHX treatment when Bid cleavage was observed (Figure 5-3A). Since caspase-8 activation does not require its cleavage [46, 47], we adopted an *in vivo* affinity labeling method to covalently biotinylate activated caspase-8 with a membrane permeable biotin-VAD-fmk [41] (Figure 5-3B). The full-length (p55)

caspase-8 was pulled-down by streptavidin beads only in cells exposed to biotin-VAD-fmk (not shown), and this p55 band was not found in *caspase-8*$^{-/-}$ fibroblasts (Figure 5-3C). The levels of biotinylated p55 caspase-8 were similar in untreated and hTNF/CHX-treated cells (Figure 5-3C and 5-3D). Detection of active caspase-8 in untreated cells may not be surprising given the recent results that caspase-8 has biological functions other than the stimulation of apoptosis [48, 49]. At 2 hours after hTNF/CHX addition, a p43 caspase-8 band was pulled-down in cells with caspase-8 but not in the *Caspase-8*$^{-/-}$ cells (Figure 5-3C and 5-3D). Previous studies have shown that the p43 caspase-8 is present in the endosomal fraction of TNF-treated cells [16]. Approximately 1% of the input p55 band was pulled-down by the streptavidin beads (Figure 5-3D), and the p43 band could not be detected in whole cell lysates (Figure 5-3A), indicating that only a small fraction of the full-length caspase-8 was activated and converted to p43 in response to hTNF/CHX. We observed biotinylated p55 and p43 bands in hTNF/CHX-treated *Rb-wt* and *Rb-MI* cells (Figure 5-3D), consistent with the previous conclusion that TNFR1-induced caspase-8 activation does occur in *Rb-MI* cells.

Enhanced death response, caspase activity and Bid cleavage through 4ºC pre-incubation with TNF

Recent reports have suggested that TNFR1 endocytosis is required for the activation of caspase-8 [16, 17], and synchronized endocytosis enhances TNFR1-induced caspase-8 activation [16]. Synchronized endocytosis can be achieved by pre-incubating cells with TNF at 4ºC and then raising the temperature to 37ºC to allow for the

simultaneous uptake of ligand-engaged TNFR1 [16]. We applied this protocol to the *Rb-wt* and *Rb-MI* cells at varying concentrations of hTNF and found that synchronization sensitized both cell types to hTNF/CHX-induced death, measured at 24 hr post temperature shift (Figure 5-4A and 5-4B). The pre-incubation protocol also enhanced IETDase activity measured at 2-3 hr after hTNF/CHX addition (Figure 5-4C), corresponding to the cleavage of Bid (and the formation of tBid) in *Rb-MI* cells (Figure 5-4D). While pre-incubation enhanced the response of *Rb-MI* cells to hTNF/CHX, it did not restore the response to that of the *Rb-wt* cells. Nevertheless, the partial rescue of Bid cleavage defect by pre-incubation suggests that the level of caspase-8 can be artificially raised in *Rb-MI* cells by synchronized endocytosis. The endocytosis of TNF receptor should be functional in *Rb-MI* cells; otherwise, we would not have been able to sensitize these cells by pre-incubation at 4ºC. However, the apoptotic signal output from the endocytic compartment is lower in *Rb-MI* cells than that of *Rb-wt* cells even under conditions of synchronized endocytosis.

One possibility for the Bid cleavage defect might be that activated caspase-8 was lost through endosomal trafficking in *Rb-MI* cells. We tested several drugs known to interfere with endocytic trafficking, and lysosomal degradation for their effects on hTNF/CHX-induced IETDase activity in *Rb-MI* cells (Figure 5-4E). Four of the compounds tested, i.e., ammonium chloride (raises intracellular pH), FCCP (a proton ionophore), 3-MA (inhibitor of autophagy) and z-FF-fmk (inhibitor of cathepsins), did not activate IETDase in the absence or presence of hTNF/CHX (Figure 5-4E). Interestingly, we found that concanamycin A and bafilomycin A, both are inhibitors of the vacuolar ATPase (V-ATPase), stimulated IETDase activity in hTNF/CHX-treated *Rb-*

MI cells but did not have any effect in the absence of TNF (Figure 5-4E). V-ATPase acidifies the endosomes to promote their trafficking along the lysosomal degradative pathway [39]. We therefore measured the pH of the endosomal compartment using a pH-sensitive fluorescent dextran [50] and found that hTNF/CHX treatment did not affect the endosomal pH in *Rb-wt* or *Rb-MI* cells (Figure 5-4F). By contrast, treatment with bafilomycin A1 (Baf) raised the endosomal pH from 5.5 to 7 irrespective of TNF treatment in both *Rb-wt* and *Rb-MI* cells (Figure 5-4F). Thus, TNF does not cause a detectable inhibition of V-ATPase activity; however, V-ATPase inhibitor can restore TNF-induced IETDase in *Rb-MI* cells.

Inhibition of V-ATPase restores caspase-8-dependent Bid cleavage in Rb-MI cells

To further examine the effect of V-ATPase inhibition, we tested whether Baf can enhance the activation of caspase-8. Using the *in vivo* biotinylation approach outlined in Figure 5-3B, we showed that Baf did not cause a significant increase in the pull-down of p55 and p43 caspase-8 in *Rb-wt* and *Rb-MI* cells (Figure 5-5A). However, Baf allowed the accumulation of cytosolic IETDase activity and the cleavage of Bid in hTNF/CHX-treated *Rb-MI* cells (Figure 5-5B and 5-5C). Baf treatment did not enhance IETDase activity or Bid cleavage in *Rb-wt* cells. Bid cleavage under the condition of Baf plus hTNF/CHX remained dependent on caspase-8 (Figure 5-5D), showing Baf did not activate an alternative Bid cleavage pathway. We found that the levels of TNFR1 and DISC component proteins were similar in *Rb-wt* and *Rb-MI* cells, and their levels were not affected by hTNF/CHX and/or Baf treatment (Figure 5-5E). We noted that Baf also

stimulated hTNF/CHX-induced Rip1 cleavage, which is mediated by caspase-8 [51], in *Rb-MI* cells but not in *Rb-wt* cells (Figure 5-5E).

To seek additional evidence that inhibition of V-ATPase can restore Bid cleavage in *Rb-MI* cells, we knocked down the B1 subunit of the cytosolic V_1 complex of the V-ATPase by siRNA. The control siRNA did not affect Bid cleavage; however, the knockdown of the V-ATPase B1 subunit rescued hTNF/CHX-induced IETDase activity and Bid cleavage in *Rb-MI* cells (Figure 5-5F, 5-5G, and 5-5H). Because pre-treatment with Baf or V1B1-knockdown did not enhance hTNF/CHX-induced IETDase or Bid cleavage in *Rb-wt* cells (Figure 5-5B, 5-5C, 5-5E, 5-5F, and 5-5G), it suggests that V-ATPase inhibition is irrelevant to Bid cleavage when Rb can be cleaved. However, in *Rb-MI* cells, V-ATPase inhibition supplants the requirement of Rb cleavage to allow Bid cleavage.

Bafilomycin A1 stimulates DSS-induced colonic apoptosis in *Rb*$^{MI/MI}$ mice

We have previously shown that *Rb-MI* promotes colon tumors in the *p53-null* genetic background, correlating with reduced apoptotic response to inflammation-associated epithelial apoptosis [52]. We induced apoptosis of colonic epithelial cells by feeding mice with water containing dextran sulfate sodium (DSS) for three days [52]. Mice were also exposed to Baf via intraperitoneal injection 16 hours prior to the collection of colonic tissue. Exposure to DSS induced TUNEL-positive nuclei in the colonic epithelium (Figure 5-6A). Exposure to Baf alone did not induce apoptosis (not shown). Following DSS exposure, the number of TUNEL-positive nuclei in the colonic

crypts was significantly lower in $Rb^{MI/MI}$ mice than that of their $Rb^{+/+}$ littermates (Figure 5-6B). However, additional exposure to Baf significantly increased the apoptotic response of $Rb^{MI/MI}$ mice to DSS feeding. Baf also significantly enhanced the apoptotic response of $Rb^{+/MI}$ mice to DSS (Figure 5-6B). By contrast, Baf did not affect the colonic apoptotic response in $Rb^{+/+}$ mice (Figure 5-6B). We have previously shown that thymocytes from $Rb^{MI/MI}$ mice are resistant to hTNF/CHX-induced apoptosis [31]. We found that treatment with Baf also enhanced hTNF/CHX-induced apoptosis of thymocytes from $Rb^{MI/MI}$ but not $Rb^{+/+}$ mice (not shown). Thus, *Rb-MI*-mediated inhibition of TNFR1-dependent apoptosis can be overridden by Baf in fibroblasts, thymocytes and colonic epithelial cells.

DISCUSSION

Sequential activation of TNFR1-induced type-1 and type-2 apoptotic pathways

In the current model of extrinsic apoptotic pathways, activation of caspase-8 leads to the simultaneous cleavage of substrates in the type-1 and the type-2 pathways (Figure 5- 7A). This parallel cleavage model cannot explain our observations with the *Rb-MI* cells where caspase-8 is activated but Bid is not cleaved. Our results suggest an alternative model where caspase-8-dependent Rb cleavage precedes caspase-8-dependent Bid cleavage (Figure 5-7B). Because Bid is not cleaved in *Rb-MI* cells, we propose that Rb cleavage via the type-1 pathway is an upstream requirement for Bid cleavage in the type-2 pathway (Figure 5-7B).

The sequential cleavage model predicts that Rb cleavage would not be required for TNF to kill cells that die by the type-1 pathway alone. In other words, Rb-MI would only protect type-2 cells from TNF-induced apoptosis. This is consistent with our previous findings that endotoxin-induced apoptosis is blocked in the intestine but not in the spleen of *Rb-MI* mice [30]. We would point out that mouse embryo fibroblasts (MEFs) are type-1 cells because TNF/CHX-induced apoptosis is observed in *Bid*-knockout and *cytochrome c*-knockout MEFs [53, 54]. In other words, the Bid-dependent cytochrome c release is not necessary for TNF/CHX to kill MEFs. In fact, we show that mTNF/CHX can indeed activate apoptosis in *Rb-MI* MEFs. Only by activating TNFR1 alone with human TNF could we reveal the type-2 pathway blockade imposed by Rb-MI in MEFs. The physiological relevance of the MEF-based experimental results is demonstrated by our observation that bafilomycin A1 can restore colonic apoptosis in DSS-treated $Rb^{MI/MI}$ mice. We have found that DSS-induced colonic apoptosis is diminished in TNFR1-deficient mice (I. C. Hunton and J.Y.J. Wang, unpublished), suggesting the involvement of TNFR1 in this *in vivo* response. This death response is diminished in $Rb^{+/MI}$ and $Rb^{MI/MI}$ mice but could be enhanced by bafilomycin. Taken together, results from *Rb-MI* MEFs and $Rb^{MI/MI}$ mice are consistent with the model that Rb cleavage is required for TNF to activate the type-2 apoptotic pathway.

Receptor endocytosis and cytosolic accumulation of activated caspase-8

Previous studies have shown that TNFR1 does not initiate DISC assembly at the plasma membrane [18, 19]. Instead, the TNFR1-DISC complex is detected in the

endosomal fraction under conditions of synchronized endocytosis in several cell types [16, 17]. A cytosolic DISC free of TNFR1 has been observed in a human fibrosarcoma cell line that ectopically expresses a constitutive inhibitor of NF-κB [18]. In the fibrosarcoma cell line, two distinct signaling complexes were identified. The complex-1 contains TNFR1, TRADD, RIP1, TRAF-2 and mediates NF-κB activation. This membrane complex appears to be further processed to recruit FADD through TRADD resulting in the formation of complex-2, i.e., the DISC complex, that dissociates from TNFR1 and accumulates in the cytosol [18]. Interestingly, while TRAIL-induced apoptosis does not require receptor endocytosis [55], internalization of FAS/CD95 and TNFR1 through endocytosis is required for the induction of apoptosis [56]. Activated FAS/CD95L directly recruits FADD and stimulates a small amount of DISC formation at the cell surface followed by endocytosis of the entire complex. In type-1 cells, this internalization step triggers further recruitment of FADD and caspase-8 to stimulate apoptosis [56]. We have found that *Rb-MI* does not interfere with apoptosis induced by anti-FAS or TRAIL (30, and unpublished). *Rb-MI* does not interfere with TNFR1 endocytosis because synchronization of endocytosis rescued Bid cleavage in *Rb-MI* cells. Taken together, these results suggest that *Rb-MI* does not block apoptosis at the step of receptor internalization. Furthermore, these results suggest that DISC complexes stimulated by activated Fas versus TNFR1 may be subjected to different regulation, despite the similar requirement for receptor endocytosis in the assembly of DISC. Because synchronized endocytosis can enhance caspase-8 activity and Bid cleavage in MEFs, irrespective of Rb cleavage, and because the inhibition of V-ATPase specifically enhanced caspase-8-dependent Bid cleavage in *Rb-MI* cells, Rb-MI is likely to exert its

anti-apoptotic effect by preventing the cytosolic accumulation of activated caspase-8 downstream of TNFR1 activation.

We propose that the endosomal TNFR1-DISC complex may activate the type-1 pathway in a manner similar to that of the endosomal FAS-DISC complex in type-1 cells (58) (Figure 5-7B). The endosomal DISC can then be released from the receptor to accumulate as cytosolic DISC or shunted down the endocytic degradation pathway (Figure 5-7B). We propose that only the cytosolic DISC is competent in cleaving Bid. We propose that the majority of activated caspase-8 is lost through endocytic trafficking in *Rb-MI* cells, thus causing the lack of cytosolic IETDase activity and the defect in Bid cleavage. Consistent with this notion is the finding that pharmacological or genetic ablation of the V-ATPase can restore cytosolic IETDase and Bid cleavage in *Rb-MI* cells. Inhibition of V-ATPase prevents endosomal fusion with multivesicular bodies and lysosome, as well as endosomal degradation [39, 57]. The rescuing of IETDase or Bid cleavage was not observed with drugs that raise the intracellular pH (NH_4Cl, FCCP), inhibit autophagy (3-MA), or inhibit cathepsins (z-FF-fmk). Furthermore, hTNF/CHX treatment did not alter the endosomal pH in *Rb-MI* cells. Taken together, these results suggest that Rb cleavage, mediated by the type-1 pathway, may regulate the release/sorting of endosomal DISC, but not the lysosomal degradation of activated caspase-8, to promote Bid cleavage.

Mechanism of Rb-dependent blockade of Bid cleavage

The nuclear Rb protein inhibits cell proliferation and apoptosis through transcriptional regulation of E2F-dependent gene expression [58]. Cleavage of Rb at the C-terminal caspase site ($DEAD^{886}G^{887}$) mutated in Rb-MI ($DEAA^{886}E^{887}$) generates a large Rb-ΔI fragment (1-886) that encompasses the two well-defined E2F-binding pockets and the Abl-binding C-pocket in the Rb protein [59, 60]. We have previously shown that Rb-ΔI is further degraded in apoptotic cells [28, 30], suggesting that C-terminal cleavage can cause the loss of Rb protein thus leading to the activation of pro-apoptotic gene expression through E2F and Abl [31, 58]. The blockade of Bid cleavage observed in this study is not likely to involve new gene expression, because Rb-ΔI was not further degraded at the time point when Bid cleavage occurred, and because cycloheximide was used in conjunction with TNF to induce cell death.

We have previously shown that thymocytes from Abl- or p73-deficient mice are resistant to TNF-induced apoptosis [31]. With Abl- or p73-deficient mouse fibroblasts, TNF/CHX-induced apoptosis was not abolished; nevertheless, re-introduction of Abl or p73 could enhance the death response in these knockout cells by stimulating cytochrome c release (31). Although Abl enhances TNF/CHX-induced fibroblast cell death, we found that the ectopic activation of Abl tyrosine kinase through inducible dimerization [59, 61] in *Rb-MI* cells did not rescue the hTNF/CHX-induced IETDase activity (http://www.jbc.org/cgi/data/M702261200/DC1/1). However, the ectopic activation of the same dimerizable Abl kinase could stimulate IETDase in hTNF (without cycloheximide)-treated p21E cells, which lack p21Cip1 and express the adenoviral E1A protein (http://www.jbc.org/cgi/data/M702261200/DC1/1). Furthermore, siRNA-mediated knockdown of Abl did not interfere with hTNF/CHX-induced IETDase activity

in *Rb-wt* cells (http://www.jbc.org/cgi/data/M702261200/DC1/1). While Abl contributes to TNF-induced type-2 apoptosis, results from this study suggest that the blockade of Bid cleavage in *Rb-MI* cells is mediated through Abl-independent mechanisms.

We considered two possibilities for how Rb cleavage might stimulate caspase-8-dependent Bid cleavage. In the first scenario, the cleaved products (Rb-ΔI and/or the C-terminal 41 aa-peptide) exert a positive effect on caspase-8 and Bid cleavage. In the second scenario, cleavage of Rb causes the release of a factor that stimulates the cytosolic accumulation of caspase-8 and thus leading to Bid cleavage. The first scenario that Rb fragments directly activate caspase-8 or Bid cleavage is inconsistent with the result that knockdown of Rb-MI rescued cytosolic caspase-8 activity and Bid cleavage. Furthermore, knockdown of Rb-wt did not affect hTNF/CHX-induced caspase-8 activation or Bid cleavage, suggesting Rb fragments are not required for Bid cleavage. While we currently favor the second scenario, i.e. Rb cleavage causes the release of a factor (X in Figure 5-7B) to stimulate Bid cleavage, we do not know the identity of such a factor. A previous report has shown that Rb-ΔI loses the ability to bind MDM2 [62]. There is considerable evidence in the literature that MDM2 functions as an inhibitor of apoptosis [63], thus, inconsistent with MDM2 being an activator of TNF-induced type-2 apoptotic pathway. Identification of the mechanism by which Rb-MI blocks Bid cleavage will await further investigation.

Rb cleavage as a nuclear checkpoint for TNF-induced type-2 apoptosis

The sequential model depicted in Figure 5-7B suggests that cleavage of Rb may serve as a nuclear checkpoint for the activation of type-2 apoptotic pathway by TNF. Previous studies have suggested that hyperphosphorylated Rb is more resistant to caspase cleavage [59, 64]. If so, Rb cleavage is less likely to occur in S/G2/M phase cells that contain hyperphosphorylated Rb. Since TNF activates NF-κB, which promotes cell growth and survival, the Rb cleavage checkpoint may help to prevent the activation of type-2 apoptotic pathway during TNF-stimulated cell proliferation. We have found that DSS-induced colonic apoptosis to occur preferentially in the differentiated and non-proliferating epithelial cells and it is this population of cells that are protected from apoptosis in the $Rb^{MI/MI}$ mice. The status of the Rb protein, i.e., phosphorylation versus degradation, may therefore regulate the proliferative versus apoptotic response to TNF.

ACKNOWLEDGEMENT

We thank Dr. David Wallach for the *Caspase-8*$^{-/-}$ MEFs, Dr. Donald Newmeyer for the recombinant NC-Bid, Ms. Rimma Levenzon and Ms. Diana Wu for technical assistance, Dr. B. Nelson Chau for insightful discussions, Dr. Shun J. Lee and Ms. Vera Huang for reading the manuscript. This work is supported by a grant from the National Cancer Institute CA58320 to JYJW.

Chapter 5, in full, is a reprint of the material as it appears in "Xiaodong Huang, Anja Masselli, Steven M. Frisch, Irina C. Hunton, Yong Jiang, and Jean Y. J. Wang, J. Biol. Chem., 2007 Oct 5;282(40):29401-13". The author of the dissertation is the primary investigator and author of this paper.

Figure 5-1: TNFR1-induced type-2 apoptotic pathway is blocked in *Rb-MI* MEFs.
A. and B. DEVDase (A) and IETDase (B) activities were not activated by hTNF/CHX in *Rb-MI* MEFs. The protease activities in whole cell lysates were measured at 5 hours after the indicated treatments. Activity in untreated lysate was set to 1 for each cell type. Values are mean and standard errors from three independent experiments.
C. IETDase dose response to hTNF/CHX or mTNF/CHX. *Rb-MI* or *Rb-wt* cells were treated with the indicated concentrations of hTNF or mTNF, plus CHX (2.5 μg/ml). The IETDase activity in whole cell lysates was measured at 5 hours after the indicated treatments and the activity in untreated lysates was set to 1. Values are mean and standard errors from three independent experiments.
D. Cytosolic cytochrome c (Cyto c) and Smac were not detected in hTNF/CHX-treated *Rb-MI* cells. *Rb-wt (+/+)* and *Rb-MI* (*MI/MI)* cell lysates were prepared 5 hours after the indicated treatments. Equal amounts of cytosolic protein were resolved by SDS-PAGE and immunoblotted with anti-cytochrome c or anti-Smac.
E. Bid is not cleaved in hTNF/CHX-treated *Rb-MI* cells. Whole cell lysates were prepared at 5 hours after the indicated treatment. Equal amounts of total protein were resolved by SDS-PAGE, Bid and tBid were detected by immunoblotting.
F. Cytosolic extracts from hTNF/CHX-treated *Rb-wt* but not *Rb-MI* cells induced cytochrome c release from liver mitochondria. Cytosolic extracts from cells prepared at the indicated time after hTNF/CHX treatment were incubated with mouse liver mitochondria at 37ºC for 45 minutes. Mitochondria were pelleted by centrifugation and supernatants and pellets were analyzed for cytochrome c and Cox -IV by immunoblotting. B, buffer-treated mitochondria.
G. Cytosolic extracts from *Rb-MI* cells did not interfere with cytochrome c release stimulated by recombinant truncated Bid (NC-Bid) [45]. The indicated extracts from hTNF/CHX-treated (+) or untreated (-) cells were incubated with liver mitochondria from wild type mice plus the indicated amounts of NC-Bid, and the incubation mixtures were analyzed for cytochrome c release as in (E).
H. Liver mitochondria from $Rb^{MI/MI}$ mice released cytochrome c in response to cytosolic extract from hTNF/CHX-treated *Rb-wt* cells. Cytosolic extracts were prepared after the indicated treatment and incubated with mitochondria isolated from the liver of $Rb^{+/+}$ or $Rb^{MI/MI}$ mice. Cytochrome c release was examined as in (F).

5-1A)

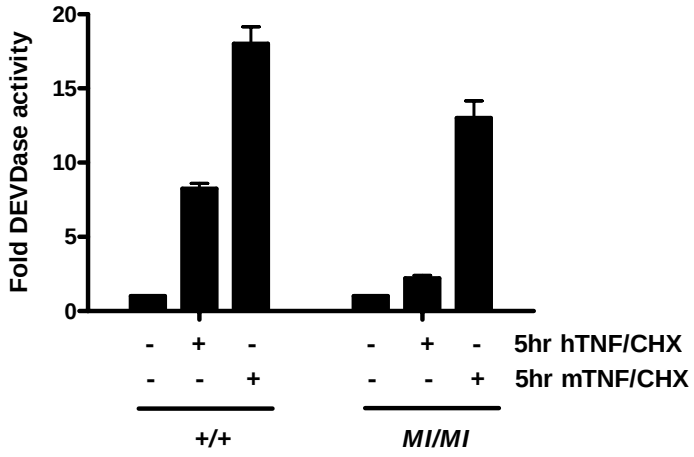

5-1B)

Whole cell lysates from +/+ and *MI/MI* cells

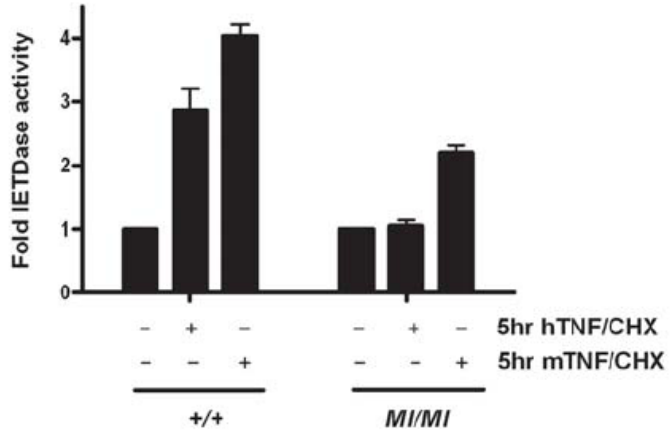

5-1C)

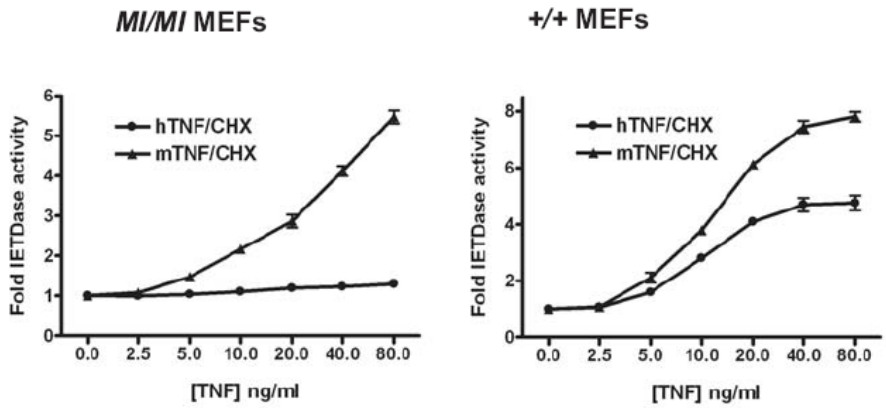

5-1D)

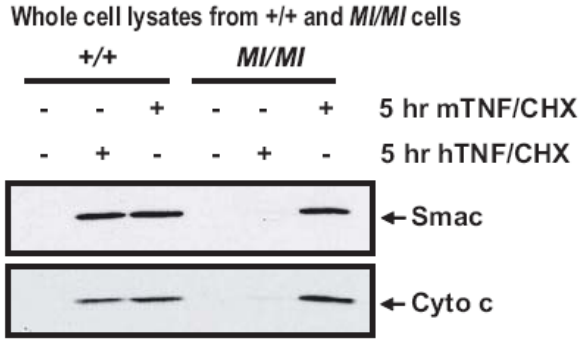

Figure 5-1 Continued

5-1E)

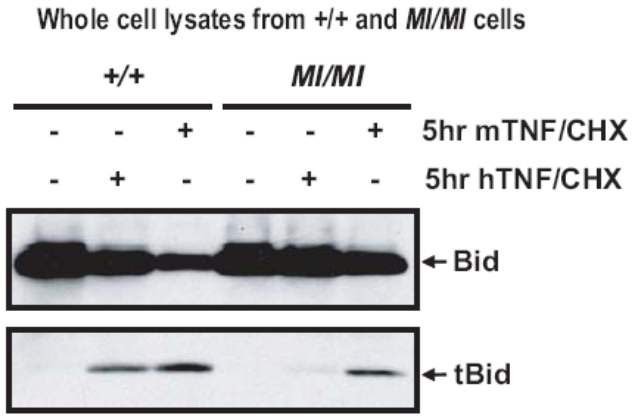

5-1F)

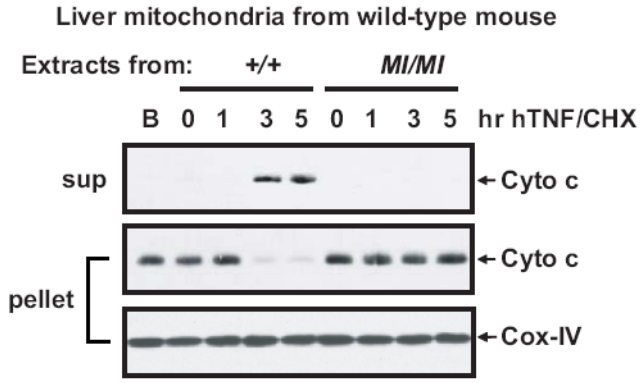

Figure 5-1 continued

5-1G)

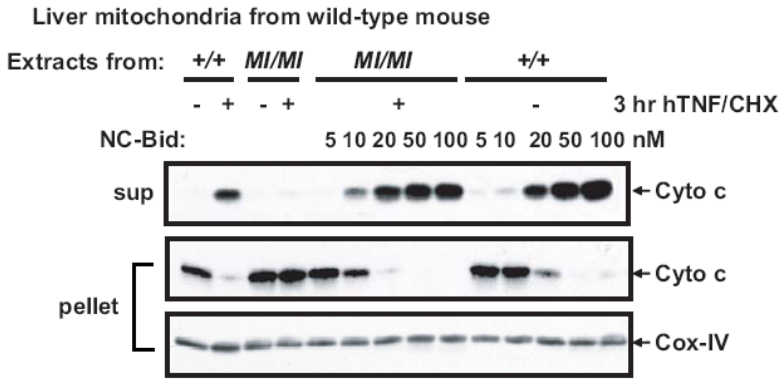

5-1H)

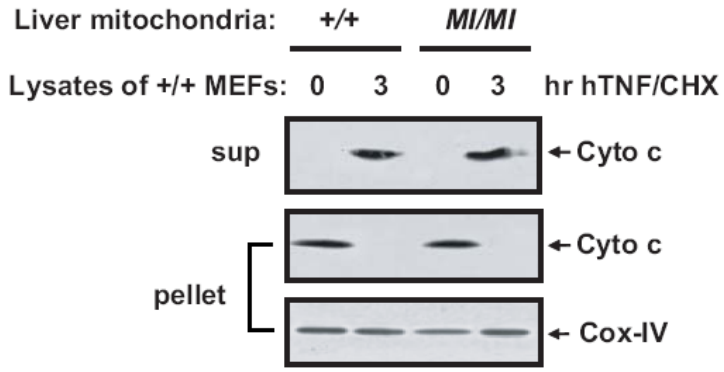

Figure 5-1 continued

Figure 5-2: TNF-induced Rb cleavage is dependent on caspase-8 and required for Bid cleavage.
A. Caspase-8 (p55) is detected in wild-type (*Casp8*$^{+/+}$) but not caspase-8 knockout (*Casp8*$^{-/-}$) cells.
B. Cells with the indicated genotypes were treated with hTNF/CHX for 5 hours and analyzed for PARP1 and cleaved caspase-3 by immunoblotting of whole cell lysates. The cleavage of Rb was detected by immunoprecipitation (IP) and immunoblotting (IB) as described in Experimental Procedures. The levels of actin are shown as loading controls.
C. and D. DEVDase (C) or IETDase (D) activity was measured in whole cell lysates after 5 hour- treatment of the indicated cells with hTNF/CHX, with the activity in untreated lysates set to 1. Values are mean and standard errors from three independent experiments.
E. The indicated cells were transfected with *control-siRNA (LacZ)* or *Rb-siRNA*, and the level of Rb protein was determined by IP/IB at 48 hours post transfection.
F. *Rb-siRNA* restored death response to hTNF/CHX in *Rb-MI* MEFs. At 48 hour post transfection with the indicated siRNA, cells of the indicated genotypes were treated with hTNF/CHX for 5 hours and cell death determined by the uptake of propidium iodide. Values are mean and standard errors from three independent experiments.
G. *Rb-siRNA* enhanced hTNF/CHX-induced IETDase activity in *Rb-MI* cells. Cells treated as in (F) were collected and the IETDase activity measured in whole cell lysates. Fold changes are relative to LacZ-siRNA transfected and untreated cells for each genotype. Means and standard errors from three independent experiments are shown.
H. *Rb-siRNA* allowed Bid cleavage in hTNF/CHX-treated *Rb-MI* MEFs. Whole cell lysates from (G) were analyzed for Bid and tBid by immunoblotting.

5-2A)

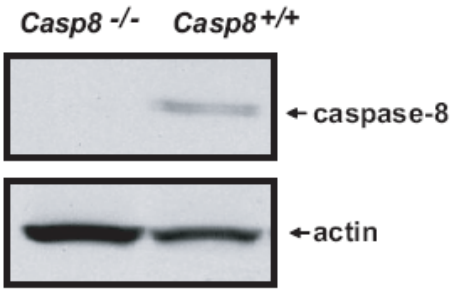
Casp8 -/-
Casp8 +/+
caspase-8
actin

5-2B)

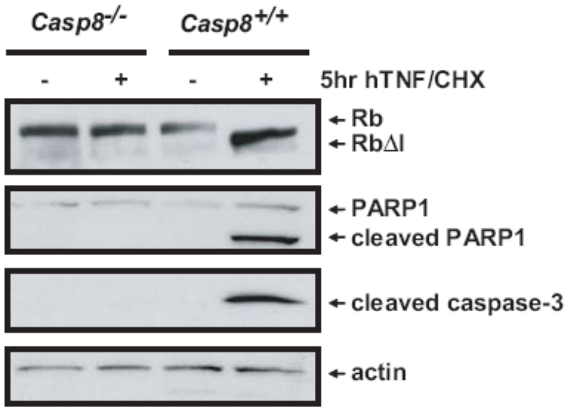
Casp8-/-
Casp8+/+
- + - +
5hr hTNF/CHX
Rb
RbΔI
PARP1
cleaved PARP1
cleaved caspase-3
actin

5-2C)

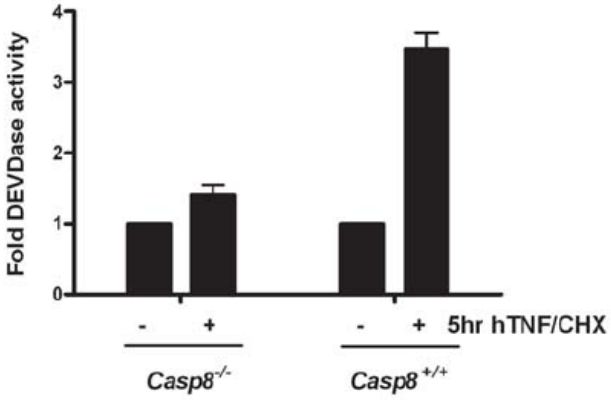
Fold DEVDase activity
0
1
2
3
4
- + - + 5hr hTNF/CHX
Casp8-/-
Casp8+/+

5-2D)

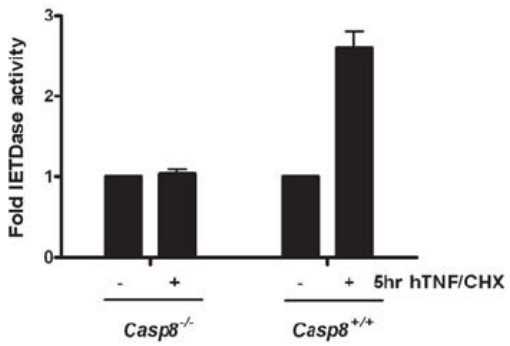

5-2E)

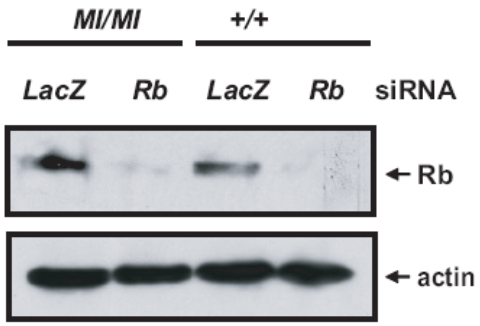

5-2F)

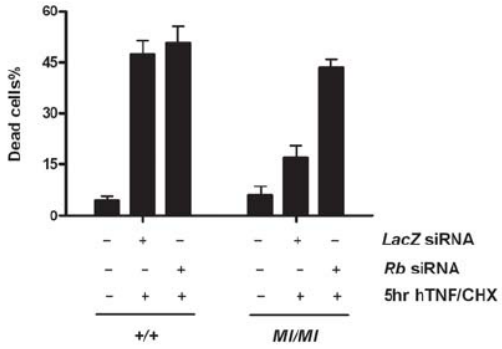

Figure 5-2 continued

5-2G)

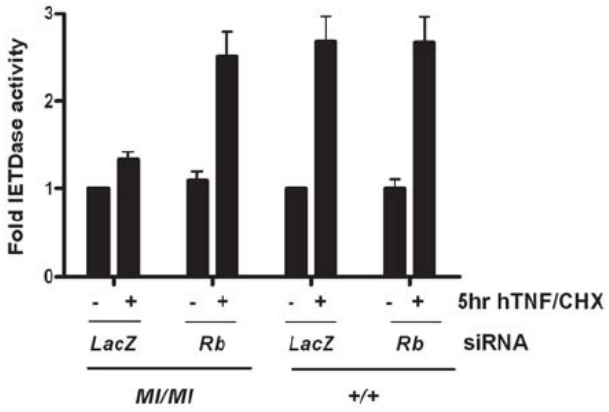

5-2H)

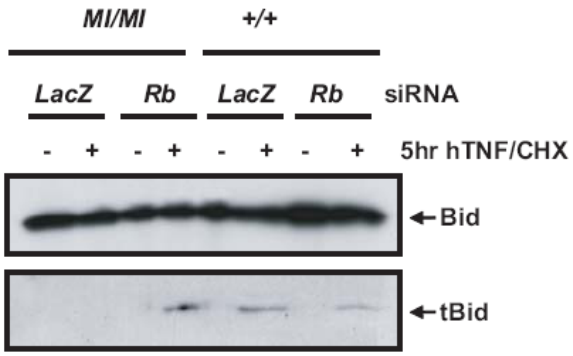

Figure 5-2 continued

Figure 5-3: In vivo affinity labeling of activated caspase-8 in Rb-wt and Rb-MI cells.
A. Caspase-8 processing was not detected in whole cell lysates prepared at 5 hours after hTNF/CHX treatment of *Rb-wt* or *Rb-MI* MEFs.
B. Outline of the affinity labeling experiments.
C. Biotinylation of caspase-8. Cells of the indicated genotypes were treated as in (B). The p55 and p43 bands were not present in caspase-8-knockout MEFs. The levels of actin in the input fractions are shown.
D. Biotinylation of caspase-8 in *Rb-wt* and *Rb-MI* cells. Cells of the indicated genotypes were collected at the indicated time after hTNF/CHX treatment, whole cell lysates (1 mg total protein) were incubated with streptavidin beads and caspase-8 was detected in the bound fractions by immunoblotting. The amounts of p55 caspase-8 in 50 μg of each input fraction are also shown.

5-3A)

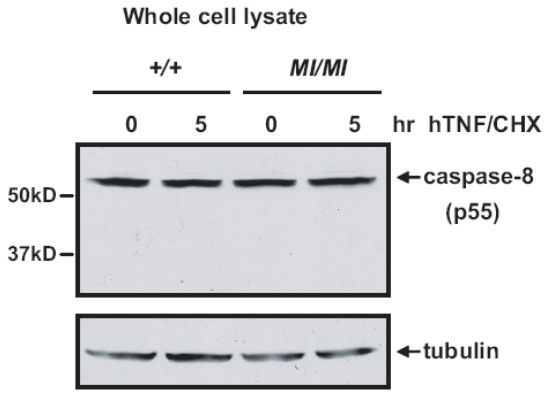
Whole cell lysate
+/+
MI/MI
0
5
0
5
hr hTNF/CHX
50kD
37kD
caspase-8
(p55)
tubulin

5-3B)

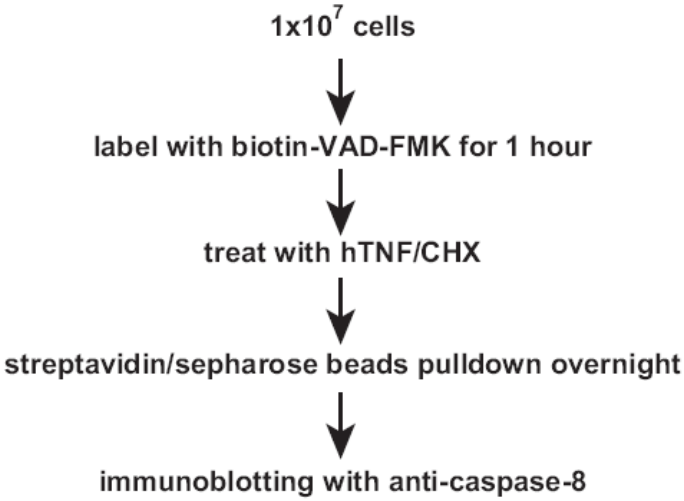
1x10^7 cells
label with biotin-VAD-FMK for 1 hour
treat with hTNF/CHX
streptavidin/sepharose beads pulldown overnight
immunoblotting with anti-caspase-8

5-3C)

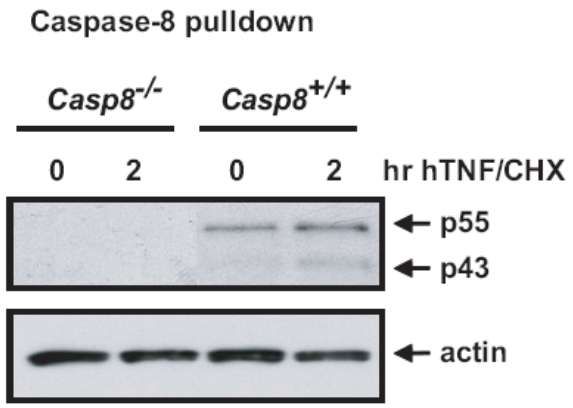

5-3D)

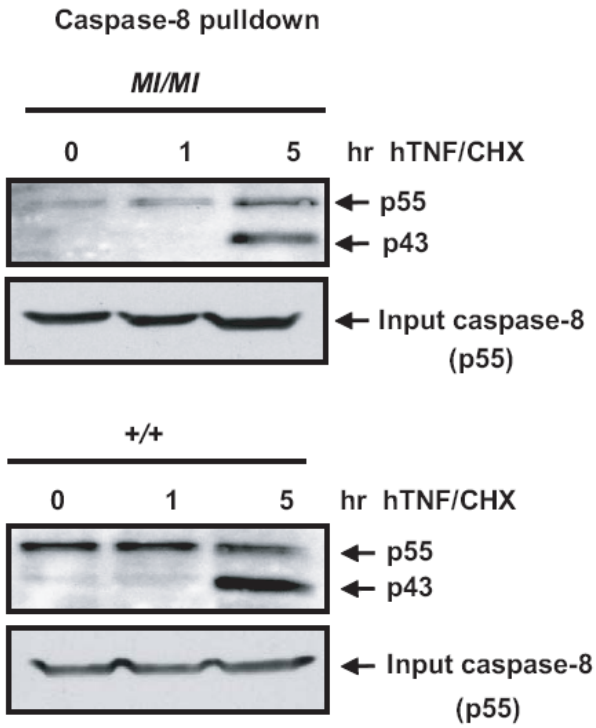

Figure 5-3 continued

Figure 5-4: Pre-incubation at 4ºC sensitized Rb-wt and Rb-MI cells to hTNF/CHX.
A. and B. Death response was enhanced by preincubation with hTNF/CHX at 4ºC. Cell death was measured by PI uptake at 24 hours after treatment with the indicated concentrations of hTNF and CHX (2.5 μg/ml) in *Rb-MI* (A) and *Rb-wt* (B) cells. Cells were treated with or without 90 min pre-incubation at 4ºC followed by warming to 37ºC to induce synchronized endocytosis. Note that pre-incubation sensitized *Rb-wt* and *Rb-MI* cells to hTNF/CHX-induced death. However, death response was lower in *Rb-MI* cells at every hTNF concentration tested.
C. IETDase activity was enhanced by preincubation with hTNF/CHX at 4ºC. *Rb-wt* and *Rb-MI* cells were incubated with hTNF (33 ng/ml) plus CHX (2.5 μg/ml) at 4°C for 90 minutes, then shifted to 37°C for the indicated times and the fold increase in IETDase activity over untreated cells was determined.
D. Bid cleavage was partially restored in *Rb-MI* cells by preincubation. Cells treated as in (C) were collected at 5 hours after warming to 37ºC. Whole cell lysates were analyzed for Bid; cytosolic extracts were analyzed for cytochrome c and Smac.
E. Effects of inhibitors on IETDase activity in *Rb-MI* cells. Cells were pre-treated with the indicated chemicals for 1 hour and then treated with hTNF/CHX for 5 hours. IETDase activity was measured in whole cell lysates and the activity in untreated cell lysate was set to 1.
F. Analysis of lysosomal pH. *Rb-wt* and *Rb-MI* cells were labeled with the pH-sensitive FITC-dextran for 1 hour and then were treated with hTNF/CHX, with or without 200 nM Bafilomycin A1 as described in Experimental Procedures. The pH values were determined by comparing the fluorescence signals to a standard curve constructed for FITC-dextran in phosphate/citrate buffers of different pH between 4.0 and 8.0.

5-4A)

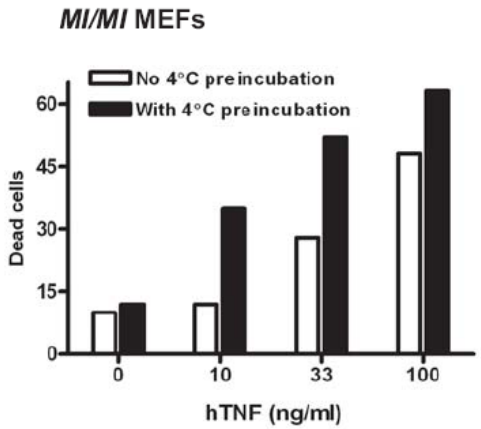
MI/MI MEFs
No 4°C preincubation
With 4°C preincubation
Dead cells
60
45
30
15
0
0
10
33
100
hTNF (ng/ml)

5-4B)

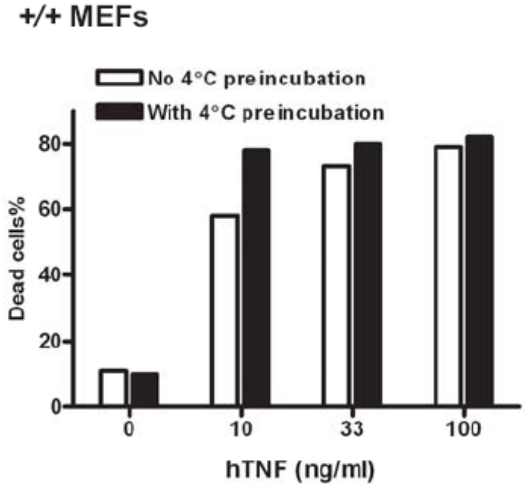
+/+ MEFs
No 4°C preincubation
With 4°C preincubation
Dead cells%
80
60
40
20
0
0
10
33
100
hTNF (ng/ml)

5-4C)

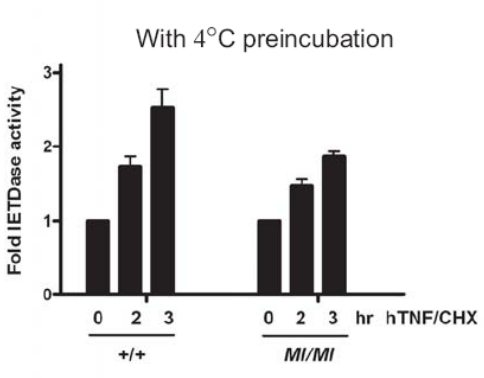

5-4D)

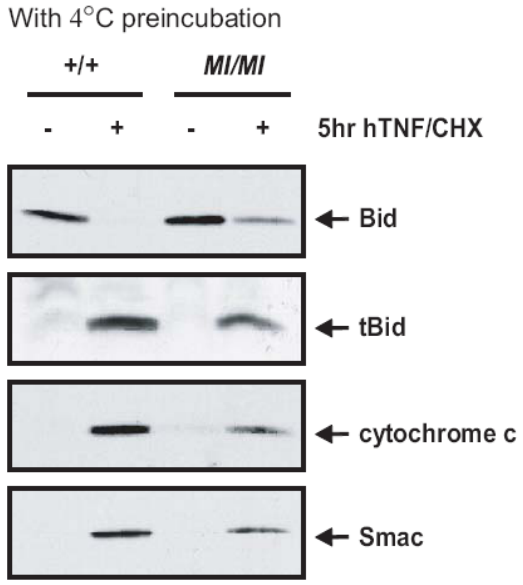

Figure 5-4 continued

5-4E)

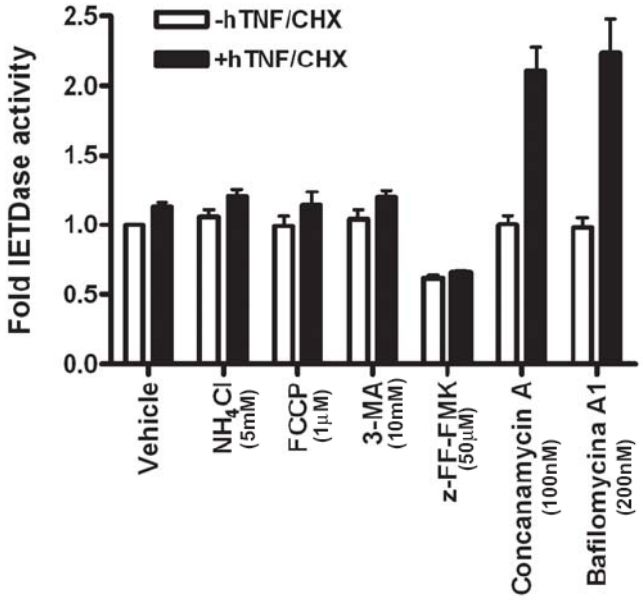

5-4F)

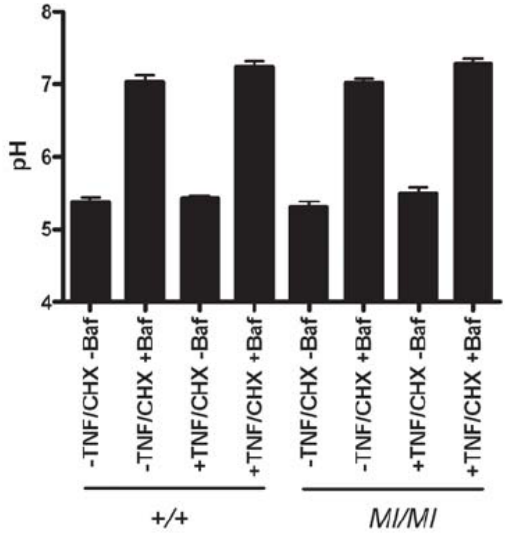

Figure 5-4 Continued

Figure 5-5: Inhibition of V-ATPase restores Bid cleavage in hTNF/CHX-treated *Rb-MI* MEFs.
A. Bafilomycin A1 (Baf) does not significantly affect the biotinylation of caspase-8. Cells of the indicated genotypes were pre-incubated with 50 μM biotin-VAD-FMK in the absence (-) or presence (+) of 200 nM Baf for 1 hour and then treated with hTNF/CHX for 5 hours. Caspase-8 in the input lysates and in the streptavidin pull down fractions was measured by immunoblotting.
B. Bafilomycin A1 (Baf) stimulated IETDase activity in hTNF-treated *Rb-MI* cells. Cells of the indicated genotypes were pre-incubated with 200 nM Baf for 1 hour followed by hTNF/CHX for 5 hours and IETDase activity measured. The activity of untreated cells of each genotype was set to 1. Fold changes represent means and standard errors from three experiments.
C. Baf rescued hTNF/CHX-induced Bid cleavage in *Rb-MI* cells. Cells treated as in (B) were analyzed for Bid and tBid by immunoblotting of whole cell lysates.
D. Baf does not induce Bid cleavage in caspase-8-knockout cells. Cells of the indicated genotypes were treated as in (B) and whole cell lysates were analyzed for Bid and tBid by immunoblotting.
E. Effects of hTNF/CHX and/or Baf on the levels of TNFR1 and DISC components. *Rb-wt* and *Rb-MI* cells were treated with or without hTNF/CHX for 5 hours, in the presence or absence of 1 hour pre-incubation with bafilomycin A1 (200 nM). Whole cell lysates were immunoblotted with the indicated antibodies. Note that Baf allowed Rip1 cleavage in hTNF/CHX-treated *Rb-MI* cells.
F. Knockdown of the B1 subunit in the V1 complex of the mouse V-ATPase (V1B1). Whole cell lysates collected at 48 hours post transfection with the indicated siRNA were immunoblotted with anti-V1B1 or anti-actin.
G. and H. Knockdown of V1B1 enhanced IETDase activity (G) and Bid cleavage (H) in *Rb-MI* cells. At 48 hours post transfection with the indicated siRNA, *Rb-MI* cells were treated with hTNF/CHX for 5 hours. Whole cell lysates were analyzed for IETDase activity, with the activity in mock transfected and untreated sample from each genotype set to 1(G).

5-5A)

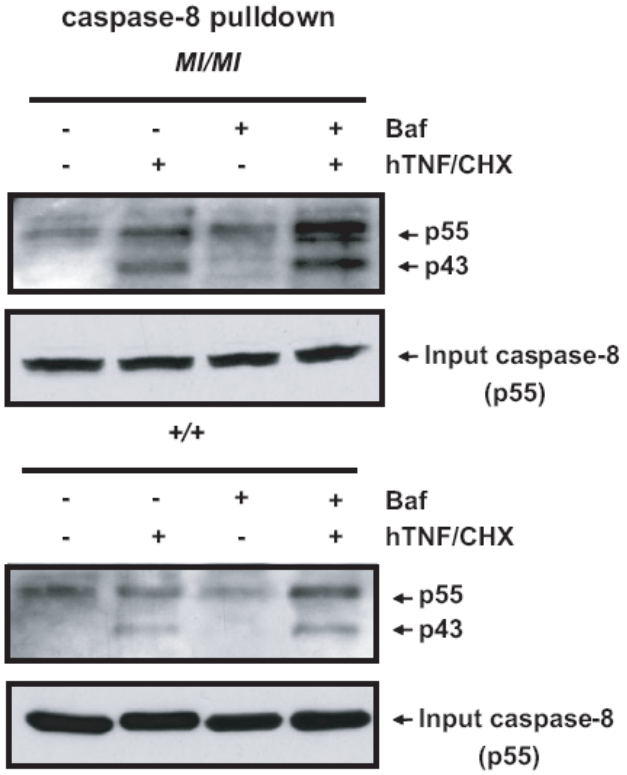
caspase-8 pulldown
MI/MI
- - + + Baf
- + - + hTNF/CHX
← p55
← p43
← Input caspase-8 (p55)
+/+
- - + + Baf
- + - + hTNF/CHX
← p55
← p43
← Input caspase-8 (p55)

5-5B)

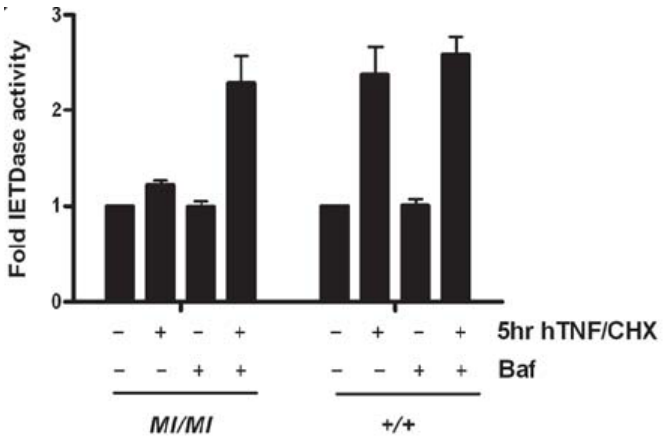
Fold IETDase activity
0
1
2
3
– + – + – + – + 5hr hTNF/CHX
– – + + – – + + Baf
MI/MI
+/+

5-5C)

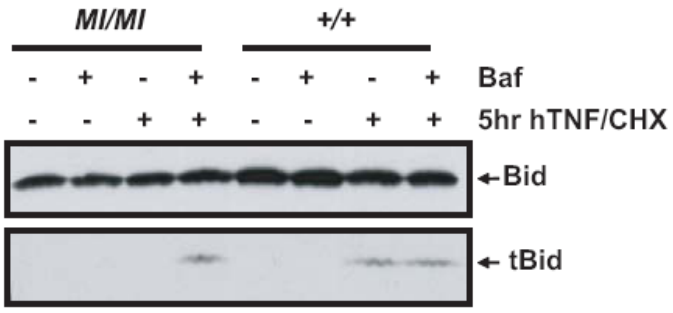

5-5D)

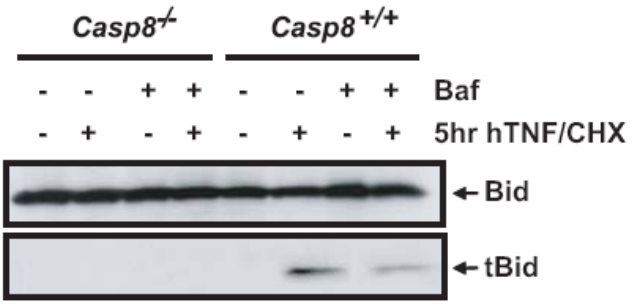

Figure 5-5 continued

5-5E)

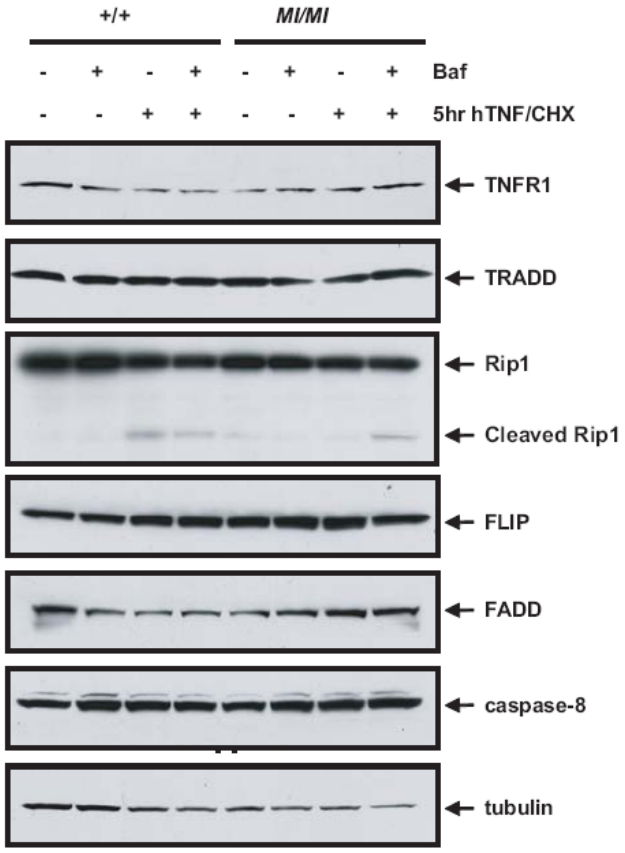

5-5F)

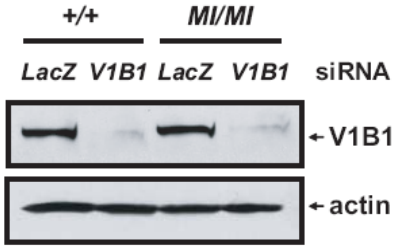

Figure 5-5 continued

5-5G)

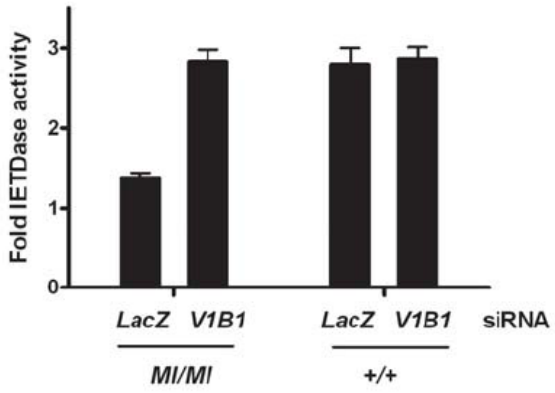

5-5H)

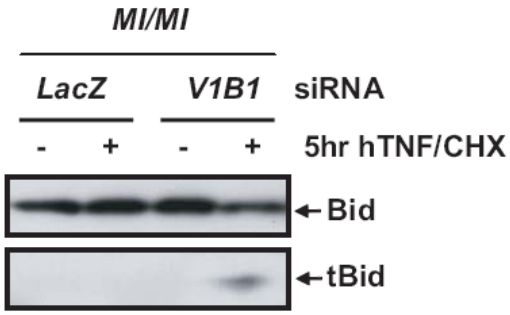

Figure 5-5 continued

Figure 5-6: DSS-induced colonic epithelial apoptosis is reduced in RbMI/MI mice but restored by bafilomycin A1.
A. Representative images of colonic tissue sections stained with DAPI (blue) or TUNEL (red). Mice of the indicated genotypes were fed with water containing 3% DSS. At 56 hour into DSS feeding, they were injected *i.p.* with either Baf (25 ng/g body weight) or vehicle (phosphate buffered saline). Mice were sacrificed 16 hours after injection and colonic apoptosis was quantitated as described in Experimental Procedures.
B. Density of TUNEL positive nuclei. The number of TUNEL-positive nuclei per crypt was determined by counting at least 25 full-crypts or 50 half-crypts in three to five sections per sample. The number of mice in each experimental group is shown, and the *p* values are determined by t-test assuming unequal variances.

5-6A)

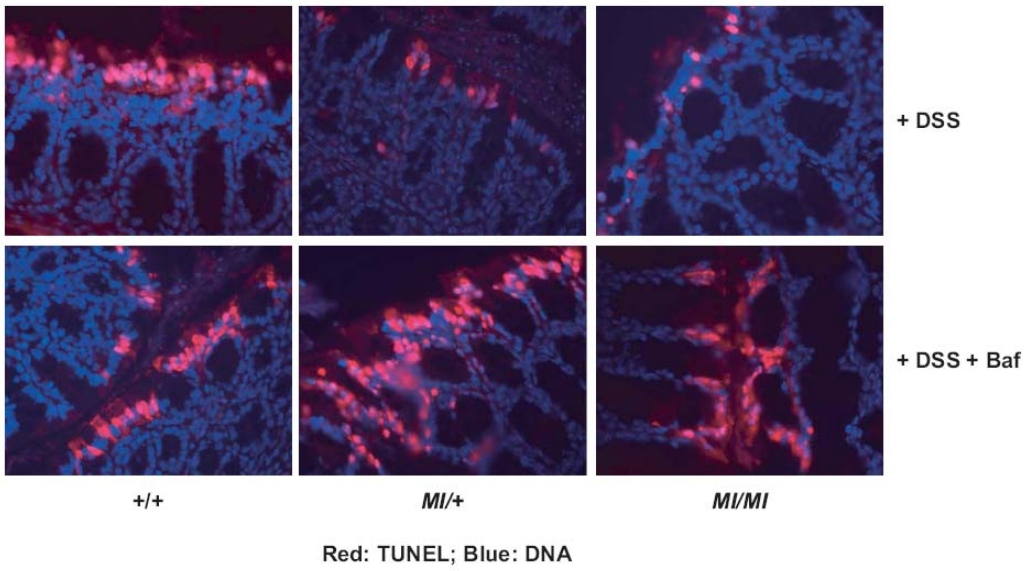
+ DSS
+ DSS + Baf
+/+
Ml/+
Ml/Ml
Red: TUNEL; Blue: DNA

5-6B)

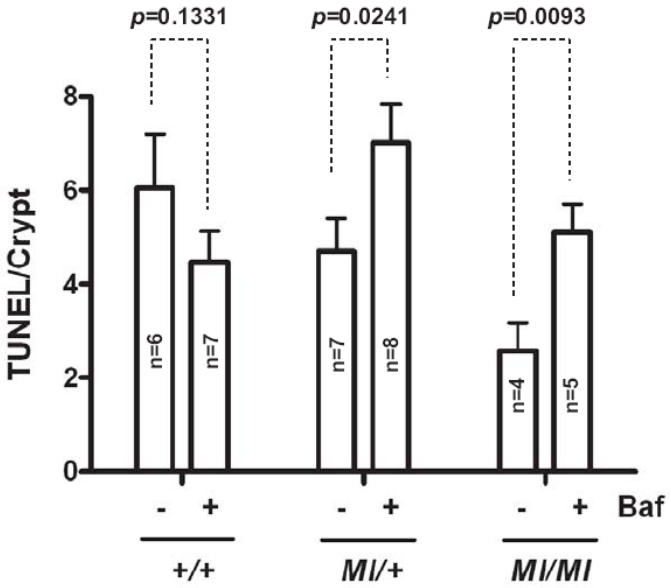
p=0.1331
p=0.0241
p=0.0093
TUNEL/Crypt
8
6
4
2
0
n=6
n=7
n=7
n=8
n=4
n=5
- + - + - + Baf
+/+
Ml/+
Ml/Ml

5-7A) **5-7B)**

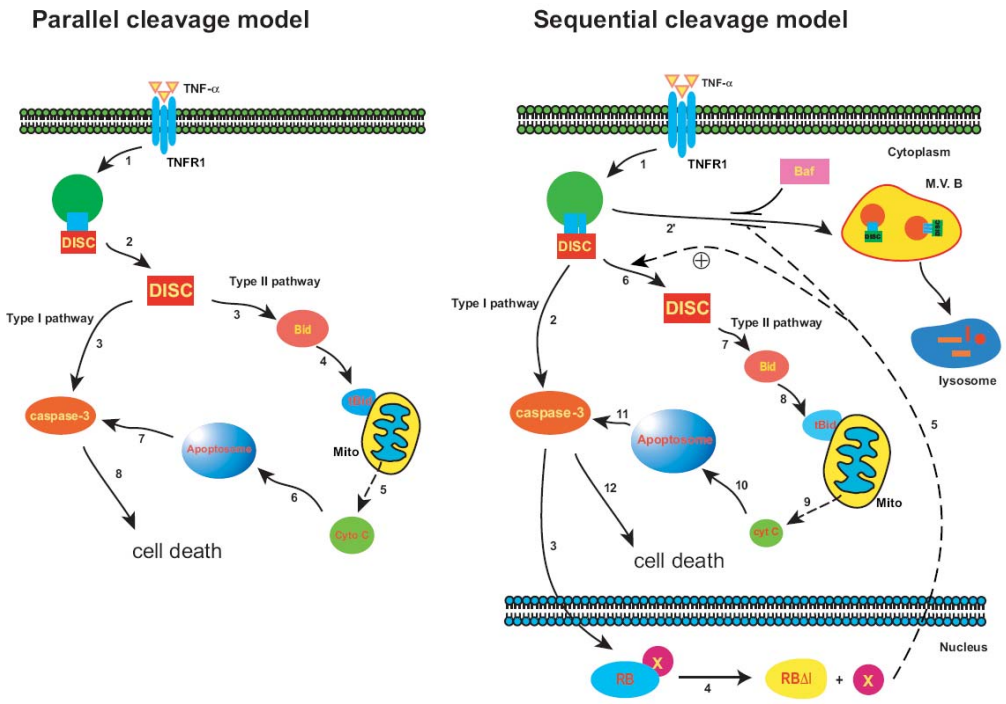

Figure 5-7: Parallel versus sequential cleavage in extrinsic apoptotic pathways. The current model (A) of extrinsic apoptosis suggests parallel cleavage of substrates in the type-1 and the type-2 pathways by receptor activated DISC. This model cannot explain our finding that Rb cleavage is required for Bid cleavage. We propose a sequential cleavage model (B), in which Rb is cleaved through the type-1 pathway and its cleavage a pre-requisite for DISC to cleave Bid. In *Rb-MI* cells where Rb cannot be cleaved, the endosomal TNFR1-DISC complex is lost through V-ATPase-dependent endocytic trafficking. Our data suggest that Rb cleavage may cause the release of a nuclear factor that either blocks endosomal trafficking of TNFR1-DISC or stimulates DISC dissociation from the endosomal-TNFR1 to allow for Bid cleavage. The sequential cleavage model can explain why Rb cleavage is not required for TNF-induced apoptosis in type-1 cells. Rb cleavage may serve as a nuclear checkpoint for TNF-induced type-2 apoptosis.

REFERENCES

1. Karin, M. and F.R. Greten, *NF-kappaB: linking inflammation and immunity to cancer development and progression.* Nat Rev Immunol, 2005. **5**(10): p. 749-59.

2. Pikarsky, E., et al., *NF-kappaB functions as a tumour promoter in inflammation-associated cancer.* Nature, 2004. **431**(7007): p. 461-6.

3. Balkwill, F. and L.M. Coussens, *Cancer: an inflammatory link.* Nature, 2004. **431**(7007): p. 405-6.

4. Chen, G. and D.V. Goeddel, *TNF-R1 signaling: a beautiful pathway.* Science, 2002. **296**(5573): p. 1634-5.

5. Locksley, R.M., N. Killeen, and M.J. Lenardo, *The TNF and TNF receptor superfamilies: integrating mammalian biology.* Cell, 2001. **104**(4): p. 487-501.

6. Ashkenazi, A., *Targeting death and decoy receptors of the tumour-necrosis factor superfamily.* Nature Reviews Cancer, 2002. **2**(6): p. 420-430.

7. Park, S.-M., R. Schickel, and M.E. Peter, *Nonapoptotic functions of FADD-binding death receptors and their signaling molecules.* Current Opinion in Cell Biology, 2005. **17**(6): p. 610-616.

8. Garg, A.K. and B.B. Aggarwal, *Reactive oxygen intermediates in TNF signaling.* Mol Immunol, 2002. **39**(9): p. 509-17.

9. Festjens, N., T. Vanden Berghe, and P. Vandenabeele, *Necrosis, a well-orchestrated form of cell demise: Signalling cascades, important mediators and concomitant immune response.* Biochimica et Biophysica Acta (BBA) - Bioenergetics, 2006. **1757**(9-10): p. 1371-1387.

10. Kim, Y.S., et al., *TNF-Induced Activation of the Nox1 NADPH Oxidase and Its Role in the Induction of Necrotic Cell Death.* Mol Cell, 2007. **26**(5): p. 675-687.

11. Kamata, H., et al., *Reactive oxygen species promote TNFalpha-induced death and sustained JNK activation by inhibiting MAP kinase phosphatases.* Cell, 2005. **120**(5): p. 649-61.

12. Kreuz, S., et al., *NF-kappaB inducers upregulate cFLIP, a cycloheximide-sensitive inhibitor of death receptor signaling.* Mol Cell Biol, 2001. **21**(12): p. 3964-73.

13. Beg, A.A. and D. Baltimore, *An essential role for NF-kappaB in preventing TNF-alpha-induced cell death.* Science, 1996. **274**(5288): p. 782-4.

14. Micheau, O., et al., *NF-{kappa}B Signals Induce the Expression of c-FLIP.* Mol. Cell. Biol., 2001. **21**(16): p. 5299-5305.

15. Dumitru, C.D., et al., *TNF-alpha induction by LPS is regulated posttranscriptionally via a Tpl2/ERK-dependent pathway.* Cell, 2000. **103**(7): p. 1071-83.

16. Schneider-Brachert, W., et al., *Compartmentalization of TNF Receptor 1 Signaling Internalized TNF Receptosomes as Death Signaling Vesicles.* Immunity, 2004. **21**(3): p. 415-428.

17. Schneider-Brachert, W., et al., *Inhibition of TNF receptor 1 internalization by adenovirus 14.7K as a novel immune escape mechanism.* J. Clin. Invest., 2006. **116**(11): p. 2901-2913.

18. Micheau, O. and J. Tschopp, *Induction of TNF receptor I-mediated apoptosis via two sequential signaling complexes.* Cell, 2003. **114**(2): p. 181-90.

19. Harper, N., et al., *Fas-associated Death Domain Protein and Caspase-8 Are Not Recruited to the Tumor Necrosis Factor Receptor 1 Signaling Complex during Tumor Necrosis Factor-induced Apoptosis.* J. Biol. Chem., 2003. **278**(28): p. 25534-25541.

20. Welch, P.J. and J.Y. Wang, *A C-terminal protein-binding domain in the retinoblastoma protein regulates nuclear c-Abl tyrosine kinase in the cell cycle.* Cell, 1993. **75**(4): p. 779-90.

21. Welch, P.J. and J.Y. Wang, *Disruption of retinoblastoma protein function by coexpression of its C pocket fragment.* Genes Dev, 1995. **9**(1): p. 31-46.

22. Lee, J.O., A.A. Russo, and N.P. Pavletich, *Structure of the retinoblastoma tumour-suppressor pocket domain bound to a peptide from HPV E7.* Nature, 1998. **391**(6670): p. 859-65.

23. Rubin, S.M., et al., *Structure of the Rb C-terminal domain bound to E2F1-DP1: a mechanism for phosphorylation-induced E2F release.* Cell, 2005. **123**(6): p. 1093-106.

24. Heinen, C.D., et al., *The APC tumor suppressor controls entry into S-phase through its ability to regulate the cyclin D/RB pathway.* Gastroenterology, 2002. **123**(3): p. 751-63.

25. Knudsen, E.S. and J.Y.J. Wang, *Differential Regulation of Retinoblastoma Protein Function by Specific Cdk Phosphorylation Sites.* J. Biol. Chem., 1996. **271**(14): p. 8313-8320.

26. Janicke, R.U., et al., *Specific cleavage of the retinoblastoma protein by an ICE-like protease in apoptosis.* EMBO J, 1996. **15**(24): p. 6969-6978.

27. Natoli, G., et al., *Activation of SAPK/JNK by TNF receptor 1 through a noncytotoxic TRAF2-dependent pathway.* Science, 1997. **275**(5297): p. 200-3.

28. Tan, X. and J.Y. Wang, *The caspase-RB connection in cell death.* Trends Cell Biol, 1998. **8**(3): p. 116-20.

29. Hiebert, S.W., et al., *The interaction of RB with E2F coincides with an inhibition of the transcriptional activity of E2F.* Genes Dev, 1992. **6**(2): p. 177-85.

30. Chau, B.N., et al., *Signal-dependent protection from apoptosis in mice expressing caspase-resistant Rb.* Nat Cell Biol, 2002. **4**(10): p. 757-65.

31. Chau, B.N., et al., *Tumor necrosis factor alpha-induced apoptosis requires p73 and c-ABL activation downstream of RB degradation.* Mol Cell Biol, 2004. **24**(10): p. 4438-47.

32. Wajant, H., *The Fas Signaling Pathway: More Than a Paradigm.* Science, 2002. **296**(5573): p. 1635-1636.

33. Scaffidi, C., et al., *Two CD95 (APO-1/Fas) signaling pathways.* The EMBO Journal, 1998. **17**: p. 1675-1687.

34. Li, H., et al., *Cleavage of BID by caspase 8 mediates the mitochondrial damage in the Fas pathway of apoptosis.* Cell, 1998. **94**(4): p. 491-501.

35. Beyenbach, K.W. and H. Wieczorek, *The V-type H+ ATPase: molecular structure and function, physiological roles and regulation.* J Exp Biol, 2006. **209**(4): p. 577-589.

36. Inoue, T., et al., *Structure and regulation of the V-ATPases.* J Bioenerg Biomembr, 2005. **37**(6): p. 393-8.

37. Sun-Wada, G.-H., Y. Wada, and M. Futai, *Diverse and essential roles of mammalian vacuolar-type proton pump ATPase: toward the physiological understanding of inside acidic compartments.* Biochimica et Biophysica Acta (BBA) - Bioenergetics, 2004. **1658**(1-2): p. 106-114.

38. Johnson, L.S., et al., *Endosome acidification and receptor trafficking: bafilomycin A1 slows receptor externalization by a mechanism involving the receptor's internalization motif.* Molecular Biology of the Cell, 1993. **4**(12): p. 1251-1266.

39. Hurtado-Lorenzo, A., et al., *V-ATPase interacts with ARNO and Arf6 in early endosomes and regulates the protein degradative pathway.* Nat Cell Biol, 2006. **8**: p. 124-136.

40. Varfolomeev, E.E., et al., *Targeted Disruption of the Mouse Caspase 8 Gene Ablates Cell Death Induction by the TNF Receptors, Fas/Apo1, and DR3 and Is Lethal Prenatally.* Immunity, 1998. **9**(2): p. 267-276.

41. Tu, S., et al., *In situ trapping of activated initiator caspases reveals a role for caspase-2 in heat shock-induced apoptosis.* Nat Cell Biol, 2006. **8**: p. 72-77.

42. Trombetta, E.S., et al., *Activation of lysosomal function during dendritic cell maturation.* Science, 2003. **299**(5611): p. 1400-3.

43. Martin, D.A., et al., *Membrane Oligomerization and Cleavage Activates the Caspase-8 (FLICE/MACHalpha 1) Death Signal.* J. Biol. Chem., 1998. **273**(8): p. 4345-4349.

44. Luo, X., et al., *Bid, a Bcl2 interacting protein, mediates cytochrome c release from mitochondria in response to activation of cell surface death receptors.* Cell, 1998. **94**(4): p. 481-90.

45. Kuwana, T., et al., *Bid, Bax, and lipids cooperate to form supramolecular openings in the outer mitochondrial membrane.* Cell, 2002. **111**(3): p. 331-42.

46. Boatright, K.M., et al., *A unified model for apical caspase activation.* Mol. Cell, 2003. **11**(2): p. 529-541.

47. Boatright, K.M. and G.S. Salvesen, *Mechanisms of caspase activation.* Current Opinion in Cell Biology, 2003. **15**(6): p. 725-731.

48. Kang, T.B., et al., *Caspase-8 Serves Both Apoptotic and Nonapoptotic Roles1.* The Journal of Immunology, 2004. **173**(5): p. 2976-2984.

49. Helfer, B., et al., *Caspase-8 Promotes Cell Motility and Calpain Activity under Nonapoptotic Conditions.* Cancer Res, 2006. **66**(8): p. 4273-4278.

50. Ohkuma, S. and B. Poole, *Fluorescence probe measurement of the intralysosomal pH in living cells and the perturbation of pH by various agents.* Proc Natl Acad Sci U S A, 1978. **75**(7): p. 3327-31.

51. Lin, Y., et al., *Tumor Necrosis Factor-induced Nonapoptotic Cell Death Requires Receptor-interacting Protein-mediated Cellular Reactive Oxygen Species Accumulation.* Journal of Biological Chemistry, 2004. **279**(11): p. 10822-10828.

52. Borges, H.L., et al., *Tumor promotion by caspase-resistant retinoblastoma protein.* Proceedings of the National Academy of Sciences, 2005. **102**(43): p. 15587-15592.

53. Li, K., et al., *Cytochrome c Deficiency Causes Embryonic Lethality and Attenuates Stress-Induced Apoptosis.* Cell, 2000. **101**(4): p. 389-399.

54. Ruffolo, S.C., et al., *BID-dependent and BID-independent pathways for BAX insertion into mitochondria.* Cell Death Differ, 2000. **7**(11): p. 1101-8.

55. Kohlhaas, S.L., et al., *Receptor-mediated endocytosis is not required for tumor necrosis factor-related apoptosis-inducing ligand (TRAIL)-induced apoptosis.* J Biol Chem, 2007. **282**(17): p. 12831-41.

56. Lee, K.H., et al., *The role of receptor internalization in CD95 signaling.* Embo J, 2006. **25**(5): p. 1009-23.

57. Clague, M.J., et al., *Vacuolar ATPase activity is required for endosomal carrier vesicle formation.* Journal of Biological Chemistry, 1994. **269**(1): p. 21-24.

58. Chau, B.N. and J.Y. Wang, *Coordinated regulation of life and death by RB.* Nat Rev Cancer, 2003. **3**(2): p. 130-8.

59. Tan, X., et al., *Degradation of Retinoblastoma Protein in Tumor Necrosis Factor- and CD95-induced Cell Death.* J. Biol. Chem., 1997. **272**(15): p. 9613-9616.

60. Whitaker, L.L., et al., *Growth suppression by an E2F-binding-defective retinoblastoma protein (RB): contribution from the RB C pocket.* Mol Cell Biol, 1998. **18**(7): p. 4032-42.

61. Vella, V., et al., *Exclusion of c-Abl from the nucleus restrains the p73 tumor suppression function.* J Biol Chem, 2003. **278**(27): p. 25151-7.

62. Xiao, Z.X., et al., *Interaction between the retinoblastoma protein and the oncoprotein MDM 2.* Nature, 1995. **375**(6533): p. 694-698.

63. Vargas, D.A., S. Takahashi, and Z. Ronai, *Mdm2: A regulator of cell growth and death.* Adv Cancer Res, 2003. **89**: p. 1-34.

64. Fattman, C.L., B. An, and Q.P. Dou, *Characterization of interior cleavage of retinoblastoma protein in apoptosis.* J Cell Biochem, 1997. **67**(3): p. 399-408.